

## **Chapter 1: Seven New Species and a New Subgenus of Forest Mice (Rodentia: Muridae: *Apomys*) from Luzon Island**

Author(s): Lawrence R. Heaney, Danilo S. Balete, Eric A. Rickart, Phillip A. Alviola, Mariano Roy M. Duya, Melizar V. Duya, M. Josefa Veluz, Lawren VandeVrede, and Scott J. Stepan

Source: Fieldiana Life and Earth Sciences, Number 2:1-60. 2011.

Published By: Field Museum of Natural History

DOI: 10.3158/2158-5520-2.1.1

URL: <http://www.bioone.org/doi/full/10.3158/2158-5520-2.1.1>

---

BioOne ([www.bioone.org](http://www.bioone.org)) is an electronic aggregator of bioscience research content, and the online home to over 160 journals and books published by not-for-profit societies, associations, museums, institutions, and presses.

Your use of this PDF, the BioOne Web site, and all posted and associated content indicates your acceptance of BioOne's Terms of Use, available at [www.bioone.org/page/terms\\_of\\_use](http://www.bioone.org/page/terms_of_use).

Usage of BioOne content is strictly limited to personal, educational, and non-commercial use. Commercial inquiries or rights and permissions requests should be directed to the individual publisher as copyright holder.

# Chapter 1: Seven New Species and a New Subgenus of Forest Mice (Rodentia: Muridae: *Apomys*) from Luzon Island

Lawrence R. Heaney<sup>1</sup>, Danilo S. Balete<sup>1</sup>, Eric A. Rickart<sup>1,2</sup>, Phillip A. Alviola<sup>1,3</sup>, Mariano Roy M. Duya<sup>4,5</sup>, Melizar V. Duya<sup>4,5</sup>, M. Josefa Veluz<sup>6</sup>, Lawren VandeVrede<sup>7,8</sup>, and Scott J. Steppan<sup>7</sup>

<sup>1</sup>Field Museum of Natural History, 1400 South Lake Shore Drive, Chicago, IL 60605, USA

<sup>2</sup>Utah Museum of Natural History, 1390 East Presidents Circle, Salt Lake City, UT 84112, USA

<sup>3</sup>Museum of Natural History, University of the Philippines, Los Baños, Laguna 4031, Philippines

<sup>4</sup>Conservation International–Philippines, 6 Maalalahanin Street, Teachers Village, Diliman, Quezon City 1101, Philippines

<sup>5</sup>Current address: Institute of Biology, University of the Philippines, Diliman, Quezon City, Philippines

<sup>6</sup>National Museum of the Philippines, Rizal Park, Ermita, Manila, Philippines

<sup>7</sup>Department of Biological Sciences, Florida State University, Tallahassee, FL 32306, USA

<sup>8</sup>Department of Medicinal Chemistry and Pharmacognosy, University of Illinois at Chicago, Chicago, IL 60608, USA

---

## Abstract

Surveys of small mammals on carefully selected mountains and mountain ranges on Luzon Island, Philippines, since 2000 have led to the discovery of seven previously unknown species of forest mice, *Apomys*, a remarkable radiation on just a portion of one island. On the basis of morphological and cytochrome (cyt) *b* DNA sequence data presented here, we propose a new subgenus, *Megapomys*, to include the large-bodied members of the genus, which form a monophyletic unit of relatively large mice (averaging ca. 65–110 g) with tails about as long as or slightly shorter than the length of the head and body; all of these species forage on the ground. Other members of the genus are assigned to the subgenus *Apomys*; they are smaller (ca. 18–41 g), have long tails, and usually or often forage above the ground surface. Members of the subgenus *Megapomys* include four previously recognized species (*A. abrae*, *A. datae*, *A. gracilirostris*, and *A. sacobianus*) and the seven new species described here (*A. aurorae*, *A. banahao*, *A. brownorum*, *A. magnus*, *A. minganensis*, *A. sierrae*, and *A. zambalensis*). All occur in northern and central Luzon Island, with the exception of one species that occurs on Mindoro Island; none is present in southern Luzon. Each species can be distinguished both morphologically and genetically. Although there are few records of *Megapomys* below 500 m elevation, they are common above about 1000 m, and some species occur near the peaks of the highest mountains on Luzon (i.e., up to nearly 2900 m). On four mountain ranges, two species of the subgenus co-occur, one at lower and one at higher elevations, although there is usually some syntopic overlap. Sister-species usually occur allopatrically in different mountain ranges, with one possible exception. Some of these species occur in areas not previously known to support endemic mammals, indicating that these areas are previously unrecognized areas of mammalian endemism where further study is warranted.

## Introduction

With 23 endemic genera of mammals within a land area of ca. 300,000 km<sup>2</sup>, the Philippine archipelago has one of the greatest concentrations of unique mammalian diversity of any place on earth (Heaney et al., 1998). Foremost among these in diversity are the murid rodents, with 16 endemic genera and at least 55 endemic species (Heaney et al., 1998; Musser & Carleton, 2005). Previously unknown murids continue to be described (e.g., Rickart et al., 2005; Balete et al., 2006, 2007, 2008; Heaney et al., 2009), many of them discovered recently as part of a continuing effort to conduct a comprehensive survey of the mammals of Luzon Island (e.g., Heaney et al., 1999, 2003; Duya et al., 2007; Balete et al., 2009; Rickart et al., 2011).

The remarkable diversity within the Philippine Muridae resides primarily within two endemic lineages: the “giant cloud

rat lineage” (= Phloeomyini *sensu* Lecompte et al., 2008), with five genera and about 15 species (Heaney et al., 1998, 2009; Jansa et al., 2006), and the “earthworm-mouse lineage” (part of the Hydromyini *sensu* Lecompte et al., 2008), with four genera and 22 species by the latest count (Steppan et al., 2003; Musser & Carleton, 2005; Jansa et al., 2006; Rowe et al., 2008). The latter is sister to all Australasian members of Hydromyini (Rowe et al., 2008; Heaney et al., 2009). The most speciose genus among these is *Apomys* Mearns 1905, generally referred to as Philippine forest mice, with 10 species previously described and recognized (Steppan et al., 2003; Musser & Carleton, 2005; Heaney & Tabaranza, 2006). In this paper, we show that past studies have undersampled, and therefore greatly underestimated, the number of species in this genus; herein, we describe seven additional species, all from Luzon. In doing so, we lay a substantial portion of the groundwork

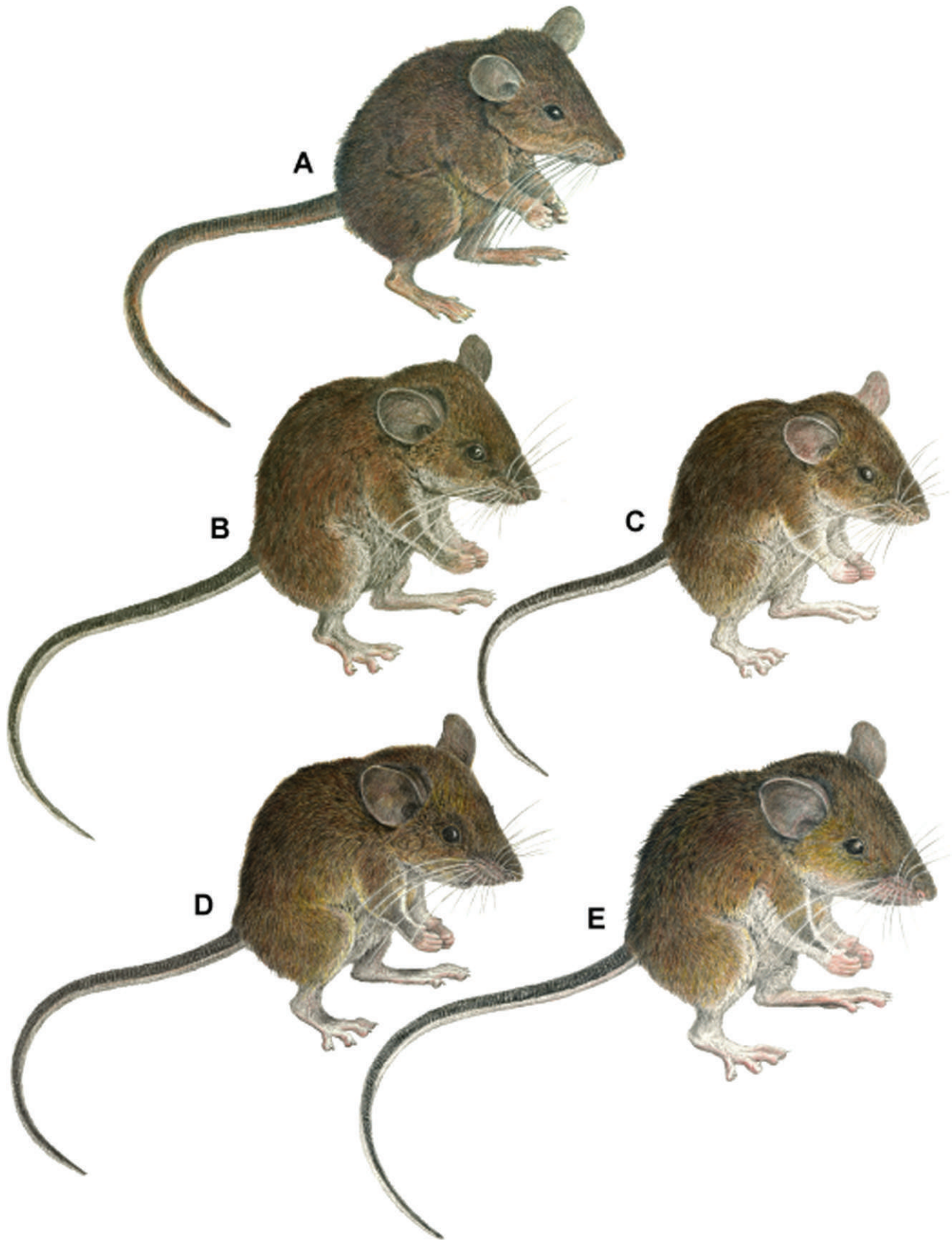


FIG. 1. Color drawings of (A) *Apomys gracilirostris*, (B) *A. datae*, (C) *A. abrae*, (D) *A. banahao* sp. nov., and (E) *A. magnus* sp. nov. to the same scale. All drawings by Velizar Simeonovski.

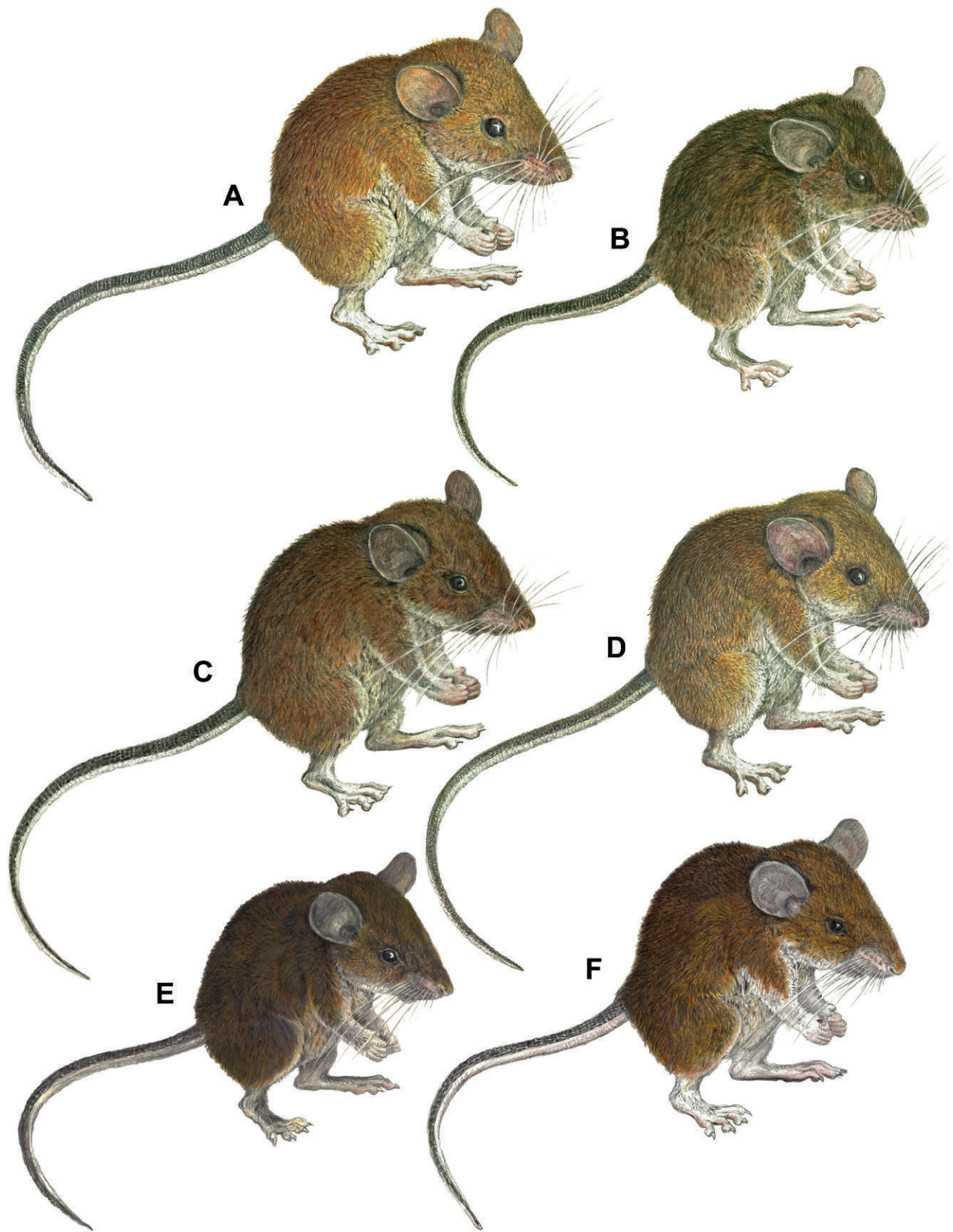


FIG. 2. Color drawings of (A) *Apomys zambalensis*, (B) *A. brownorum*, (C and D) *A. sierrae* (from Mt. Cetaceo and Mt. Palali, respectively), (E) *A. minganensis*, and (F) *A. aurorae* spp. nov., to the same scale. All drawings by Velizar Simeonovski.



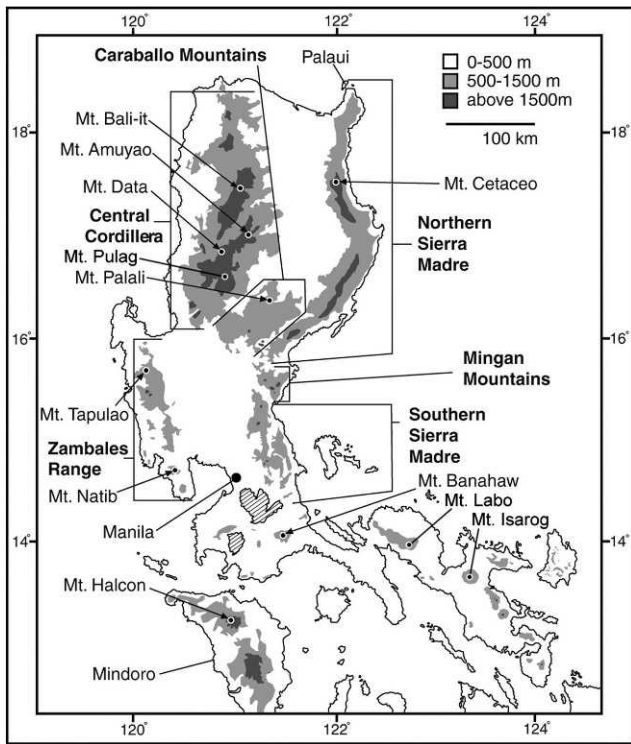


FIG. 3. Map of Luzon and Mindoro, showing mountains and ranges referred to in the text.

for a detailed examination of the geographic patterns of mammalian biodiversity on Luzon Island, the largest island in the Philippines at 102,000 km<sup>2</sup>, and the site of remarkable geological and geographical heterogeneity for such limited area.

Mice of the genus *Apomys* occur on most of the oceanic islands of the Philippines, being absent from only three areas: the Palawan region, which is faunistically more closely associated with the Sunda Shelf than with the oceanic Philippines; the Sulu Archipelago, a poorly known but seemingly species-poor set of islands that lie between Mindanao and Borneo; and the small, isolated islands of the Batanes and Babuyan groups that lie in deep water north of Luzon (Musser, 1982; Heaney, 1985, 1986, 2000; Musser & Heaney, 1992; Steppan et al., 2003; Catibog-Sinha & Heaney, 2006; Heaney et al., 2006a). At many of our sampling localities, these mice were the most abundant small mammals, especially at elevations above about 1200 m. As many as four species can occur on a given mountainside, with up to three species occurring syntopically. On Luzon, two ecological groups can be readily identified: small-bodied *Apomys* that forage primarily in vegetation (grass, shrubs, and trees) above the ground, and large-bodied species that forage primarily on the ground (Musser, 1982; Heaney et al., 1998, 1999, 2003, 2006a,b; Steppan et al., 2003; Balete et al., 2009, this volume; Alviola et al., this volume; Rickart et al., 2011).

During the 2004–2006 period of the comprehensive survey of Luzon mammals referred to above, we noted extensive variation in the external morphology of the large-bodied *Apomys* (Figs. 1, 2) that we captured in the northern and central parts of Luzon (Fig. 3), and we subsequently noted consistent cranial variation in parallel with the external morphology. As described below, our mitochondrial gene

phylogeny has revealed the presence of clades that corresponded to those morphological units. In this paper, we describe each of these morphologically distinct, genetically monophyletic units as a new species, discuss their patterns of distribution and phylogeny in the context of the previously described species of large-bodied *Apomys*, and consider their distribution patterns within the complex geography of Luzon Island.

## Materials and Methods

Specimens examined and/or referred to in this study are housed in the following museums, with their standard acronyms and some “synonyms”:

BM(NH)—British Museum (Natural History) = The Natural History Museum (London)

CMNH—Cincinnati Museum of Natural History, Cincinnati, OH

FMNH—Field Museum of Natural History, Chicago = Chicago Museum of Natural History

NMP—National Museum of the Philippines, Manila

USNM—United States National Museum of Natural History, Washington, D.C. = NMNH

For murid taxonomy and nomenclature, we follow Musser and Carleton (2005) unless otherwise noted.

Heaney examined the holotypes of the following species (housed at the indicated institutions): *Apomys abrae* (FMNH), *A. gracilirostris* (NMP), *A. sacobianus* (USNM), and *A. major* (USNM). We did not examine the holotype of *Apomys datae*, housed at the Staatliches Museum für Tierkunde, Dresden, Germany; for information on this holotype, we relied on Musser (1982).

Most of the specimens obtained during and after 2000 were initially preserved in formalin in the field then rinsed in water and transferred to ethanol. Many have had their skulls removed and cleaned by dermestid beetles, followed by soaking in a dilute ammonia solution, rinsing in water, and picking by hand. Before fixation with formaldehyde, specimens in the field had small amounts of muscle tissue, usually from the thigh, removed and stored in either 90% ethanol or dimethyl sulfoxide (DMSO). Additionally, some specimens were skeletonized in the field, and the skeletons were soaked and stored in ethanol before cleaning by the same procedure for skulls. A few specimens were karyotyped in the field, as detailed below. Once the specimens arrived at FMNH, the tissue samples were stored in the vapor from liquid nitrogen. Older specimens were skinned and stuffed as standard museum study skins in the field, and the skulls were removed and cleaned. Pre-1970 specimens at FMNH had their skulls cleaned by maceration, which sometimes caused teeth to loosen, fall out, or both and cranial sutures to loosen, come apart, or both.

With one exception, uncoated skulls were imaged with an AMRAY 1810 scanning electron microscope (SEM). The specimens were not coated with gold. Because the size of the skulls and mandibles exceeded the photographic frame, SEM photographs were taken of the front, middle, and back of the skull in each view and digitally matched and merged to make the images presented here. The skull of the holotype of *A. sacobianus* was photographed with a digital camera.

Our investigations used qualitative aspects of the external, cranial, and dental morphology; quantitative assessment of

mensural craniodental similarities and differences by principal components analysis (PCA); and genetic data. We conducted these studies simultaneously, with the results of each causing us to re-examine and extend our examination of the others. In this paper, we take the results of quantitative morphometric studies as our starting point then present the results from our genetic studies that provide a phylogenetic context generally lacking from the quantitative morphological studies. We also present information on the karyology of four of the species. We follow this with detailed descriptions and comparisons of anatomy for each species, emphasizing the distinctive features that are not captured by measurements. Within the individual species accounts, we also include additional quantitative assessments of craniodental morphometric variation within individual species and among sets of closely related species, and often include bivariate plots to document differences among them and as an aid to identification for future studies.

All specimens collected since 2000 have been prepared and cataloged at FMNH, as described above. Upon completion of this study, approximately half of the specimens will be permanently deposited at the NMP, including all of the holotypes of the species named here. All of the authors of this publication are intended as authors of all species names proposed herein.

Specimens collected before about 1970 often had localities with elevation recorded in feet. Inspection of the elevations indicates that these were estimates, often rounded to the nearest 500 or 1000 feet. We retain these original data in the following text but also provide the elevation converted to meters, rounded to the nearest 100 m for the convenience of the reader.

### Measurements and Morphometric Analyses

Measurements of total length (TL), length of tail vertebrae (TV), length of hind foot including claws (HF), length of ear from notch (EAR), and weight in grams (WT) were taken from our field catalogs housed at FMNH or from the tags on older specimens. Our field measurements were taken with plastic rulers graduated to 1 mm or with Pesola scales graduated to 1 g. The length of head and body (HBL) was determined by subtracting length of tail from total length.

Eighteen cranial and dental measurements were taken from individuals, with sample sizes listed in the tables. For our sample, we chose adults that had complete skulls. Adults were defined as those individuals with adult pelage (not the grayer pelage of young animals), cranial sutures (especially the basicranial sutures) fused or nearly so, and molar teeth showing at least moderate wear. Most adult females had enlarged nipples, and most males had testes of relatively large size. Heaney took all cranial measurements with dial calipers graduated to 0.01 mm. The following measurements were taken: basioccipital length (BOL; from anterior edge of premaxillary to posterior edge of occipital condyles); least interorbital breadth (IB); greatest zygomatic breadth (ZB); mastoid breadth (MB); nasal length (NL); length of incisive foramen (LIF); rostral depth (RD; taken from the midpoint of the premaxillary–maxillary suture to the nearest point on the dorsum of the rostrum); rostral length (RL; taken from anteriormost point of orbit to the tip of the nasals); orbitotemporal length (OL; taken from the anteriormost point of the orbit to the posteriormost point of the temporal fossa); alveolar length of maxillary molariform teeth ( $M^1$ – $M^3$ ); labial

palatal breadth at the first upper molar ( $PBM^1$ ); diastema length (DL); postpalatal length (PPL; from the posterior edge of palate to anterior edge of foramen magnum); lingual palatal breadth at the upper third molar ( $LBM^3$ ); braincase height (BH; taken at the midline); breadth of  $M^1$  ( $BM^1$ ); breadth of upper incisors (BIT; near tip but below the wear surface); and width of the zygomatic plate (ZP; at its midpoint).

We used Microsoft Excel for Windows (version 2007) to calculate descriptive statistics (mean, standard deviation, and observed range) for sample groups. We assessed quantitative phenetic variation in craniodental morphology through PCA with the use of the correlation matrix of log-transformed measurements of adult specimens using SYSTAT 10 for Windows (SPSS Inc., 2000). Samples included adults of both sexes, usually 10–12 individuals per sex per locality or species, as shown in the tables. Samples were smaller only when more adult individuals were not available. We conducted analyses that included several combinations of taxa, such as all species, sets of closely related species, and geographic populations within species, as described below. We considered any component with an eigenvalue of less than 1.5 to be not meaningfully interpretable and have dealt cautiously with eigenvalues between 2.0 and 1.5, as indicated in the text.

### DNA Sequencing and Phylogenetic Analyses

We extracted DNA from and sequenced the entire cytochrome (cyt) *b* gene for 107 individuals of *Apomys*. Sequences have been submitted to GenBank under accession numbers HM370984–HM371090; accession numbers for all analyzed individuals are listed in Appendix 1. The alignment and trees have been deposited with TreeBASE accession S10997. Our use of informal species designations for undescribed species in the small-bodied group (e.g., “sp. F”) follows Heaney et al. (1998) and Stepan et al. (2003), except that their “sp. D” has been described as *A. camiguinensis* by Heaney and Tabaranza (2006).

We extracted total genomic DNA from liver or muscle tissue stored in ethanol according to standard phenol/chloroform extraction techniques. We amplified the entire cyt *b* gene by polymerase chain reaction (PCR) following procedures described in Stepan et al. (2003). All PCR reactions included a negative control (no template DNA), intended to identify any instances of contamination of reagents, and were visualized on agarose gels with ethidium bromide. Successful reactions were prepared directly by enzymatic digestion with Exo-SAP-IT (USB Corp., USA). Both strands of each PCR product were completely sequenced with PCR and internal primers. Products were sequenced by automated DNA sequencing on an ABI 3100 with the use of big-dye terminator chemistry (Applied Biosystems, USA). Sequences were aligned by Sequencher 4.1 (Genecodes).

To verify the taxonomy of individuals attributed to *A. datae* and *A. abrae*, we also sequenced individuals collected from the type localities. For specimens from the 1940s and 1950s, we conducted extractions on bits of dried tissue left adhering to museum skulls (FMNH 62709, 62724, 62749, 92759, 92760), the sequencing products of which are referred to as “ancient DNA.” Standard procedures were modified by the addition of 10  $\mu$ l *N*-phenacylthiazolium bromide (PTB) solution to the 200  $\mu$ l of extraction buffer to break DNA–protein cross-linking (Poinar et al., 2003), incubating for 36 hours rather than overnight. All extractions were conducted in an isolated

lab free of PCR products, and ancient DNA PCR and cloning were conducted in a lab that had never worked on mammalian DNA. We amplified a portion of *cyt b* in two overlapping fragments of approximately 110 base pairs in length each, with the use of primer pairs S205/S206 (CCCCCTCCAAYATTT-CATCCTGATGAAA/GTKACTGAGGAGAAGGCAGT) and S207/S208 (TCTAGCCATACACTATAACATCAG/CGTCCTACGTGTAGAAATAAGCAG), modified from primers L14841/H14927 and L14925/H15052, respectively, from Kuch et al. (2002), tailored to match *Apomys*. PCR products were then cloned with the TOPO TA cloning kit from Invitrogen and vector pCR 2.1-TOPO (3.9 kb). The recombinant plasmids were isolated with Qiaprep spin columns from Qiagen. Presence of insert and the size of the insert were verified by *Eco*R1 restriction digest and gel electrophoresis. Three to five clones of each ancient sample were sequenced using the vector primers m13r and m13f.

Phylogenetic analyses were conducted using maximum-likelihood (ML) and Bayesian approaches as implemented in PAUP\* 4.0b10 (Swofford, 2002) and MrBayes ver. 3.1.2 (Huelsenbeck & Ronquist, 2003). Support values are reported below for ML analyses as bootstrap values (bp) and for Bayesian analyses as posterior probabilities (pp). The analytical model (GTR with invariant sites and gamma distributed rates) was identified using Akaike's Information Criterion as implemented in Modeltest 3.04 (Posada & Crandall, 1998) on one of the maximum parsimony (MP) trees. We then conducted a ML search using the preferred model with parameters fixed at the values estimated on the MP tree. A heuristic search was conducted with ten random-addition replicates and TBR branch swapping. Bayesian analysis was run with two heated chains and default settings for 10 million generations each. The data were partitioned by codon, and all parameter values were estimated for each partition separately (unlinked). Convergence was estimated by means of diagnostics from AWTY (Wilgenbusch et al., 2004) as well as by examination of likelihood plots and posterior probabilities of individual clades for subsets of the runs. Trees were recorded every 2000 generations and the first 20% were discarded as burn-in. Nonparametric ML bootstrapping (Felsenstein, 1985) was performed with 200 replicates, each consisting of five random-sequence addition replicates, each of which was limited to 2000 rearrangements.

### Karyology

Karyotype preparations were made in the field from freshly caught specimens of some taxa. For live-trapped animals, bone marrow cells were processed with the use of *in vivo* methods (Patton, 1967, as modified by Rickart et al., 1989). For specimens captured in snap traps and recovered shortly after death, cells were processed with a modified *in vitro* technique (Rickart et al., 1998). Fixed cell preparations were stored at  $-70^{\circ}\text{C}$  within one month of field processing, and standard karyotypes (undifferentially stained with giemsa) were prepared after several months of storage. A minimum of 10 chromosome spreads was examined from each preparation. Chromosome terminology follows Rickart and Musser (1993). As used here, fundamental number (FN) refers to the total number of chromosome arms (including those of sex chromosomes) in the female karyotype. Because of variation in preparation quality and the presence of very tiny secondary arms on some chromosomes, we use the symbol " $\geq$ " to indicate what we consider to be minimum FN values.

## Results

### The Definition of *Apomys*

*Apomys* is defined as including the most recent common ancestor of *A. datae*, *A. gracilirostris*, *A. hylocoetes*, *A. musculus*, and all its descendants. They are medium to small mice, with adults weighing from as little as 18 g (*Apomys musculus*; Heaney et al., 1999) to as much as 128 g. The general appearance (Figs. 1, 2) resembles individuals of *Peromyscus*, *Apodemus*, *Praomys*, and many other muroid genera. The tail is nearly equal in length to, or longer than, the head and body and usually is dark dorsally and pale to white ventrally, usually with a sharp boundary. The eyes and ears are large. The fur is soft and thick, darker dorsally than ventrally; the ventral fur is paler, often nearly white with an ochraceous wash. The hind feet are moderately long and narrow, have six plantar pads, and have digits 2–4 notably longer than digit 5 and the hallux. All species have two pairs of inguinal mammae.

The skull (Fig. 4) is similar in general appearance to those of many murids of similar size, but a combination of eight characters uniquely diagnoses the genus (Musser, 1982; Musser & Heaney, 1992). 1) The rostrum is moderately to distinctly long and narrow. The premaxillaries project well beyond the anterior edges of the incisors; together, with the equally elongate nasals, this forms a somewhat tubular structure. 2) The incisive foramina are rather broad, especially relative to their length. 3) The bony palate is wide and long, ending posterior to the last molar, with a ridge along the posterior margin. It is textured by many tiny pits and perforations, particularly on the posterior half to one-third of its length. 4) Each upper third molar is small and peg-like, but with a small cusp at the anterolabial margin (absent on worn teeth). 5) The occlusal surface of each first and second upper molar consists of three chevron-shaped laminae on which cusps are barely evident or absent. 6) The occlusal surface of each first lower molar consists of a large, inverted, heart-shaped structure at the front that forms about half of the tooth, followed by a chevron-shaped lamina and a small posterior cingulum. 7) Each auditory bulla is separated from the squamosal and alisphenoid by a gap of variable size; the gap represents the coalesced postglenoid foramen, the postalar fissure, and the middle lacerate foramen. 8) Most species have a subsquamosal fenestra (= squamoso-mastoid fenestra) that is evident as a notch dorsal to the auditory bulla. Additionally, we note that adult male *Apomys* have the posterior tip of the scrotum (roughly 10% of the scrotum) covered with a densely pigmented, dark spot. A similar pigmented area occurs in *Chrotomys* and *Rhynchomys*.

*Apomys* is the basal member of a clade that also includes *Archboldomys*, *Chrotomys*, and *Rhynchomys* (Jansa et al., 2006; Heaney et al., 2009). Although no gene sequence data are available from some Indo-Australian genera of interest, this Philippine clade is well supported by multiple nuclear and mitochondrial genes as most closely related to the remaining members of the Hydromyini *sensu* Rowe et al. (2008), all of which are confined to New Guinea, Australia, and adjacent islands (Rowe et al., 2008). *Chiropodomys*, a genus confined to continental SE Asia, the Sunda Shelf, and Palawan, is the sister-group to the Hydromyini *sensu* Rowe et al. (2008; see also Heaney et al., 2009).





FIG. 4. Crania and mandibles of *Apomys (Megapomys) datae* (A, C, E, F; FMNH 188445) and *Apomys (Apomys) hylocoetes* (B, D, G, H; FMNH 148146), dorsal (A, B), ventral (C, D), lateral (E–H); scale bar = 5 mm.

#### Carotid Circulatory Patterns

As noted by Musser (1982), the basicranial arterial circulatory patterns in *A. abrae* and *A. datae* have discrete and fundamental differences; we follow him in referring to these as the “abrae pattern” (Fig. 5A) and “datae pattern” (Fig. 5B). In *A. datae* (Fig. 5B), the carotid artery produces a branch, the stapedial artery, near the posterior margin of the bulla. The carotid artery continues anteriorly through the carotid canal into the cranial cavity where it passes beneath the brain. The stapedial artery enters the bulla through a canal that leads to the stapedial foramen, which lies between the

bullar capsule and the petrosal portion of the petromastoid bone. This stapedial foramen is visible on the bulla of a clean skull under low magnification and is visible to the naked eye of many people. The artery proceeds through the bulla and emerges in the middle lacerate foramen as the internal maxillary artery, which courses through a groove in the pterygoid plate and through the foramen ovale into the alisphenoid canal and sphenoidal fissure and eventually into the orbit. This configuration of the carotid circulatory pattern is widespread in murids, and it is present in *Archboldomys*, *Chrotomys*, and *Rhynchomys*, which form the sister-group to *Apomys* (Balette et al., 2006, 2007; Jansa et al., 2006); we



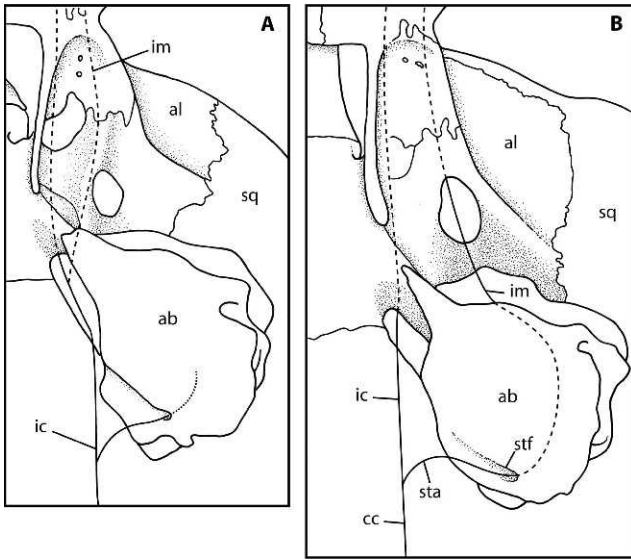


FIG. 5. Diagrammatic drawing of the basicranial region of *Apomys* in ventral view, showing the two types of carotid circulatory patterns. (A) The “abrae type”; (B) the “datae type.” Redrawn from Musser, 1982. Abbreviations: **ab**, auditory bulla; **al**, alisphenoid bone; **cc**, carotid canal; **ic**, internal carotid artery; **im**, internal maxillary artery; **sq**, squamosal bone; **sta**, stapedial artery; **stf**, stapedial foramen.

presume it to be the primitive condition in *Apomys*. It is present in *A. datae*, *A. aurorae* sp. nov., *A. gracilirostris*, *A. magnus* sp. nov., *A. minganensis* sp. nov., and *A. zambalensis* sp. nov., as detailed below.

In *A. abrae* (Fig. 5A), the carotid artery produces a stapedial artery that enters the bulla through a foramen that is too small to be seen with the naked eye and is seen only with difficulty under low magnification. This artery ends within the otic region of the bulla. The carotid artery proceeds anteriorly through the carotid canal into the cranial cavity; at the point of entering the cranial cavity, it produces the internal maxillary artery. The internal maxillary proceeds through a conspicuous groove in the alisphenoid wing of the pterygoid plate, thence through the sphenoidal fissure into the orbit. This condition is present in *A. abrae*, *A. banahao* sp. nov., *A. brownorum* sp. nov., *A. sacobianus*, and *A. sierrae* sp. nov.; we have noted no variation within any of these species. Because this condition is unusual within murids and absent in the sister-clade to *Apomys*, we consider it to be derived within *Apomys*.

On the basis of our assessment of polarity, the molecular phylogeny presented below implies that the primitive “datae pattern” is retained in *A. gracilirostris* (the basal species in the clade), *A. datae*, and the clade that includes *A. minganensis* sp. nov., *A. magnus* sp. nov., *A. aurorae* sp. nov., and *A. zambalensis* sp. nov. The derived condition (the “abrae pattern”) developed independently three times: in *A. brownorum* sp. nov. and *A. banahao* sp. nov., in *A. abrae*, and in *A. sierrae* sp. nov. Because the phylogenetic position of *A. sacobianus* is unknown, we do not know whether its possession of the derived condition is shared with one of the other species or is also derived independently. The basicranial arterial patterns are highly useful as diagnostic features of species in *Apomys*, but apparently they are not consistent indicators of phylogenetic relationships as inferred from *cyt b* sequence data analysis.

TABLE 1. Character loadings, eigenvalues, and percent variance explained on the first four components of a principal components analysis of log-transformed measurements of adult large-bodied *Apomys* (see Fig. 6 and Methods).

Variable	Principal component			
	1	2	3	4
Basioccipital length	0.924	0.131	-0.210	0.023
Zygomatic breadth	0.843	0.125	0.147	-0.097
Rostral depth	0.839	-0.028	-0.094	-0.221
Labial palatal breadth at M <sup>1</sup>	0.789	-0.485	0.070	0.122
Mastoid breadth	0.766	0.211	0.232	0.002
Orbitotemporal length	0.762	-0.300	-0.120	-0.216
Maxillary tooththrow length	0.715	-0.525	0.037	-0.075
Lingual palatal breadth at M <sup>3</sup>	0.711	-0.319	-0.237	0.072
Nasal length	0.690	0.405	0.109	0.275
Interorbital breadth	0.650	0.082	0.276	0.285
Diastema length	0.644	0.320	-0.462	0.216
Postpalatal length	0.625	0.272	-0.394	-0.320
Breadth of incisors at tip	0.621	0.105	0.123	-0.507
Width of zygomatic plate	0.618	-0.184	0.049	0.279
Rostral length	0.600	0.616	0.059	0.270
Incisive foramen length	0.541	-0.306	-0.372	0.133
Breadth of M <sup>1</sup>	0.488	-0.401	0.584	0.112
Braincase height	0.479	0.374	0.448	-0.302
Eigenvalue	8.665	1.947	1.363	0.965
Percent variance explained	48.14	10.82	7.57	5.36

#### Quantitative Morphometric Variation within Large-Bodied *Apomys*

We conducted a PCA of 18 craniodental measurements of individuals representing all of the genetic units identified below on the basis of data summarized in the tables of measurements that appear below. Because the genetic data showed that animals from high elevations are often distinct from those at low elevations in a given area, we measured specimens along as complete a portion of the elevational gradient as possible in every case. We included individuals from every geographic region from which we have specimens with complete skulls, to determine whether the operational units apparent in the craniodental morphometric data are evident as monophyletic groups in the genetic data also. In this analysis, we excluded the Mindoro species *A. gracilirostris*. Compared with the other species, it is morphologically divergent, possessing an elongate rostrum, globose braincase, and narrow incisors, conformations not seen in any of the Luzon species. Including this distinctive species with the others, which resemble each other more closely, would have dominated the pattern of variation and obscured fine discrimination among the remaining taxa.

The PCA produced four axes with eigenvalues that exceed or nearly equal 1.0 (Table 1), which explained 48.1%, 10.8%, 7.6%, and 5.4% of the variance in the data set (71.9% total). Loadings on the first axis are all positive and fairly high, indicating that this is an axis that primarily shows overall size. The second axis has strong positive loadings for nasal, rostral, and diastema length and braincase height, and strong negative loadings for the length of the maxillary tooththrow, labial breadth of the palate at M<sup>1</sup>, lingual palatal breadth at M<sup>3</sup>, and breadth of M<sup>1</sup>. This axis thus contrasts individuals with long rostra, nasal bones, and diastema, high braincase, short molar tooththrows, narrow palates, and narrow M<sup>1</sup>, with individuals having the converse.

The third axis (Table 1), with a marginally interpretable eigenvalue of 1.4, had high positive loadings for breadth of M<sup>1</sup>

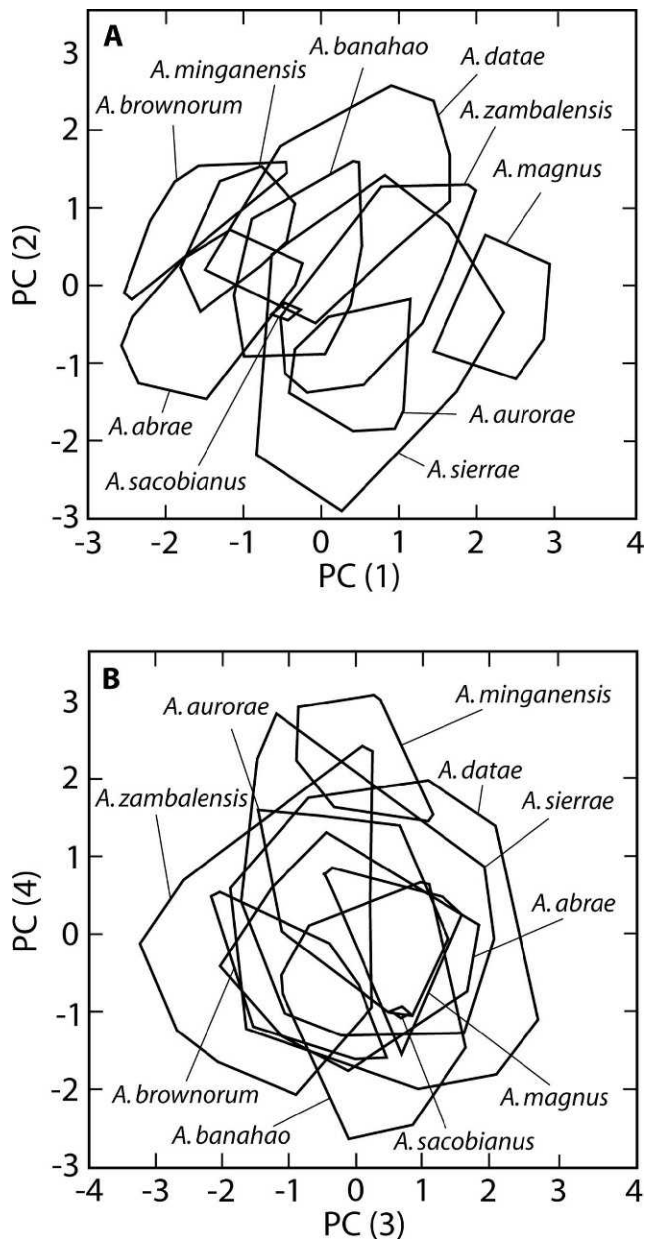


FIG. 6. Results of the principal components analysis of all taxa; see Table 1 and text for details. (A) Principal component (PC) 2 vs. PC 1; (B) PC 4 vs. PC 3.

and braincase height and high negative loadings for diastema length, length of the incisive foramina, and postpalatal length. This axis contrasts individuals with wide  $M^1$ ; high braincases; and short diastemas, incisive foramina, and postpalatal regions with those that have the converse.

The fourth axis is not interpretable, with an eigenvalue of 0.965. It primarily contrasts individuals with upper incisors that are narrow at the tip with those that are wider at the tip.

A plot of the first two axes (Fig. 6A) shows overlap among many named species and previously unnamed, geographically defined populations, but clear patterns and differences are nevertheless evident. Specimens from the lowlands of Mt. Banahaw (*A. magnus* sp. nov.) scored highest on the first axis, and specimens of *A. abrae* and those from the high elevations on the Zambales Mountains (*A. brownorum* sp. nov.) scored lowest, reflecting their status as the largest and smallest of

these species. Other species fell toward the middle of the range and overlapped extensively. *Apomys datae* scored highest on the second axis, reflecting its long rostral region (including the diastema), high braincase, narrow  $M^1$ , and narrow palate (and, we note from examination of skulls, the palate is also short). Most individuals from the Sierra Madre (*A. sierrae* sp. nov.) scored low on this axis, reflecting their shorter rostrum, low braincase, and wide  $M^1$ .

Close inspection of Figure 6A shows additional patterns. *Apomys abrae* and *A. datae*, which co-occur in the Central Cordillera, show limited overlap on these two axes. Specimens from high (*A. brownorum* sp. nov.) and low (*A. zambalensis* sp. nov.) in the Zambales Mountains show no overlap; the same is true for specimens from high (*A. banahao* sp. nov.) and low (*A. magnus* sp. nov.) on Mt. Banahaw, and from high (*A. minganensis* sp. nov.) and low (*A. aurorae* sp. nov.) in the Mingan Mountains. Those from high in the Zambales (*A. brownorum* sp. nov.) and on Mt. Banahaw (*A. banahao* sp. nov.) do not overlap, nor do those from low in Zambales (*A. zambalensis* sp. nov.) and on Mt. Banahaw (*A. magnus* sp. nov.). This suggests that each of these is a distinct morphotype, compared with a sympatric or parapatric morphotype. But this analysis also leaves ambiguity among some geographic populations. Individuals from the Sierra Madre and Caraballos Mountains (described below as *A. sierrae* sp. nov.) vary widely, and overlap broadly with individuals from the Mingan lowlands and Zambales lowlands. *Apomys datae* overlaps fairly extensively with individuals from the high elevations on Mt. Banahaw (*A. banahao* sp. nov.) and the Zambales lowlands (*A. zambalensis* sp. nov.), and there is some overlap between *A. datae* and individuals from the Sierra Madre and Caraballos Mountains (*A. sierrae* sp. nov.).

Figure 6B, which is marginally interpretable because of low eigenvalues, plots the scores of individual specimens on axes 3 and 4 of the PCA. *Apomys* from the lowlands of Zambales (*A. zambalensis* sp. nov.), which fall near the center in Figure 6A, score lowest on axis 3, indicating that they have narrow  $M^1$ , low braincases, and long diastemas and incisive foramina. *Apomys datae* and specimens from the highlands of Mt. Banahaw (*A. banahao* sp. nov.) have the reverse. On axis 4, specimens from the Mingan highlands (*A. minganensis* sp. nov.) score high, indicating that their incisors are especially narrow at the tip. Specimens from the highlands of Mt. Banahaw (*A. banahao* sp. nov.) scored especially low on this axis. Specimens of *A. sierrae* are notably variable on this axis.

These morphometric analyses provide an overview of differences in size and shape among geographic populations of large-bodied *Apomys*, and many of these differences imply that many distinct species are present. However, clear resolution of species requires further data, which we provide next in the form of genetic data from the mitochondrial DNA genome, specifically from *cyt b*, followed by detailed comparisons of external and craniodental morphology. In the descriptions of species that follow, we also present PCAs of selected sets of species, and of populations in geographically widespread species, as a means of further investigating patterns of variation, similarity, and dissimilarity.

#### Molecular Evidence of Relationships within *Apomys*

Maximum likelihood analysis of the mitochondrial gene *cyt b* yielded 14 trees, all of which agreed on the among-species

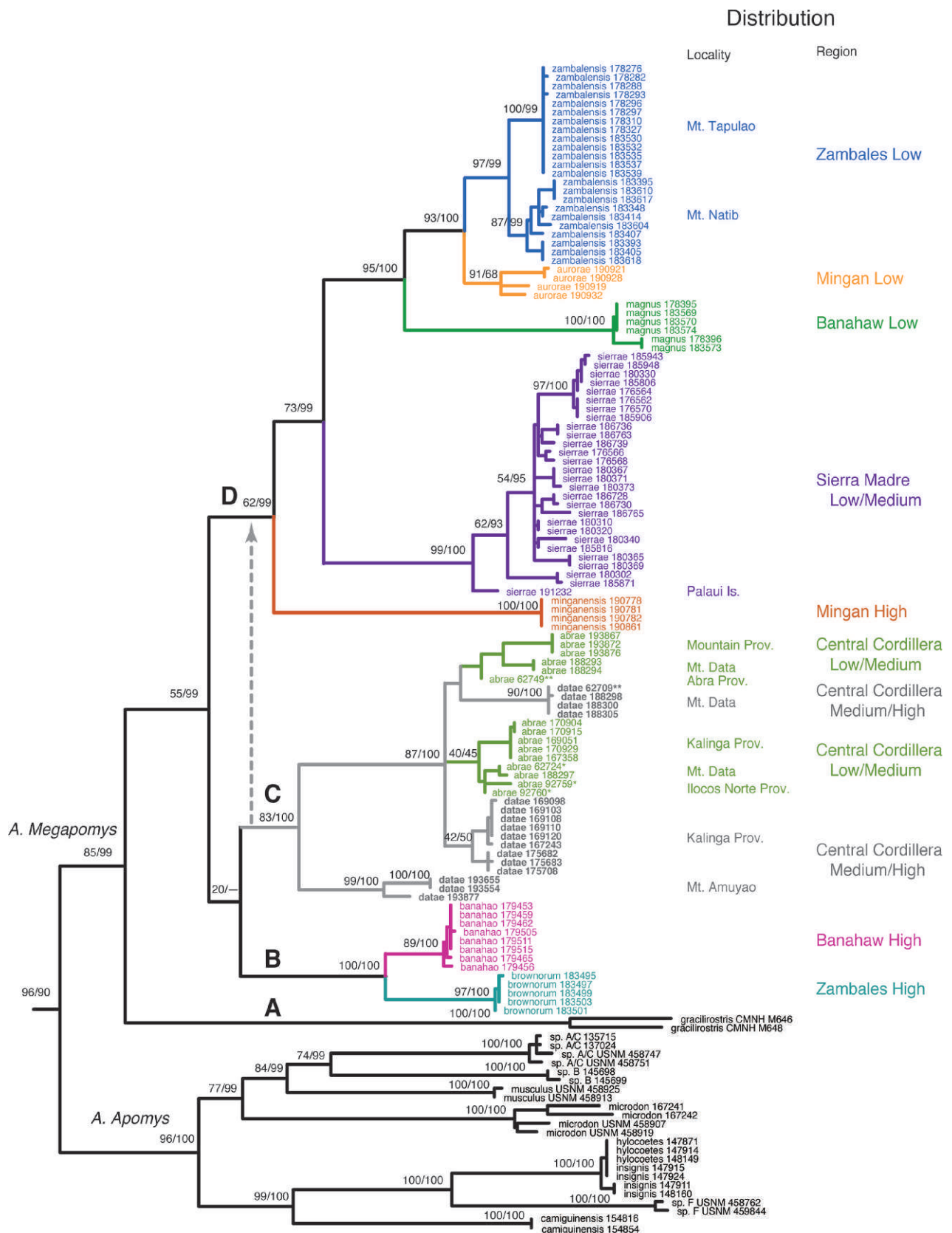


FIG. 7. Maximum likelihood phylogeny of *Apomys* based on the mitochondrial gene *cyt b*. Pictured is one of 14 most likely trees, chosen randomly. The trees vary topologically only with respect to apparent polytomies within species and among three lineages of *A. abrae* and *A. datae*. Support values are ML bootstrap and Bayesian posterior probabilities, respectively, expressed as percentages, for selected nodes. The **long dash symbol** (—) indicates clades B and C are not sister-groups in the maximum credible tree from Bayesian analysis. The **dashed grey arrow** indicates the Bayesian placement of clade C. Unless otherwise specified, all specimen numbers are FMNH. An **asterisk** (\*) on the specimen name indicates source for ancient DNA or degraded frozen sample. A **double asterisk** (\*\*) indicates an ancient DNA specimen collected from type locality. Outgroups are pruned for visual clarity. Clades are color-coded by morphologically defined species. Localities and regions of selected clades are indicated on the right. Low, medium, and high refer to relative elevation ranges.



topology. The only differences among the ML trees occurred within regions of near-zero branch lengths: at the base of *A. aurorae*, within *A. sierrae*, and among three population-level clades of *A. datae* and *A. abrae*. Our analysis of the phylogeny showed clear structure, with most nodes significantly resolved down to a low divergence level (Fig. 7). Two primary clades are evident. The first of these (*A. Apomys* in Fig. 7) includes all of the small species (average 18–41 g) in the genus (*A. camiguinensis*, *A. hylocoetes*, *A. insignis*, *A. microdon*, *A. musculus*, and unnamed taxa labeled “sp. A,” “sp. B,” “sp. C,” and “sp. F”; see Heaney et al., 1998; Steppan et al., 2003). This clade occurs widely within the Philippines except for three areas: the Palawan region, which shares many species with Borneo and may have been connected to Asia (via Borneo) at some point during the Pleistocene glaciations (Heaney, 1985, 1986; Sathiamurthy & Voris, 2006); the small, isolated islands of the Babuyan and Batanes groups that lie north of Luzon; and the Sulu Archipelago, a seemingly depauperate but poorly known set of small islands between Mindanao and Borneo. These species all have tails that are substantially longer than the length of the head and body (from 120% to 140%), and all apparently forage frequently or primarily above ground in grass, shrubs, trees, or a combination thereof, often in sympatry with large-bodied species in northern and central Luzon (Heaney et al., 1989, 1998, 1999, 2006a,b; Rickart et al., 1993, 2011; Balete et al., 2009).

The second primary clade within *Apomys* (*A. Megapomys* in Fig. 7) includes large-bodied animals (mean weight 66–109 g) that occur only on Luzon and Mindoro islands, represented among previously described species by *A. abrae*, *A. datae*, *A. gracilirostris*, and *A. sacobianus* (the last of which could not be included in Fig. 7 because it is known only from the holotype collected in 1956). In addition to these species, which are treated in detail below, many monophyletic lineages are represented by specimens that have been obtained by our field surveys since 2000. All of these mice have tails that are usually about equal to but sometimes shorter than or slightly longer than the length of head and body (84–110%), and they forage on or occasionally slightly above the surface of the ground (Heaney et al., 2003; Duya et al., 2007, this volume; Balete et al., 2009, this volume; Alviola et al., this volume; Rickart et al., 2011).

Within the large-bodied *Apomys*, four secondary clades are evident in the genetic data (Fig. 7). The first of these (“A”) consists of *A. gracilirostris* from Mt. Halcon, Mindoro Island, sister to all other species. This is the only large-bodied species of *Apomys* currently known from an island other than Luzon, with the exception of a population on a small, shallow-water island (Palau) of a species described below that occurs on the adjacent portion of Luzon.

The second large-bodied clade (“B”) includes two monophyletic populations from high elevations on Mt. Banahaw and on Mt. Tapulao in the Zambales Mountains (Fig. 3), described herein as the new species *A. banahaw* and *A. brownorum*, respectively. Although the genetic distance between them is not great (3.6% uncorrected distance), the support values are high (ML bootstrap 89–97 bp, 1.00 Bayesian pp), and the clade containing these two species is genetically quite distinct from their sister-clade. These populations were easily distinguished from each other on principal components 1 and 2 (PC1, PC2) in the PCA described above and differ in anatomical details described below.

The third large-bodied clade (“C”) includes two named species, *A. abrae* and *A. datae*. The results are equivocal as to the exact placement of this clade; ML places it as sister to clade “B,” Bayesian analysis places it as sister to clade “D,” as discussed below, but neither position is well supported (20% bp, 0.63 pp, respectively). Therefore, we consider the relationships among clades B–D to be unresolved and effectively a polytomy, pending further data. Monophyly of clade C is moderately well supported, with 83% bp and 100 pp. These two species are easily distinguished by morphological details provided below in the species descriptions. The remarkable pattern here is the paraphyly of both species with respect to each other. Individuals assignable morphologically to *A. datae* belong to three mitochondrial lineages, one of which (FMNH 193554, 193655, 193877) is from Mt. Amuyao and is moderately divergent from the rest of the complex. The other two interdigitate with two lineages assignable to *A. abrae*. Specimens from the type localities of these two species are indicated by “\*\*\*” and are part of this polytomy. Within clade C, *cyt b* data do not support the species limits that are indicated by morphology. There are two leading alternative explanations for this discordance. The species could have diverged only very recently, with the tree reflecting a lack of sorting of the mitochondrial genome. Given that the mitochondrial genome is quickly evolving and rapidly sorting, we believe that this hypothesis is unlikely. Alternatively, mitochondrial introgression might obscure the true phylogeny, as seen in chipmunks (Good et al., 2008). In contrast to the *cyt b* results, preliminary phylogenies from several nuclear genes indicate that these species might not even be close relatives (S. J. Steppan, unpubl. data). We are currently testing these alternatives with additional nuclear sequence data and will present the results elsewhere. Although we consider their current phylogenetic placement tentative pending these further studies, on the basis of their distinctive morphology and extensively overlapping geographic distributions, we retain *A. abrae* and *A. datae* as distinct species.

The fourth major clade (“D” in Fig. 7) includes five distinct monophyletic groups from 1) lowland portions of Mt. Banahaw (described here as *A. magnus* sp. nov.), 2) Mt. Natib and lowland portions of Mt. Tapulao in the Zambales Mountains (described here as *A. zambalensis* sp. nov.), 3) the upper and 4) lower elevations in the Mingan Mountains (described here as *A. minganensis* and *A. aurorae* spp. nov., respectively), and 5) individuals from the northern Sierra Madre, the Caraballo Mountains, and the near-shore, shallow-water island of Palau (described here as *A. sierrae* sp. nov.). Clade D is the least well supported of the major large-bodied clades, with 62% bp and 0.99 pp.

The first species to diverge in this group is *A. minganensis* sp. nov. from the highlands of the Mingan Mountains. Its genetic distance to other groups is high (7–8% uncorrected, 11–12% ML distances), and support values are strong (100% bp, 1.00 pp), clearly showing this as an evolutionarily distinct species. As described below, this species overlaps syntopically with individuals of *A. aurorae* sp. nov. from the lowlands of the Mingan Mountains, a species that is more closely related to lowland populations from Mt. Banahaw (*A. magnus* sp. nov.) and the Zambales/Natib area (*A. zambalensis* sp. nov.). The absence of evidence of gene flow and the ease of morphological differentiation evident in the PCA (Fig. 6A) mark the two clades in the Mingan Mountains as necessarily representing different species. The clades from lowland

Banahaw (*A. magnus* sp. nov.) and lowland Zambales/Natib (*A. zambalensis* sp. nov.) are genetically similar to each other and the clade from lowland Mingan, but each of these three allopatric clades is well supported, they have limited overlap in the PCA (Fig. 6A), and they can be easily distinguished anatomically from one another. We conclude that each should be recognized as a distinct species.

The “Zambales Low” clade (Fig. 7) is made up of individuals from two sampling regions: Mt. Tapulao in the Zambales Mountains and Mt. Natib in Bataan Province. The two populations form reciprocally monophyletic groups, but the subtending branches are very short. The PCA results and anatomical comparisons of specimens from these areas (described below) show no clear evidence of differences, and we note that these two mountains are at nearly opposite ends of a mountain chain that runs 150 km with only a few narrow lowland gaps (Fig. 3). We predict that individuals collected in intervening areas will show evidence of low-level isolation by distance, consistent with recognition of the single species that we describe here as *A. zambalensis* sp. nov.

The remaining clade consists of individuals from a broad portion of the Sierra Madre and Caraballo Mountains in northeastern Luzon, including Cagayan, Quirino, and Nueva Viscaya provinces and the small offshore island of Palau. They are separated by a long, well-supported branch (99% bp, 1.00 pp) from any other clade. However, within this clade, little if any geographic structure is apparent: individuals from Mt. Cetaceo in Cagayan Province, from the Mungiao Mountains in Quirino Province, and from Mt. Palali in Nueva Viscaya are scattered almost randomly within the clade, and the internal branches are short. The individual from Palau Island (FMNH 191232) is slightly divergent from the others, which is not surprising for a population on a small island that has been isolated by a shallow sea-channel for about 12,000 years, and periodically during earlier Pleistocene interglacial periods. A PCA of these populations, presented below, showed no evidence of structure within this set of individuals, and we see no evidence of anatomical differences, aside from pelage (see below), among any of these populations, including the one from Palau Island. It is therefore our hypothesis that all of these individuals are members of a single species, *Apomys sierrae* sp. nov.

We note that two genetically distinct populations occur in the Mingan Mountains: two in the Zambales Mountains and two on Mt. Banahaw. In each of these cases, there is no evidence of hybridization or intermediacy in any individual, and indeed, none of the pairs consists of sister-species. *Apomys abrae* and *A. datae*, on the other hand, which are sympatric over much of the Central Cordillera, currently have ambiguous relationships discussed above and below.

### Karyotypic Variation

Karyotype data are available for nine species of *Apomys*, more than half of the 17 species currently known (including the 7 described here). The level of karyotypic variation within *Apomys* is extreme: only two species share a common karyotype (*A. abrae* and *A. datae*), whereas the remaining species have highly divergent karyotypes with diploid numbers ranging from 30 to 48 and fundamental numbers from 50 to 88 (Rickart & Musser, 1993; Rickart & Heaney, 2002). Much of this karyotypic diversity is encompassed among species belonging to the small-bodied clade as defined above.

Among the *Apomys* that have been karyotyped, four belong to the large-bodied clade (Fig. 8). *Apomys datae* (Fig. 8A) and *A. abrae* (Fig. 8B) both have karyotypes of  $2n = 44$  that are very similar, if not identical, consisting of a majority of telocentric elements, including a large telocentric X chromosome, and distinctive pairs of biarmed autosomes. *Apomys zambalensis* sp. nov. from Mt. Natib in Bataan Province also has a karyotype of  $2n = 44$  (Fig. 8C) but differs in a number of important respects from the *datae-abrae* arrangement, including a submetacentric X chromosome. The karyotype of *A. banahaw* sp. nov., from the high elevations on Mt. Banahaw in Quezon Province, has  $2n = 48$  (Fig. 8D), but otherwise is most similar to that of *A. zambalensis* sp. nov. Each of these karyotypes of large-bodied *Apomys* is similar to a common karyotype of  $2n = 44$  seen in species belonging to the other genera of “earthworm-mice,” *Archboldomys*, *Chrotomys*, and *Rhynchomys* (Rickart & Musser, 1993; Rickart & Heaney, 2002; E. A. Rickart, unpubl. data).

Patterns of karyotype diversity within *Apomys* and related genera suggest that the large-bodied species are more conservative, with arrangements that resemble the presumed ancestral karyotype, whereas members of the small-bodied clade have more highly derived karyotypes. Clearly, diversification within *Apomys* has often been accompanied by major chromosomal evolution.

## The Subgenera and Species of Large-Bodied *Apomys*

To recognize the fundamental morphological, genetic, and ecological dichotomy within *Apomys*, we recognize two subgenera within the genus. The subgenus *Apomys* includes the small-bodied species, as listed below, retaining *A. hylocoetes* Mearns 1905 as the type species. For the large-bodied species, we propose the new subgenus *Apomys* (*Megapomys*).

### *Apomys* (*Megapomys*) New Subgenus

TYPE SPECIES—*Mus datae* Meyer, 1899 (= *Apomys datae sensu* Ellerman, 1941, and others).

ETYMOLOGY—From the Greek “megas,” meaning large or great; “apo,” from Mt. Apo, the highest mountain in the Philippines, and meaning “grandfather” in local languages; and the Greek “mys,” meaning mouse. The gender is masculine.

INCLUDED SPECIES—The previously described *A. abrae* (Sanborn, 1952), *A. datae* (Meyer, 1899), *A. gracilirostris* Ruedas, 1995, and *A. sacobianus* Johnson, 1962, and the seven new species described below: *A. aurorae*, *A. banahaw*, *A. brownorum*, *A. magnus*, *A. minganensis*, *A. sierrae*, and *A. zambalensis*.

DIAGNOSIS—The subgenus *Megapomys* is defined phylogenetically as the most recent common ancestor of *A. gracilirostris*, *A. datae*, and *A. zambalensis* and all of its descendants (Fig. 7), and by the following combination of morphological characters (contrasted with the subgenus *Apomys*): size large, averaging 66–109 g (vs. 18–41 g in *A. (Apomys)*); average tail length ranging from 84% to 110% of the length of head and body (vs. 120–140%); hind foot typically relatively broader and wider (vs. longer and narrower; see Heaney & Tabaranza, 2006); braincase more

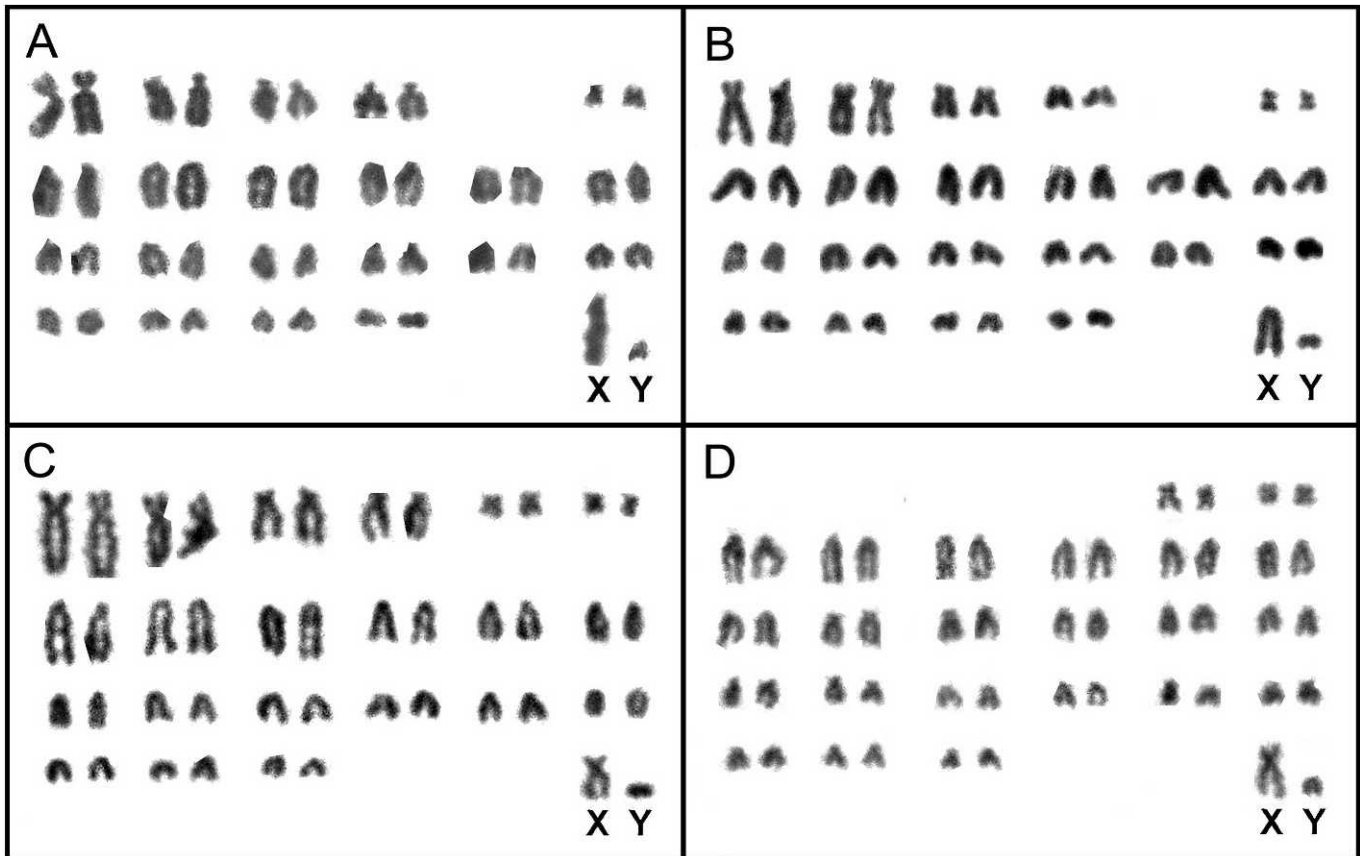


FIG. 8. Male karyotypes of four species of the subgenus *Megapomys* from Luzon. (A) *Apomys datae*, Mt. Amuyao, Mountain Province (FMNH 193662). (B) *Apomys abrae*, Balbalasang, Kalinga Province (FMNH 169051). (C) *Apomys zambalensis* sp. nov., Mt. Natib, Bataan Province (FMNH 183368). (D) *Apomys banahao* sp. nov., Mt. Banahaw, Quezon Province (FMNH 178468).

robust, less globose (vs. more delicate and globose; Fig. 4); rostrum proportionately broader and heavier, except in *A. (M.) gracilirostris* (vs. thinner and more gracile); upper incisors deeper in anteroposterior axis, except in *A. (M.) gracilirostris* (vs. narrower); posterior bony palate more heavily pitted and fenestrated (vs. less pitted and fenestrated); incisive foramina proportionately broader (vs. broad, but less so); and zygomatic arches more robust (vs. more gracile). Some of these characters are associated with *Megapomys*, being a clade of larger, more ground-living species, compared with the smaller and more arboreal subgenus *Apomys*. These two ecomorphological lineages are clearly evident in the mitochondrial DNA-based analysis (Fig. 7).

The genus *Apomys* has *A. hylocoetes* as its type species, and thus the nominotypical subgenus necessarily does as well. This subgenus contains the following recognized species: *A. camiguinensis*, *A. hylocoetes*, *A. insignis*, *A. littoralis*, *A. microdon*, and *A. musculus*, plus several as yet undescribed species listed by Heaney et al. (1998) on the basis of the cyt *b* phylogenies presented by Steppan et al. (2003) and in Figure 7. These species are widespread in the Philippines, with the exception of the Palawan and Babuyan/Batanes groups of islands and the Sulu Archipelago. On Luzon, *A. microdon* and *A. musculus* often occur sympatrically with members of the subgenus *Megapomys* (e.g., Heaney et al., 1998; Balete et al., 2009; Rickart et al., 2011).

Because the morphometrically distinctive populations of *Megapomys* are concordant with mitochondrial clades (except *A. abrae* and *A. datae*, as discussed) and with units defined on

the basis of qualitative external and craniodental traits (as discussed below), we recognize each of them as a distinct species in the following pages. In the diagnoses and comparisons that follow, we emphasize differences that separate species from their sister-taxa and from the geographically closest species of *Megapomys*.

#### *Apomys datae* (Meyer, 1899)

*Mus datae* Meyer, 1899: 52.

*Apomys major* Miller, 1910: 402. Musser 1982: 73, synonym of *A. datae*.

*Apomys datae*. Ellerman, 1941: 225. First use of current name combination.

HOLOTYPE—Staatliches Museum für Tierkunde, Dresden B3100 obtained in 1892 by John Whitehead. Prepared as stuffed skin plus skull.

TYPE LOCALITY—"Monte Data, Lepanto [Province], North Luzon, Philippines" (= Mt. Data, currently in Mountain Province; see Musser, 1982).

SPECIMENS EXAMINED (n = 882)—LUZON ISLAND: Benguet Prov.: Haight's-in-the-Oaks, 7000 ft [ca. 2100 m] (USNM 151513); Mt. Pulag National Park, 0.5 km S, 0.4 km W Mt. Babadak peak, 2480 m (FMNH 198620–198632, 198638, 198639, 198643–198653, 198662–198665, 198669–198672, 198827, 198828, 198831–198833, 198835–198840); Mt. Pulag National Park, 0.7 km S, 0.4 km W Mt. Babadak peak, 2445 m (FMNH 198536, 198583–198604, 198611–198615); Mt. Pulag National Park, 0.8 km S, 0.4 km W Mt. Babadak peak, 2420 m (FMNH 198579–198582, 198640, 198641, 198654, 198673, 198811–198819, 198834); Mt. Pulag National Park, 0.8 km S, 0.9 km





FIG. 9. Dorsal (A), ventral (B), and lateral (D) views of the cranium and lateral view of the mandible (C) of *Apomys datae* (FMNH 188445; adult female from Mt. Data); scale bar = 5 mm.

W Mt. Babadak peak, 2285 m (FMNH 198616, 198617, 198633–198637, 198642, 198655–198659, 198667, 198668, 198674–198676, 198825, 198826, 198830); Mt. Pulag National Park, 0.9 km S, 0.9 km W Mt. Babadak peak, 2335 m (FMNH 198605–198610, 198618, 198619, 198660, 198661, 198666, 198677, 198820–198824, 198829); Mt. Pulag National Park, 0.5 km S, 0.7 km E Mt. Pulag peak, 2800 m (FMNH 198539–198543, 198549, 198798, 198801); Mt. Pulag National Park, 0.6 km S, 0.65 km E Mt. Pulag peak, 2730 m (FMNH 198550–198555, 198565–198568, 198570, 198571, 198804–198807); Mt. Pulag National Park, 1.15 km S, 1.35 km E Mt. Pulag peak, 2695 m (FMNH 198556–198564, 198572–198578, 198802, 198803, 198808–198810, 202538); Mt. Pulag National Park, 1.2 km S, 1.15 km E Mt. Pulag peak, 2780 m (FMNH 198544, 198545, 198548, 198799, 198800); Mt. Pulag National Park, 1.35 km S, 0.8 km E Mt. Pulag peak, 2740 m (FMNH 198537, 198538, 198546, 198547, 198569); Mt. Pulag National Park, 1.75 km S, 0.9 km E Mt. Pulag peak, 2650 m (FMNH 198678–198707, 198841–198852).

Ifugao Prov.: Kiangnan Munic.: Brgy. Duwit (=Brgy. Duit), 4000 ft [ca. 1200 m] (USNM 557717). Ilocos Norte Prov.: Tagudin (AMNH 252474–252475).

Kalinga Prov.: Balbalan Munic.: Balbalasang Brgy.: Am-licao, 1800 m (FMNH 169071–169121, 170931–170964, 170982); Balbalan Munic.: Balbalasang Brgy.: Magdallao, 1600 m (FMNH 167243, 167244, 167246–167253, 167255–167257, 167260, 167263–167272, 167278–167284, 167288–167291, 167293, 167295–167298, 167302, 167329–167341, 167345, 167348, 167350–167354, 167357, 167359, 167360, 167362–167366); Balbalasang Brgy.: Mt. Bali-it, 1950 m (FMNH 175415–175498, 175630–175681, 175732); Balbalan Munic.: Balbalasang Brgy.: Mt. Bali-it, 2150 m (FMNH 175499–175546, 175682–175717, 175733).

Mountain Prov. (no specific locality; FMNH 62761, 62762); 0.6 km N Barlig Munic. Hall, 1800 m (FMNH 193548, 193549, 193877); 0.4 km N, 0.4 km W Mt. Amuyao peak, 2480 m (FMNH 193599–193614, 193884–193886); 0.5 km N, 0.5 km W Mt. Amuyao peak, 2530 m (FMNH 193550–193559, 193878–193883); 0.75 km W Mt. Amuyao peak, 2300 m (FMNH 193615–193636, 193910–193919); 1.0 km N, 1.0 km W Mt. Amuyao peak, 2150 m (FMNH 193637–193659, 193920–193931); 1.25 km N, 0.5 km W Mt. Amuyao peak, 1990 m (FMNH

193660–193662); 1.75 km N, 0.4 km W Mt. Amuyao peak, 1885 m (FMNH 193932–193940, 193663–193675); 1.75 km N, 1.5 km W Mt. Amuyao peak, 1950 m (FMNH 193676–193680); Mt. Amuyao peak, 2690 m (FMNH 193560–193598, 193887–193909); Mt. Data (FMNH 62697, 62698, 62701–62705, 62707, 62708, 62710, 62713–62718, 62721, 62722, 62729, 62730, 62732, 62735–62737, 62742, 62745–62747); Mt. Data, 5300 ft [ca. 1600 m] (FMNH 62731); Mt. Data, 7500 ft [ca. 2300 m] (FMNH 62695–62696, 62699, 62720, 62725); Mt. Data, 8000 ft [ca. 2400 m] (FMNH 62727, 62733–62734, 62741, 62744); Mt. Data, 8200 ft [ca. 2500 m] (FMNH 62706, 62709, 62711); Mt. Data, 8300 ft [ca. 2500 m] (FMNH 62712); Mt. Data, Cotcot (FMNH 62743, 62748); 0.1 km E south peak Mt. Data, 2310 m (FMNH 188298–188306, 188310–188312, 188438–188445); 0.75 km N, 0.6 km E south peak Mt. Data, 2241 m (FMNH 188245–188277, 188425–188427, 188429–188436, 188493); 0.75 km N, 0.75 km E south peak Mt. Data, 2289 m (FMNH 188287–188291, 188448); 0.75 km N, 1.0 km E south peak Mt. Data, 2289 m (FMNH 188278–188286, 188307–188309, 188446, 188447).

EMENDED DIAGNOSIS AND DESCRIPTION—A large mouse (HBL averaging 137–144 mm, BOL averaging 34–36 mm in populations summarized in Table 2), with a tail that averages shorter than the length of head and body (89–95%; Table 2; Figs. 1B, 9). The fur is dense, soft, and dark brown with a slight rusty-orange tint dorsally. The ventral fur is either white at the tips, or with a pale ochraceous wash, and dark gray at the base. The fur on the dorsal surface of the forepaws and hind feet is white on the distal half, with dark fur extending over approximately the basal half. The tail is darker dorsally than ventrally, often with a sharp line demarcating the upper and lower halves, but some scattered black hairs are often present on the ventral surface of the tail. The skin of the lips and lower rhinarium is darkly pigmented, as is the inside surface of the base of the pinna. The hind feet are of moderate length, with fairly large and well-separated pads, and usually

are darkly pigmented over the proximal half to two-thirds of the ventral surface. The plantar pads are large, and the toes are slightly short and stocky (Fig. 10B). The cranium is relatively large and robust, with a deep, squarish braincase and a long, stout rostrum that is associated with a long diastema. The interparietal bone is of variable shape, but usually moderately wide (anteroposteriorly) and roughly oval in shape. The maxillary toothrow is moderately short, the palate is narrow, and the toothrows diverge slightly posteriorly (Fig. 9B; Table 2). The postpalatal region is of moderate length. The stapedia artery enters each bulla through a distinct foramen between the bullar capsule and the petrosal portion of the petromastoid bone (the “datae pattern”; Fig. 5B). The mandible is robust and deep. The coronoid process is slender, sharply pointed, and moderately long; the angular process is sturdy, with the posterior margin of the mandible sweeping down in a shallow arc from the condylar process (Fig. 9C).

On the basis of two males from Mt. Amuyao, Mountain Province (FMNH 193558, 193662), and one from Mt. Bali-it, Kalinga Province (FMNH 169111), the karyotype of *A. datae* has  $2n = 44$  and  $FN \geq 54$  (Fig. 8A). The available preparations are of marginal quality, but the karyotype appears to be very similar to that of *A. abrae* (described below in greater detail).

To assess geographic variation, we conducted a PCA of 18 craniodental measurements in Table 2 from the four populations of *A. datae* from which we have adequate samples: Mt. Pulag (Benguet Province), Mt. Data and Mt. Amuyao (Mountain Province), and Mt. Bali-it and vicinity (Kalinga Province); these represent populations from the southern, central, and northern portions of the species’ range. The first principal component (PC1), which accounted for 36% of the variation, had moderate to high positive loadings for all variables, with the exception of length of incisive foramen, which has a loading barely above zero (Table 4); this component appears to represent overall size. The second component (PC2), which accounted for 11% of the variation, had high positive loadings on length of incisive foramen and diastema and labial breadth at  $M^3$  and high negative loadings on length of the molar toothrow, braincase height, and breadth of  $M^1$ . The next two components had eigenvalues of 1.2 or less. Individuals from all four areas overlapped extensively on the first two PCs, with no evident geographic pattern (Fig. 11). Given this lack of quantitative craniodental differences, and the consistent qualitative cranial and external morphology, we regard all of the specimens included in Specimens Examined as being examples of a single species.

COMPARISONS—Relative to most other *Megapomys*, the cranium of *A. datae* is large and robust, with a deep, squarish braincase, a long, stout rostrum, and a long diastema. As detailed below, relative to some other species, the maxillary toothrow is short, the palate is narrow, and the postpalatal region is of moderate length (Fig. 9; Table 2). In *A. datae*, the stapedia artery enters each bulla through a distinct foramen between the bullar capsule and the petrosal portion of the petromastoid bone (the “datae pattern”; Fig. 5B), as discussed above under Carotid Circulatory Patterns.

Compared with *A. abrae*, the tail is short relative to the length of head and body, averaging 89–95% (97–101% of HBL in *A. abrae*; Table 2). A plot of weight and relative length of the tail (Fig. 12A) shows overlap, but most individuals are outside of the area of overlap. The dorsal pelage of *A. abrae* (Fig. 1C) typically is a rich, dark brown, whereas that of *A.*

*datae* is equally dark, but has a rusty, slightly orange tinge (Fig. 1B); although, as noted below, some specimens of *A. abrae* are much paler. *Apomys abrae* rarely have any black hairs on the ventral surface of the tail, whereas scattered black hairs are often present on *A. datae*, and the scales are usually pale gray, not white as in *A. abrae*. The fur on the dorsal surface of the forepaws and hind feet of *A. abrae* is white or with very few scattered dark hairs (vs. having dark hairs extending over much of the tops of the feet). The hind feet of *A. abrae* (Fig. 10A) are paler, slightly shorter on average, and proportionately narrower, than those of *A. datae* (Table 2). Additionally, the toes are slightly longer, and the plantar pads are smaller and more widely separated than those of *A. datae* (Fig. 10B).

The cranium of *A. datae* is larger than that of *A. abrae* in nearly every dimension, with little overlap in zygomatic breadth, mastoid breadth, nasal length, rostral depth, rostral length, width of the zygomatic plate, and postpalatal length (Table 2). For example, plots of zygomatic breadth and mastoid breadth (Fig. 12B) and rostral length and rostral depth (Fig. 12C) show very little overlap, and serve to easily distinguish most individuals. The interparietal bone is variable in both species but is usually anteroposteriorly wider in *A. datae* than in *A. abrae*. Relative to *A. datae*, the mandible of *A. abrae* is shorter and less deep, with a shorter coronoid process, less robust angular process, and more concave posterior margin between the condylar and coronoid processes.

A PCA of individuals that we refer to *A. datae* and *A. abrae* using 18 craniodental measurements (Tables 2, 3) showed significant and interpretable variation on two components (Fig. 13; Table 5). The first component loaded heavily on nearly all measurements (Table 5) and accounted for 51% of the total variation; only length of incisive foramen had a low loading. This axis was thus an overall measure of size and robustness. The second component loaded heavily and positively on length of incisive foramen and diastema length and negatively on length of the molar toothrow, palatal breadth at  $M^1$ , and breadth of  $M^1$ . A plot of these two components (Fig. 13) showed that specimens with qualitative features associated with *A. abrae* scored low on PC1, and *A. datae* scored high; this is consistent with our observation regarding relative size and robustness of these two species, with some overlap that we suspect is associated with age-related variation in size. PC2 had great overlap, such that it does not assist in distinguishing between these species. Taking all of the available data together, it appears that the differences in carotid artery circulatory patterns, pelage coloration, and overall size are the best means to distinguish between these two species.

DISTRIBUTION—*Apomys datae* occurs widely in the high mountains of the Central Cordillera of northern Luzon Island. Verified records are from Benguet, Ifugao, Kalinga, and Mountain provinces, from 1500 to 2800 m in elevation (Figs. 3, 14). This species overlaps broadly with *A. abrae*, but *A. datae* usually occurs in more mature forests, in moister habitats, and at higher elevations, although they occur syntopically in some places (Rickart et al., 2011; Fig. 15). Surveys are needed to determine the distribution of this species in the northernmost Central Cordillera, in Abra, Apayao, and Ilocos Norte provinces, and in the southeastern Central Cordillera where this range abuts with the Caraballo Mountains, which support *A. sierrae* sp. nov.

TABLE 2. Cranial and external measurements (mean  $\pm$  1 S.D. and range) of *Apomys datae* and *A. abrae* (part).

Measurement	<i>Apomys datae</i>					
	Mt. Data, Mountain Prov.		Balbalasang, 1900–2150 m, Kalinga Prov.		Mt. Amuyao, Mountain Prov.	
	M (n = 10)	F (n = 10)	M (n = 10)	F (n = 10)	M (n = 10)	F (n = 10)
Basioccipital length	35.51 $\pm$ 0.75 34.14–36.77	34.82 $\pm$ 0.62 34.06–35.90	34.75 $\pm$ 0.72 33.65–35.82	33.94 $\pm$ 0.55 33.24–34.76	35.02 $\pm$ 0.92 33.58–36.58	35.07 $\pm$ 0.47 34.46–35.64
Interorbital breadth	6.14 $\pm$ 0.28 5.60–6.50	6.07 $\pm$ 0.36 5.29–6.50	5.79 $\pm$ 0.35 5.20–6.58	5.89 $\pm$ 0.23 5.42–6.21	6.21 $\pm$ 0.26 5.91–6.71	6.21 $\pm$ 0.18 5.90–6.52
Zygomatic breadth	18.55 $\pm$ 0.40 17.85–18.99	18.60 $\pm$ 0.27 18.09–19.15	18.34 $\pm$ 0.41 (9) 17.90–18.98	18.19 $\pm$ 0.23 (9) 17.87–18.63	18.15 $\pm$ 0.39 (9) 17.60–18.84	18.16 $\pm$ 0.40 17.64–18.73
Mastoid breadth	14.68 $\pm$ 0.36 14.23–15.48	14.53 $\pm$ 0.35 13.86–14.94	14.08 $\pm$ 0.30 13.53–14.49	13.99 $\pm$ 0.31 13.39–14.46	14.34 $\pm$ 0.25 13.85–14.66	14.34 $\pm$ 0.21 14.11–14.72
Nasal length	15.15 $\pm$ 0.50 14.14–15.85	14.61 $\pm$ 0.54 13.89–15.42	14.07 $\pm$ 0.32 13.61–14.64	13.76 $\pm$ 0.24 13.38–14.23	14.66 $\pm$ 0.49 14.03–15.52	14.90 $\pm$ 0.45 14.42–15.91
Incisive foramen length	4.94 $\pm$ 0.27 4.58–5.29	4.77 $\pm$ 0.20 4.48–5.13	5.37 $\pm$ 0.17 5.14–5.78	5.28 $\pm$ 0.38 4.75–5.87	5.15 $\pm$ 0.32 4.58–5.57	5.20 $\pm$ 0.26 4.86–5.65
Rostral depth	7.73 $\pm$ 0.30 7.14–8.21	7.70 $\pm$ 0.22 7.43–8.02	7.42 $\pm$ 0.24 7.17–7.91	7.38 $\pm$ 0.16 7.16–7.66	7.49 $\pm$ 0.17 7.26–7.73	7.45 $\pm$ 0.17 7.20–7.69
Rostral length	16.43 $\pm$ 0.50 15.51–17.02	16.15 $\pm$ 0.40 15.71–17.09	15.58 $\pm$ 0.32 15.21–16.16	15.14 $\pm$ 0.37 14.61–15.89	16.01 $\pm$ 0.62 15.16–17.09	15.97 $\pm$ 0.21 15.71–16.36
Orbitotemporal length	11.64 $\pm$ 0.27 11.21–11.98	11.68 $\pm$ 0.39 11.28–12.60	11.69 $\pm$ 0.32 11.23–12.30	11.72 $\pm$ 0.34 11.07–12.08	11.31 $\pm$ 0.37 10.85–11.84	11.57 $\pm$ 0.20 11.31–11.91
Maxillary tooth-row length	7.06 $\pm$ 0.23 6.82–7.53	7.09 $\pm$ 0.16 6.89–7.34	6.93 $\pm$ 0.23 6.49–7.25	6.78 $\pm$ 0.26 6.48–7.26	6.80 $\pm$ 0.19 6.53–7.18	6.86 $\pm$ 0.18 6.65–7.21
Labial palatal breadth at M <sup>1</sup>	7.31 $\pm$ 0.21 7.07–7.70	7.37 $\pm$ 0.14 7.22–7.70	7.22 $\pm$ 0.16 6.92–7.51	7.17 $\pm$ 0.26 6.77–7.50	7.34 $\pm$ 0.26 6.96–7.81	7.28 $\pm$ 0.22 6.91–7.62
Diastema length	9.45 $\pm$ 0.33 9.11–10.06	9.22 $\pm$ 0.25 8.89–9.71	9.13 $\pm$ 0.23 8.76–9.52	9.18 $\pm$ 0.23 8.80–9.59	9.38 $\pm$ 0.40 8.95–10.21	9.52 $\pm$ 0.27 9.10–9.89
Postpalatal length	12.11 $\pm$ 0.32 11.72–12.61	11.89 $\pm$ 0.38 11.28–12.36	11.81 $\pm$ 0.53 11.09–12.60	11.34 $\pm$ 0.36 10.87–12.07	11.64 $\pm$ 0.19 11.38–12.00	11.83 $\pm$ 0.27 11.46–12.29
Lingual palatal breadth at M <sup>3</sup>	5.03 $\pm$ 0.23 4.57–5.38	5.08 $\pm$ 0.28 4.59–5.47	4.95 $\pm$ 0.22 4.60–5.30	4.97 $\pm$ 0.22 4.66–5.42	5.02 $\pm$ 0.15 4.79–5.28	5.13 $\pm$ 0.18 4.88–5.44
Braincase height	11.42 $\pm$ 0.32 11.00–11.96	11.45 $\pm$ 0.34 10.58–11.81	10.92 $\pm$ 0.44 10.23–11.58	10.80 $\pm$ 0.28 10.28–11.30	10.55 $\pm$ 0.40 9.77–11.02	10.81 $\pm$ 0.30 10.40–11.22
Breadth of M <sup>1</sup>	1.87 $\pm$ 0.05 1.81–1.95	1.90 $\pm$ 0.06 1.84–2.03	1.82 $\pm$ 0.07 1.69–1.92	1.81 $\pm$ 0.08 1.70–1.93	1.83 $\pm$ 0.07 1.74–2.01	1.83 $\pm$ 0.09 1.71–1.95
Breadth of incisors at tip	2.32 $\pm$ 0.11 2.13–2.48	2.24 $\pm$ 0.09 2.08–2.37	2.26 $\pm$ 0.14 2.02–2.43	2.23 $\pm$ 0.07 2.12–2.32	2.17 $\pm$ 0.10 2.01–2.30	2.21 $\pm$ 0.08 2.13–2.40
Width of zygomatic plate	3.55 $\pm$ 0.17 3.20–3.74	3.43 $\pm$ 0.22 3.12–3.78	3.53 $\pm$ 0.14 3.37–3.82	3.55 $\pm$ 0.20 3.22–3.88	3.41 $\pm$ 0.16 3.12–3.59	3.55 $\pm$ 0.26 3.28–3.96
Length of head and body	144.7 $\pm$ 6.9 130–154	141.0 $\pm$ 6.0 (9) 129–149	139.4 $\pm$ 2.9 (8) 134–142	137.8 $\pm$ 4.9 (8) 133–149	138.7 $\pm$ 7.2 127–151	139.9 $\pm$ 5.2 132–147
Total length	279.5 $\pm$ 7.6 260–287	273.3 $\pm$ 8.0 (9) 257–286	269.4 $\pm$ 5.6 (8) 261–277	261.3 $\pm$ 6.9 (8) 256–276	268.9 $\pm$ 14.3 250–292	271.5 $\pm$ 5.3 262–278
Length of tail vertebrae	134.8 $\pm$ 4.6 126–141	132.1 $\pm$ 3.6 128–139	130.0 $\pm$ 3.9 (8) 125–136	123.5 $\pm$ 2.8 (8) 121–127	130.2 $\pm$ 7.9 121–141	131.6 $\pm$ 4.2 128–142
Length of hind foot	37.3 $\pm$ 0.9 36–38	36.2 $\pm$ 1.5 33–38	35.5 $\pm$ 0.7 34–36	34.5 $\pm$ 0.7 33–35	37.0 $\pm$ 1.1 35–38	35.8 $\pm$ 1.3 34–38
Length of ear	21.0 $\pm$ 0.7 20–22	20.3 $\pm$ 0.9 18–21	21.1 $\pm$ 0.7 20–22	20.7 $\pm$ 1.1 19–22	20.6 $\pm$ 0.5 20–21	20.5 $\pm$ 0.7 20–22
Weight (g)	91.6 $\pm$ 7.0 78–102	81.8 $\pm$ 9.8 (9) 70–97	72.2 $\pm$ 4.6 66–79	70.7 $\pm$ 5.9 63–82	77.5 $\pm$ 6.4 68–88	79.2 $\pm$ 10.2 65–90

COMMENTS—Because this species was the best known of the Luzon *Megapomys* for many years, the few scattered specimens from other parts of Luzon were often tentatively, but incorrectly, referred to this species in collections and in some publications (e.g., Danielsen et al., 1994; Heaney et al., 1998). We have examined the holotype of *A. major* Miller 1910, and agree with Musser (1982) that it is not distinguishable from *A. datae* and should be treated as a junior synonym.

#### *Apomys abrae* (Sanborn, 1952)

*Rattus (Apomys) abrae* Sanborn, 1952: 133.

*Apomys abrae*. Johnson 1962. First use of current name combination.

HOLOTYPE—FMNH 62750, young adult male, obtained 14 May 1946. Field number H. H. Hoogstraal 460. Prepared as stuffed skin plus skull. Measurements in Table 2.

TYPE LOCALITY—Philippines: Luzon Island: Abra Province: Massisiat, 3500 feet [ca. 1100 m] (approximately 17.583°N, 120.833°E; our estimate from topographic maps). Taken in “thick growth along mountain creek” (from specimen tag).

SPECIMENS EXAMINED (n = 183)—LUZON ISLAND: Abra Prov.: Massisiat, 3500 ft [ca. 1100 m] (FMNH 62749; 62750).

Benguet Prov.: Baguio (USNM 151510, 399580); Baguio, 3000 ft [ca. 900 m] (USNM 399573–399577); Baguio, 3600 ft [ca. 1100 m] (USNM 399579); Baguio, 4000 ft [ca. 1200 m] (USNM 399578); Haight’s-in-the-Oaks, 7000 ft [ca. 2100 m] (USNM 151507–151509, 151530, 261170); near Baguio (MCZ 35034, 35035); near Baguio, Mt. Santo Tomas (AMNH 242099, 242100; FMNH 202181); Sablan (FMNH 92763, 92764).



TABLE 2. *Extended.*

<i>Apomys datae</i>		<i>Apomys abrae</i>					
Mt. Pulag, Benguet Prov.		Massiasiat, Abra Prov.		Mt. Data, Mountain Prov.		Balbalasang, 900 m, Kalinga Prov.	
M (n = 10)	F (n = 10)	M-holotype FMNH 62750		M (n = 2)	F (n = 4)	M (n = 1)	F (n = 1)
35.68 ± 0.61	35.19 ± 0.91	31.09	31.70	32.64 ± 0.90	32.40 ± 0.44	32.39	32.55
34.65–36.59	33.90–37.04	—	—	32.00–33.27	31.80–32.74	—	—
6.23 ± 0.28	6.00 ± 0.22	5.50	—	5.83 ± 0.25	5.69 ± 0.19	6.09	5.50
5.80–6.74	5.73–6.31	—	—	5.65–6.00	5.54–5.96	—	—
18.57 ± 0.47	18.45 ± 0.51	—	—	17.42 (1)	17.02 ± 0.30 (3)	16.74	16.81
18.12–19.50	17.68–19.47	—	—	—	16.84–17.37	—	—
14.69 ± 0.41	14.53 ± 0.27	—	—	13.73 ± 0.88	13.89 ± 0.35	13.29	13.50
14.20–15.42	14.11–14.92	—	—	13.10–14.35	13.52–14.35	—	—
14.75 ± 0.45	14.84 ± 0.58	12.59	13.03	13.39 ± 0.22	13.67 ± 0.40	14.05	13.64
14.21–15.65	13.54–15.41	—	—	13.23–13.54	13.26–14.11	—	—
5.26 ± 0.19	5.47 ± 0.22	4.60	4.75	5.07 ± 0.04	5.07 ± 0.21	5.09	4.79
4.95–5.51	5.18–5.96	—	—	5.04–5.10	4.88–5.36	—	—
7.63 ± 0.26	7.46 ± 0.38	6.39	6.55	7.09 ± 0.27	6.92 ± 0.21	6.82	7.05
7.38–8.23	6.89–7.95	—	—	6.90–7.28	6.67–7.18	—	—
16.59 ± 0.45	16.24 ± 0.60	13.62	14.17	15.20 ± 0.12	14.60 ± 0.56	14.93	14.66
15.93–17.38	15.40–17.19	—	—	15.11–15.28	14.10–15.19	—	—
11.64 ± 0.32	11.62 ± 0.36	10.84	—	10.75 ± 0.77	11.13 ± 0.20	11.00	11.26
11.01–12.14	10.99–12.00	—	—	10.20–11.29	10.86–11.30	—	—
7.09 ± 0.25	7.10 ± 0.28	6.69	6.62	6.68 ± 0.11	6.94 ± 0.08	6.54	7.09
6.71–7.46	6.48–7.57	—	—	6.60–6.75	6.85–7.01	—	—
7.49 ± 0.29	7.41 ± 0.27	6.75	—	6.97 ± 0.04	7.18 ± 0.12	7.13	7.14
7.00–7.93	7.10–7.93	—	—	6.94–7.00	7.08–7.33	—	—
9.72 ± 0.32	9.51 ± 0.30	7.79	8.62	8.68 ± 0.61	8.48 ± 0.19	8.83	8.33
9.30–10.28	9.05–9.94	—	—	8.25–9.11	8.31–8.75	—	—
11.86 ± 0.29	11.72 ± 0.44	10.62	—	11.36 ± 0.34	10.99 ± 0.15	11.77	11.68
11.54–12.28	11.10–12.37	—	—	11.12–11.60	10.83–11.18	—	—
5.23 ± 0.29	5.00 ± 0.26	4.23	—	4.82 ± 0.45	4.82 ± 0.34	4.67	4.96
4.72–5.65	4.57–5.44	—	—	4.50–5.13	4.44–5.14	—	—
11.13 ± 0.42	11.14 ± 0.37	10.43	—	10.03 ± 0.69	10.63 ± 0.43	10.47	10.57
10.57–11.95	10.55–11.66	—	—	9.54–10.52	10.09–11.03	—	—
1.92 ± 0.13	1.88 ± 0.09	1.93	1.78	1.71 ± 0.14	1.80 ± 0.03	1.83	1.81
1.71–2.13	1.74–2.03	—	—	1.61–1.81	1.77–1.83	—	—
2.24 ± 0.08	2.29 ± 0.13	2.06	2.09	1.99 ± 0.04	2.01 ± 0.05	2.08	2.05
2.08–2.40	2.08–2.50	—	—	1.96–2.01	1.95–2.05	—	—
3.63 ± 0.22	3.56 ± 0.24	3.01	3.15	3.10 ± 0.07	3.17 ± 0.21	3.13	3.22
3.22–3.94	3.16–3.92	—	—	3.05–3.15	2.90–3.36	—	—
143.8 ± 6.7	139.7 ± 7.4	125	139	136 (1)	133.0 ± 3.6 (3)	—	—
131–155	132–153	—	—	—	129–136	—	—
273.9 ± 9.2	268.5 ± 11.1	255	278	271 (1)	267.7 ± 5.9 (3)	—	—
261–292	255–287	—	—	—	261–272	—	—
130.1 ± 4.0	128.8 ± 6.3	130	139	135 (1)	134.7 ± 3.1 (3)	137	129
122–137	121–136	—	—	—	132–138	—	—
36.8 ± 1.0 (9)	35.9 ± 1.3	34	35	36 (1)	35.0 ± 0.0 (3)	35	35
35–38	35–39	—	—	—	35	—	—
22.1 ± 0.6	21.1 ± 1.0	—	—	21 (1)	20.7 ± 0.6 (3)	21	21
21–23	20–22	—	—	—	20–21	—	—
87.8 ± 10.6	77.2 ± 6.2 (9)	—	—	72 (1)	68.0 ± 8.5 (2)	—	—
70–105	70–86	—	—	—	62–74	—	—

Ilocos Norte Prov.: Mt. Simminublar (FMNH 92753–92756, 92758–92760, 92762); Mt. Simminublar, 4000 ft [ca. 1200 m] (FMNH 92757); Mt. Simminublar, 4300 ft [ca. 1300 m] (FMNH 92761); Mt. Simminublar, 4350 ft [ca. 1300 m] (FMNH 92752); Tagudin (AMNH 252473).

Kalinga Prov.: Balbalan Munic.: Balbalasang Brgy.: Balbalasang, 900 m (FMNH 169182, 169183); Balbalasang Brgy.: Magdallao, 1600 m (FMNH 167245, 167254, 167258, 167259, 167261–167262, 167273–167277, 167285–167287, 167292, 167294, 167299–167301, 167303, 167342–167344, 167346, 167347, 167349, 167355, 167356, 167358, 167361, 167367); Balbalan Munic.: Balbalasang Brgy.: Mapa, 1050 m (FMNH 169021–169067, 169069, 169070, 170904–170930).

Mountain Prov.: 0.3 km N Barlig Munic. Hall, 1730 m (FMNH 193532); 0.4 km N Barlig Munic. Hall, 1790 m (FMNH 193533, 193534, 193867, 193868); 0.6 km N Barlig Munic. Hall, 1800 m (FMNH 193535–193547, 193869–193876); Mt. Data (FMNH 62738); Mt. Data, 5300 ft [ca. 1600 m] (FMNH 62719, 62728); Mt. Data, 6500 ft [ca. 2000 m] (FMNH 62700); Mt. Data, 7500 ft [ca. 2300 m] (FMNH 62723–

62724, 62726); 8000 ft [ca. 2400 m] (FMNH 62739, 62740); Mt. Data: 0.9 km N, 1.75 km E south peak, 2228 m (FMNH 188294–188297, 188483); Mt. Data: 1.0 km N, 1.25 km E south peak, 2231 m (FMNH 188292, 188293, 188437).

EMENDED DIAGNOSIS AND DESCRIPTION—A medium-sized *Megapomys*, averaging smaller than *A. datae* in nearly all measurements (Tables 2, 3). The tail is long relative to the head and body, with TV/HBL of our sampled populations averaging 97–101%. The dorsal pelage is a rich and dark brown, with little or no rusty-orange tint (Fig. 1C). The fur on the dorsal surface of the forepaws and hind feet is white or with very few scattered dark hairs (vs. having dark hairs extending over much of the tops of the feet). *Apomys abrae* rarely have any black hairs on the ventral surface of the tail,

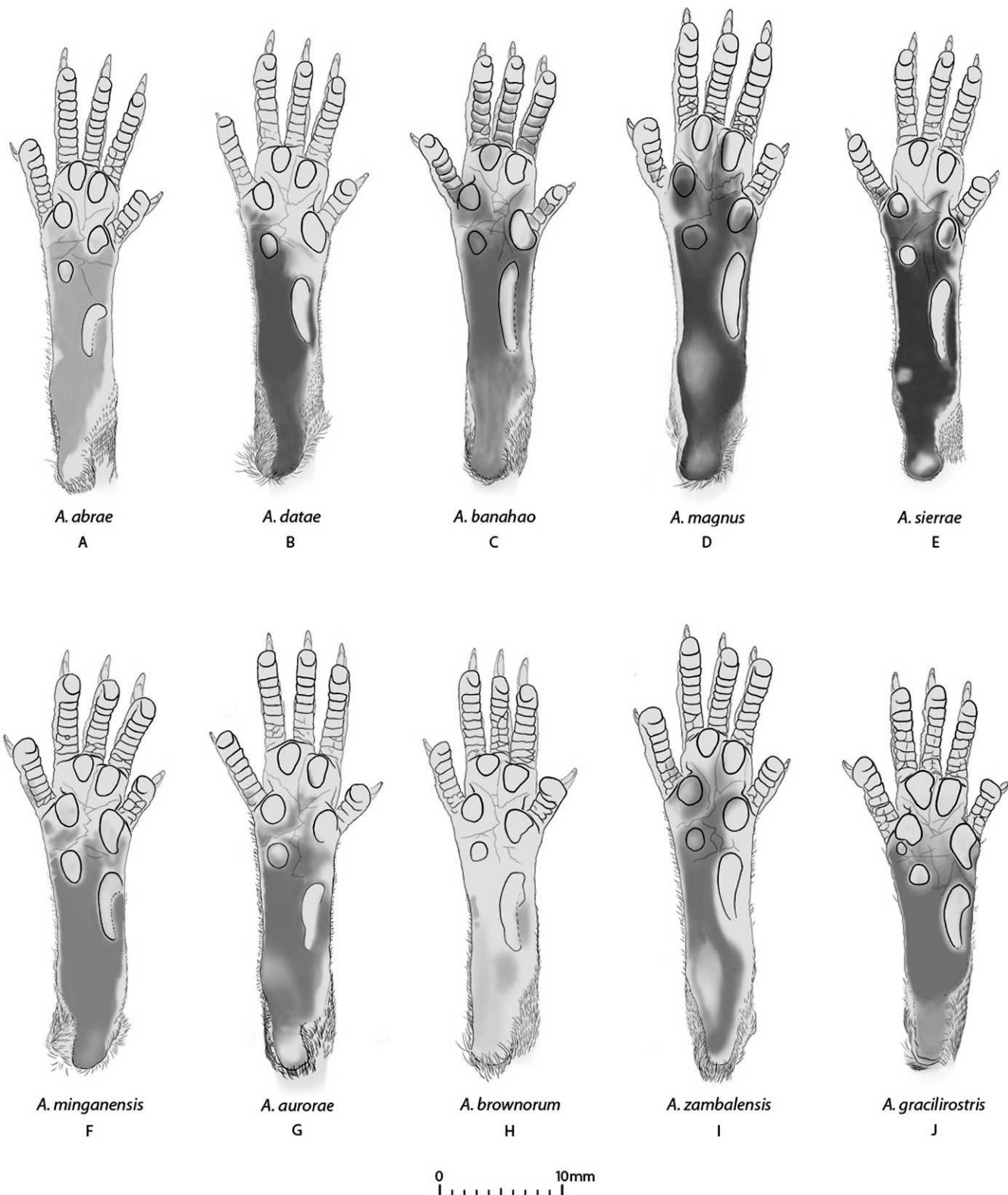


FIG. 10. Ventral surface of the right hind feet of *Apomys* subgenus *Megapomys*, all shown to the same scale.

and the scales are white (when clean). The hind feet are proportionately somewhat narrow, the toes are long, and the plantar pads are relatively small and well separated (Fig. 10A). The ventral surface of the hind foot typically has little pigment. Specimens from Abra and Ilocos Norte have dorsal pelage much paler than specimens from Benguet,

Kalinga, or Mountain province, approaching sandy-brown with orange tints. We suspect this is due to fading in these older specimens (1940s–1960s); field surveys in Abra and Ilocos Norte are needed to test this hypothesis.

The cranium of *A. abrae* (Fig. 16) is one of the smallest within *Megapomys*, with a moderately short and slender rostrum,

rounded braincase, narrow palate, short maxillary toothrow, and short postpalatal region (Tables 2, 3). Its small size is clearly apparent on the first axis of the PCA of craniodental measurements, on which *A. abrae* and *A. brownorum* sp. nov. have the lowest scores (Fig. 6A). The foramen in the bulla for the stapedia artery is lacking in *A. abrae* (Fig. 5A); that is, it has the “abrae pattern” (see Carotid Circulatory Patterns above). The interparietal bone is variable in shape, but usually oval and, anteroposteriorly, relatively narrow. The mandible (Fig. 16C) is relatively small and slender, with a relatively short coronoid process, narrow angular process, and deeply concave margin between the condylar and angular processes.

The karyotype of *A. abrae*, based on two males from Kalinga Province (FMNH 169051, 169065), has  $2n = 44$ ,  $FN \geq 54$  (Fig. 8B). The autosomal complement includes two pairs of large submetacentric, two pairs of small to medium-sized subtelocentric, one pair of very small metacentric, and 16 pairs of telocentric (or subtelocentric) chromosomes. Both the large X chromosome and the very small Y are telocentric. This karyotype was mistakenly reported earlier as representing *A. datae* (Rickart & Heaney, 2002). The two species have very similar karyotypes, although there may be minor variation in the number and size of secondary arms on some autosomes. In contrast, both *A. zambalensis* sp. nov. and *A. banahao* sp. nov. have submetacentric X chromosomes and  $FN \geq 58$ ; the former has  $2n = 44$  and the latter  $2n = 48$ .

To assess geographic variation among individuals we refer to this species, we conducted a PCA of the 18 craniodental measurements in Tables 2 and 3. This included specimens from Mt. Data (Mountain Province), from three elevations on Mt. Bali-it (Kalinga Province), and from Mt. Amuyao. Because the specimens from Abra (including the holotype) and Ilocos Norte provinces have damaged skulls, they could not be included in this analysis. The first component, which accounted for 34% of the variance, loaded heavily on most measurements, with the exception of orbitotemporal length, braincase height, and breadth of  $M^1$  (Table 6). The second component, which accounted for 15% of the variance, loaded most heavily on length of the molar toothrow, palatal breadth at  $M^1$ , diastema length, braincase height, breadth of  $M^1$ , and width of the zygomatic plate. The remaining components had eigenvalues below 2.0 and were not interpretable. A plot of individual scores on PC1 and PC2 (Fig. 17) shows a high degree of overlap among the five groups, with no evident means to distinguish among them. Because we can detect no apparent differences among the crania of any of the specimens listed above as *A. abrae*, and because the cyt *b* data (Fig. 7) show specimens from Abra and Ilocos Norte provinces to be very similar to samples from Mt. Data and Mt. Amuyao, we conclude that these represent a single species.

COMPARISONS—As noted above, *A. abrae* differs from *A. datae* in being smaller overall, usually with little or no overlap in the features measured (Tables 2, 3), but the tail is proportionately longer (in our sampled populations, averaging 97–101% vs. 89–95% in *A. datae*), and a plot of relative length of the tail and weight (Fig. 12A) shows little overlap. The dorsal fur of *A. abrae* (Fig. 1C) has little of the rusty, slightly orange tint that *A. datae* (Fig. 1B) typically possesses. The tail of *A. abrae* is white ventrally, whereas scattered black hairs are often present on *A. datae*, and the scales are pale gray, not white. The toes of *A. abrae* are relatively longer and narrower than those of *A. datae*, the plantar pads are smaller and more widely separated than in *A. datae*, and much less pigment on

the ventral surface is present than in *A. datae* (Fig. 10B). The cranium of *A. abrae* is consistently smaller than that of *A. datae*, with little overlap in zygomatic breadth, mastoid breadth, nasal length, rostral depth, rostral length, width of the zygomatic plate, and postpalatal length (Tables 2, 3). Bivariate plots of zygomatic breadth and mastoid breadth (Fig. 12B) and of rostral length and rostral depth (Fig. 12C) show the differences clearly. The interparietal bone of *A. abrae* is usually anteroposteriorly narrower than that of *A. datae*. The mandible of *A. datae* is larger and more robust, as described under that species.

Musser (1982) noted that morphological differences between *A. abrae* and *A. sacobianus* are slight in most respects and suggested that they might be conspecific. With our larger sample of *A. abrae*, it is clear that the holotype and still only known specimen of *A. sacobianus* is larger in all respects and differs in having a narrow line of dark hairs reaching to the base of the toes on the dorsal surface of the forefeet (vs. white fur only). The cranium is generally larger and more robust with a deeper and wider rostrum, but the palate is narrower. Additional details are discussed in the *A. sacobianus* species account below.

DISTRIBUTION—*Apomys abrae* occurs widely over the Central Cordillera of northern Luzon, with records from Benguet to Ilocos Norte (Figs. 3, 18). It has been recorded from 950 to 2200 m elevation (Fig. 15) in habitats ranging from mixed grass and shrubs beneath pines to dense montane rain forest. Compared with *A. datae*, with which it overlaps broadly, it often occurs at lower elevations and in relatively drier and more open habitats, including, but not restricted to, pine forest with broad-leaved undergrowth (Heaney et al., 1998, 2003; Rickart et al., 2007, 2011). Additional surveys are needed to determine its distribution at lower and middle elevations in Abra, Apayao, Ilocos Norte, and Ilocos Sur provinces in the Cordillera and at the boundary of the Central Cordillera and the Caraballo Mountains, where *A. sierrae* sp. nov. occurs.

COMMENTS—Given the conspicuous and easily recognized diagnostic features of this species, it is remarkable that the mitochondrial data (Fig. 7) fail to separate *A. abrae* and *A. datae*. We hypothesize that this is an instance of introgression because analysis of some nuclear genes reveals a subsample of individuals to be reciprocally monophyletic and not sister-species (S. J. Stepan, unpubl. data); details will be published elsewhere.

#### *Apomys gracilirostris* Ruedas, 1995

*Apomys gracilirostris* Ruedas, 1995: 305.

HOLOTYPE—NMP 3482. Adult male collected 12 June 1992. Field number NMP/CMNH 1136. Prepared as stuffed skin plus skull.

TYPE LOCALITY—Philippines: Mindoro Island: Mindoro Occidental Province: San Teodoro Munic.: North Ridge approach to Mt. Halcon, ca. 1580 m, ca. 13°16'48"N, 121°59'19"E.

SPECIMENS EXAMINED ( $n = 2$ ): MINDORO ISLAND: Mindoro Occidental Prov.: San Teodoro Munic.: North Ridge approach to Mt. Halcon (NMP 3476, 3478).

EMENDED DIAGNOSIS AND DESCRIPTION—The pelage of this species both dorsally and ventrally is dark brown, but slightly paler ventrally (Fig. 1A). The tail is proportionately longer than in other *Megapomys*, averaging about 105% of head and



TABLE 3. Cranial and external measurements (mean  $\pm$  1 S.D. and range) of *Apomys abrae*, *A. gracilirostris*, *A. sacobianus*, and *A. brownorum*.

Measurement	<i>Apomys abrae</i>					
	Balbalasang, 1100 m, Kalinga Prov.		Balbalasang, 1600 m, Kalinga Prov.		Mt. Amuyao, Mountain Prov.	
	M (n = 10)	F (n = 11)	M (n = 2)	F (n = 3)	M (n = 5)	F (n = 5)
Basioccipital length	33.47 $\pm$ 0.59 32.62–34.32	32.86 $\pm$ 0.67 31.73–34.28	33.14 $\pm$ 0.87 32.52–33.75	33.02 $\pm$ 0.25 32.74–33.20	32.45 $\pm$ 0.37 32.00–32.97	33.42 $\pm$ 0.94 (4) 32.16–34.40
Interorbital breadth	5.72 $\pm$ 0.15 5.50–6.01	5.61 $\pm$ 0.15 5.42–5.95	5.69 $\pm$ 0.13 5.59–5.78	5.60 $\pm$ 0.16 5.46–5.78	5.60 $\pm$ 0.15 5.47–5.86	5.55 $\pm$ 0.07 5.43–5.60
Zygomatic breadth	17.41 $\pm$ 0.45 16.87–18.13	17.00 $\pm$ 0.34 16.53–17.69	16.83 $\pm$ 0.18 16.70–16.95	17.00 $\pm$ 0.47 (2) 16.66–17.33	16.56 $\pm$ 0.48 16.04–17.17	16.65 $\pm$ 0.35 16.19–16.98
Mastoid breadth	13.89 $\pm$ 0.28 (9) 13.45–14.30	13.73 $\pm$ 0.15 13.51–14.03	13.99 $\pm$ 0.06 13.95–14.03	13.53 $\pm$ 0.26 13.29–13.81	13.25 $\pm$ 0.33 12.88–13.74	13.38 $\pm$ 0.12 (4) 13.27–13.53
Nasal length	13.82 $\pm$ 0.34 13.24–14.15	13.61 $\pm$ 0.34 13.22–14.29	13.52 $\pm$ 0.06 13.48–13.56	13.78 $\pm$ 0.28 13.47–13.99	13.48 $\pm$ 0.24 13.24–13.83	13.93 $\pm$ 0.45 13.15–14.33
Incisive foramen length	5.05 $\pm$ 0.27 4.57–5.44	5.02 $\pm$ 0.23 4.61–5.41	5.31 $\pm$ 0.22 5.15–5.46	5.24 $\pm$ 0.35 4.91–5.60	5.07 $\pm$ 0.29 4.76–5.47	5.03 $\pm$ 0.24 4.80–5.34
Rostral depth	7.23 $\pm$ 0.15 7.06–7.56	7.10 $\pm$ 0.19 6.86–7.44	7.25 $\pm$ 0.07 7.20–7.30	7.09 $\pm$ 0.24 6.83–7.30	6.77 $\pm$ 0.15 6.62–7.02	6.98 $\pm$ 0.22 6.71–7.28
Rostral length	14.86 $\pm$ 0.29 14.42–15.28	14.52 $\pm$ 0.42 13.91–15.23	14.54 $\pm$ 0.10 14.47–14.61	14.74 $\pm$ 0.26 14.48–15.00	14.57 $\pm$ 0.22 14.33–14.92	14.99 $\pm$ 0.46 14.22–15.37
Orbitotemporal length	11.13 $\pm$ 0.35 10.57–11.82	11.14 $\pm$ 0.26 10.72–11.57	11.51 $\pm$ 0.57 11.10–11.91	10.95 $\pm$ 0.34 10.63–11.31	11.24 $\pm$ 0.29 10.80–11.50	11.50 $\pm$ 0.19 11.31–11.81
Maxillary tooththrow length	6.93 $\pm$ 0.25 6.55–7.40	6.82 $\pm$ 0.21 6.56–7.23	7.05 $\pm$ 0.06 7.00–7.09	6.69 $\pm$ 0.07 6.61–6.74	6.69 $\pm$ 0.15 6.51–6.87	6.76 $\pm$ 0.09 6.65–6.89
Labial palatal breadth at M <sup>1</sup>	7.27 $\pm$ 0.15 7.07–7.48	7.06 $\pm$ 0.19 6.72–7.33	7.20 $\pm$ 0.03 7.18–7.22	6.85 $\pm$ 0.09 6.79–6.95	7.06 $\pm$ 0.25 6.82–7.43	7.05 $\pm$ 0.19 6.79–7.30
Diastema length	9.04 $\pm$ 0.26 8.69–9.42	8.85 $\pm$ 0.36 8.14–9.32	8.72 $\pm$ 0.16 8.61–8.83	9.00 $\pm$ 0.30 8.65–9.18	8.86 $\pm$ 0.36 8.54–9.47	9.10 $\pm$ 0.16 8.93–9.34
Postpalatal length	11.77 $\pm$ 0.32 11.24–12.35	11.55 $\pm$ 0.20 11.20–11.87	11.44 $\pm$ 0.23 11.28–11.60	11.54 $\pm$ 0.10 11.42–11.60	10.86 $\pm$ 0.13 10.66–10.99	11.25 $\pm$ 0.76 (4) 10.34–12.15
Lingual palatal breadth at M <sup>3</sup>	5.09 $\pm$ 0.14 (9) 4.90–5.34	4.89 $\pm$ 0.17 4.44–5.07	4.91 $\pm$ 0.21 4.76–5.05	4.93 $\pm$ 0.38 4.61–5.35	4.54 $\pm$ 0.23 4.29–4.78	4.96 $\pm$ 0.17 4.70–5.16
Braincase height	10.52 $\pm$ 0.36 10.07–11.12	10.46 $\pm$ 0.21 10.09–10.70	10.86 $\pm$ 0.08 10.80–10.91	10.43 $\pm$ 0.14 10.30–10.58	10.42 $\pm$ 0.33 9.92–10.71	10.33 $\pm$ 0.17 (4) 10.08–10.42
Breadth of M <sup>1</sup>	1.82 $\pm$ 0.04 1.76–1.90	1.79 $\pm$ 0.09 1.61–1.91	1.80 $\pm$ 0.02 1.78–1.81	1.65 $\pm$ 0.06 1.60–1.72	1.84 $\pm$ 0.03 1.80–1.87	1.83 $\pm$ 0.05 1.79–1.89
Breadth of incisors at tip	2.15 $\pm$ 0.09 1.94–2.27	2.09 $\pm$ 0.07 1.99–2.24	2.15 $\pm$ 0.04 2.12–2.18	2.12 $\pm$ 0.02 2.10–2.14	1.96 $\pm$ 0.07 1.86–2.02	2.05 $\pm$ 0.10 1.89–2.12
Width of zygomatic plate	3.31 $\pm$ 0.11 3.08–3.44	3.23 $\pm$ 0.15 2.93–3.49	3.20 $\pm$ 0.13 3.10–3.29	3.36 $\pm$ 0.29 3.03–3.58	3.09 $\pm$ 0.09 3.00–3.21	3.03 $\pm$ 0.14 2.90–3.24
Length of head and body	134.6 $\pm$ 5.6 (9) 124–141	131.4 $\pm$ 5.0 (10) 121–137	131.5 $\pm$ 2.1 130–133	132.7 $\pm$ 1.2 132–134	126.2 $\pm$ 4.0 122–132	133.6 $\pm$ 4.7 126–137
Total length	269.6 $\pm$ 6.8 (9) 258–283	262.6 $\pm$ 8.6 242–275	259.0 $\pm$ 1.4 258–260	262.7 $\pm$ 4.6 260–268	254.0 $\pm$ 8.6 242–265	264.2 $\pm$ 7.8 252–272
Length of tail vertebrae	135.9 $\pm$ 6.7 125–144	130.8 $\pm$ 6.3 (10) 121–140	127.5 $\pm$ 0.7 127–128	130.0 $\pm$ 3.5 128–134	127.8 $\pm$ 4.9 120–133	130.6 $\pm$ 3.9 126–135
Length of hind foot	37.0 $\pm$ 0.7 (9) 36–38	35.8 $\pm$ 1.4 (10) 34–39	36.0 $\pm$ 0.0 36	35.7 $\pm$ 0.6 35–36	34.4 $\pm$ 0.5 34–35	34.2 $\pm$ 1.1 33–35
Length of ear	22.0 $\pm$ 0.5 (9) 21–23	21.6 $\pm$ 0.5 (10) 21–22	23.0 $\pm$ 1.4 22–24	22.7 $\pm$ 0.6 22–23	21.4 $\pm$ 0.5 21–22	21.2 $\pm$ 0.4 21–22
Weight (g)	72.6 $\pm$ 4.7 (9) 66–79	66.7 $\pm$ 6.5 (10) 59–76	71.5 $\pm$ 3.5 69–74	57.0 $\pm$ 4.6 53–62	56.6 $\pm$ 5.9 50–66	62.6 $\pm$ 5.2 54–68

body length (Ruedas, 1995), and is thicker at the base than in other species. The tail is dark brown both dorsally and ventrally, slightly paler ventrally, and often white at the tip. The hind feet are shorter and broader than those of other *Megapomys*, with proportionately larger plantar pads and a hallux that reaches to the top or slightly beyond the top of the adjacent plantar pad; the ventral surface is moderately heavily pigmented except for the pads (Fig. 10J; Table 3). The upper incisors are laterally compressed relative to depth, 1.56–1.76 mm at the tip; the lower incisors are unpigmented and elongate (Fig. 19). The rostrum is long and slender and turns up slightly near the tip. The braincase is more globose than in other *Megapomys*. The maxillary molars are narrow and the

tooththrow is short. The postpalatal region is long. A foramen is present in the bulla for the stapedia artery (the “datae pattern”). The interparietal bone is variable in shape but is usually moderately wide anteroposteriorly. The mandible (Fig. 19C) is long and slender, with a short coronoid process and a short, blunt angular process (see Ruedas [1995] for additional details). No other species of rodent on Mindoro is similar in size and overall morphology.

COMPARISONS—*Apomys gracilirostris* differs from *A. datae* in having darker pelage dorsally and much darker pelage ventrally, with a proportionately longer and thicker tail and shorter and broader hind feet. The crania are of similar total length, but that of *A. datae* is more robust overall, with a

TABLE 3. *Extended.*

<i>Apomys abrae</i> Mt. Simminublan, Ilocos Norte Prov.	<i>Apomys gracilirostris</i> Mt. Halcon, Mindoro Island	<i>Apomys sacobianus</i>		<i>Apomys brownorum</i>	
		Sacobia River, Pampanga Prov.	M-holotype USNM 304352	M-holotype FMNH 183524	M (n = 10)
32.10 ± 0.46 (5)	33.85 ± 0.71	34.29	33.57	33.55 ± 0.91	32.43 ± 0.33
31.43–32.58	33.34–34.35	—	—	32.41–34.85	31.96–32.75
5.48 ± 0.16 (7)	6.02 ± 0.21	6.02	5.75	5.65 ± 0.13	5.60 ± 0.13
5.27–5.71	5.87–6.17	—	—	5.38–5.87	5.46–5.78
16.65 ± 0.52 (4)	17.57 ± 0.20	17.97	17.54	17.44 ± 0.45	17.14 ± 0.24
15.93–17.17	17.43–17.71	—	—	16.69–18.09	16.88–17.45
13.17 ± 0.83 (3)	14.48 ± 0.04	14.04	14.01	14.09 ± 0.33	13.91 ± 0.26 (4)
12.21–13.65	14.45–14.51	—	—	13.63–14.70	13.69–14.28
13.18 ± 0.50 (8)	14.42 ± 0.28	13.91	13.62	13.88 ± 0.49	13.17 ± 0.31
12.18–13.70	14.22–14.62	—	—	12.90–14.63	12.74–13.58
5.08 ± 0.19 (8)	4.77 ± 0.13	5.70	4.86	5.03 ± 0.23	4.99 ± 0.16
4.89–5.52	4.67–4.86	—	—	4.66–5.48	4.80–5.16
6.85 ± 0.17 (7)	7.00 ± 0.11	7.96	7.06	7.05 ± 0.17	6.79 ± 0.16
6.62–7.11	6.92–7.08	—	—	6.73–7.36	6.54–6.97
14.22 ± 0.43 (7)	16.08 ± 0.55	15.04	14.92	15.12 ± 0.54	14.65 ± 0.25
13.60–14.68	15.69–16.47	—	—	14.27–15.83	14.28–14.93
11.24 ± 0.40 (4)	10.53 ± 0.23	11.73	11.59	11.28 ± 0.33	11.14 ± 0.34
10.81–11.77	10.36–10.69	—	—	10.63–11.70	10.81–11.58
6.59 ± 0.27 (7)	6.25 ± 0.09	6.92	6.53	6.59 ± 0.17	6.60 ± 0.18
6.19–6.99	6.19–6.31	—	—	6.37–6.81	6.38–6.80
6.79 ± 0.35 (5)	7.33 ± 0.01	7.20	6.87	6.82 ± 0.20	6.75 ± 0.10
6.42–7.31	7.32–7.34	—	—	6.56–7.09	6.57–6.83
8.47 ± 0.36 (7)	9.52 ± 0.54	8.55	9.44	9.44 ± 0.29	8.89 ± 0.16
7.98–8.98	9.13–9.90	—	—	8.79–9.77	8.67–9.09
10.99 ± 0.53 (4)	11.53 ± 0.27	11.88	11.66	11.51 ± 0.42	10.95 ± 0.18
10.26–11.42	11.34–11.72	—	—	11.03–12.10	10.75–11.21
4.51 ± 0.08 (2)	5.27 ± 0.01	4.10	4.80	4.87 ± 0.26	4.69 ± 0.30
4.45–4.56	5.26–5.27	—	—	4.46–5.29	4.35–5.05
10.23 ± 0.66 (3)	10.71 ± 0.71	10.30	11.13	10.65 ± 0.38	10.72 ± 0.34
9.50–10.76	10.20–11.21	—	—	10.12–11.13	10.32–11.25
1.72 ± 0.10 (7)	1.76 ± 0.01	1.97	1.76	1.69 ± 0.05	1.71 ± 0.06
1.58–1.85	1.75–1.77	—	—	1.63–1.76	1.65–1.79
2.06 ± 0.09 (7)	1.74 ± 0.03	2.27	2.13	2.09 ± 0.08 (9)	2.03 ± 0.07
1.93–2.23	1.72–1.76	—	—	1.94–2.18	1.92–2.08
3.08 ± 0.19 (8)	3.28 ± 0.12	3.46	2.70	2.71 ± 0.09	2.55 ± 0.20
2.84–3.33	3.19–3.36	—	—	2.56–2.82	2.23–2.78
—	—	141	135	134.3 ± 5.3 (9)	128.0 ± 4.6
—	—	—	—	125–140	123–135
—	—	290	250	246.9 ± 6.3 (9)	238.6 ± 6.2
—	—	—	—	235–255	230–247
—	147.0 ± 8.5	149	115	112.6 ± 2.7 (9)	110.6 ± 2.6
—	141–153	—	—	110–116	107–114
—	36.0 ± 0.0	40	34	33.8 ± 1.3	33.4 ± 1.5
—	36	—	—	32–36	31–35
—	18.0 ± 0.0	22	21	21.5 ± 0.5	21.6 ± 0.5
—	18	—	—	21–22	21–22
—	—	—	71	77.1 ± 5.5	69.4 ± 8.9
—	—	—	—	69–84	60–82

heavier rostrum, broader and more squarish braincase, broader zygomatic plate and zygomatic arches, broader incisive foramina, and a longer toothrow. Both species have the “datae pattern” of carotid circulatory pattern (Fig. 5). The mandible of *A. gracilirostris* is similar in length to that of *A. datae* but is more slender, with the bony sheath of the anterior portion of the mandible extending less far onto the incisor. The coronoid process of the mandible is shorter and less pointed than in *A. datae*, and the angular process is shorter and blunter.

DISTRIBUTION—*Apomys gracilirostris* is currently known only from 1250 to 1950 m on the North Ridge of Mt. Halcon (Fig. 18). This species should be sought widely in the

mountains that make up the central core of Mindoro, at elevations from 700 m to more than 2000 m, areas from which no data on small mammals are currently available. The long tail and short, broad hind foot implies to us that it could be partially arboreal.

COMMENTS—The combination of the dark pelage, long tail, short and broad hind feet, and slender rostrum, globose braincase, and narrow incisors easily distinguish *A. gracilirostris* from all other *Megapomys*. The long tail and slender rostrum are characters shared with the subgenus *Apomys*, which suggests that they represent primitive character states, whereas the short tail and robust rostrum of the remaining species of *Megapomys* might represent shared, derived characters.

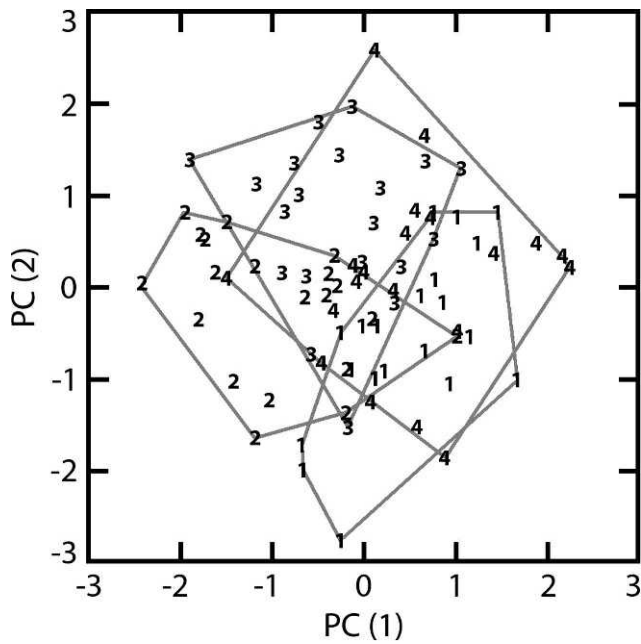


FIG. 11. Results of the principal components analysis of *Apomys datae* (see text and Table 4) based on specimens included in Table 2. 1 = Mt. Data, Mountain Province; 2 = Mt. Bali-it and vicinity, Kalinga Province; 3 = Mt. Amuyao, Mountain Province; 4 = Mt. Pulag, Benguet Province.

***Apomys sacobianus* Johnson, 1962**

*Apomys sacobianus* Johnson, 1962: 317–319.

HOLOTYPE—USNM 304352. Adult male, collected 16 August 1956. Field number D. H. Johnson 8555. Prepared as stuffed skin plus skull. Measurements in Table 3.

TYPE LOCALITY—Philippine Islands: Luzon: Pampanga Province: Clark Air Base, Sacobia River, in a narrow forested canyon of the Sacobia River “just above the point where it

TABLE 4. Character loadings, eigenvalues, and percent variance explained on the first four components of a principal components analysis of log-transformed measurements of adult *Apomys datae* (see Fig. 11 and Methods).

Variable	Principal component			
	1	2	3	4
Basioccipital length	0.879	0.253	0.168	0.011
Interorbital breadth	0.454	0.145	-0.527	-0.228
Zygomatic breadth	0.725	-0.131	-0.211	0.325
Mastoid breadth	0.788	-0.010	-0.281	-0.128
Nasal length	0.767	0.190	0.034	-0.152
Incisive foramen length	0.036	0.397	0.433	0.518
Rostral depth	0.730	0.042	-0.105	0.162
Rostral length	0.778	0.193	0.150	-0.312
Orbitotemporal length	0.381	-0.230	-0.302	0.619
Maxillary tooththrow length	0.591	-0.537	0.402	-0.157
Labial palatal breadth at M <sup>1</sup>	0.581	-0.213	0.308	-0.307
Diastema length	0.611	0.598	0.093	0.097
Postpalatal length	0.693	0.051	0.056	-0.004
Lingual palatal breadth at M <sup>3</sup>	0.431	0.466	-0.129	-0.152
Braincase height	0.495	-0.343	-0.510	0.069
Breadth of M <sup>1</sup>	0.507	-0.660	0.311	-0.153
Breadth of incisors at tip	0.309	-0.339	-0.092	0.398
Width of zygomatic plate	0.358	0.029	0.466	0.409
Eigenvalue	6.451	1.969	1.610	1.477
Percent variance explained	35.84	10.94	8.95	8.21

TABLE 5. Character loadings, eigenvalues, and percent variance explained on the first four components of a principal components analysis of log-transformed measurements of adult *Apomys abrae* and *A. datae* (see Fig. 13 and Methods).

Variable	Principal component			
	1	2	3	4
Basioccipital length	0.937	0.144	0.123	0.010
Interorbital breadth	0.686	0.094	-0.344	-0.137
Zygomatic breadth	0.902	0.071	-0.135	0.110
Mastoid breadth	0.871	0.017	-0.192	-0.112
Nasal length	0.843	0.035	0.033	-0.074
Incisive foramen length	0.241	0.455	0.557	0.473
Rostral depth	0.861	0.122	-0.050	-0.096
Rostral length	0.884	0.059	0.068	-0.074
Orbitotemporal length	0.587	-0.005	-0.281	0.444
Maxillary tooththrow length	0.543	-0.645	0.274	-0.060
Labial palatal breadth at M <sup>1</sup>	0.646	-0.400	0.283	-0.236
Diastema length	0.738	0.455	0.174	0.054
Postpalatal length	0.690	0.051	0.129	-0.203
Lingual palatal breadth at M <sup>3</sup>	0.512	0.315	0.071	-0.575
Braincase height	0.663	-0.159	-0.512	0.183
Breadth of M <sup>1</sup>	0.468	-0.745	0.171	0.151
Breadth of incisors at tip	0.695	-0.046	-0.087	0.238
Width of zygomatic plate	0.694	-0.014	0.185	0.203
Eigenvalue	9.173	1.730	1.127	1.072
Percent variance explained	50.96	9.61	6.26	5.96

emerges from the foothills of the Zambales Mountains onto the plains of Pampanga” (Johnson, 1962: 319).

SPECIMENS EXAMINED—The holotype (and only known specimen).

EMENDED DIAGNOSIS AND DESCRIPTION—A large *Megapomys*, within the range of large individuals of *A. datae*, but larger than *A. abrae*. The tail is slightly longer than the length of head and body (149 mm/141 mm = 106%). The dorsal pelage is shorter and less dense than that of other *Megapomys* and grayish-brown rather than dark brown with red, orange, or yellow tones. The ventral pelage is pale whitish-gray, creamy along the midline and throat. The dorsal surfaces of the hind feet are white. The dorsal surfaces of the forefeet have a narrow stripe of dark hairs reaching from the forearm to the base of the central toes. Because the holotype is a dried museum study skin, no description of the ventral surface of the hind feet is possible, beyond noting that they are longer than those of most species of *Megapomys* (Table 3). The tail is sharply bicolored, dark grayish-brown dorsally and nearly white ventrally. The cranium (Fig. 20) is large and robust, with a deep, squarish braincase and a broad, deep rostrum. The incisive foramina are long (5.8 mm), as is the upper tooththrow (7.1 mm). The palate is narrow, with the premaxillary tooththrows diverging only slightly posteriorly. The postpalatal region is of moderate length. There is no foramen in the bulla for the stapedial artery (the “abrae pattern”; Fig. 5). The interparietal bone is of moderate anteroposterior width. The mandible (Fig. 20C) is of moderate length and is robust overall. The coronoid process is short, sturdy, and sharply pointed, and the angular process is deep and moderately pointed.

COMPARISONS—Because only the holotype is known, and USNM policy does not allow destructive sampling of holotypes, no material is available for genetic analysis. Here, we make comparisons to the four geographically nearest and most morphologically similar species.



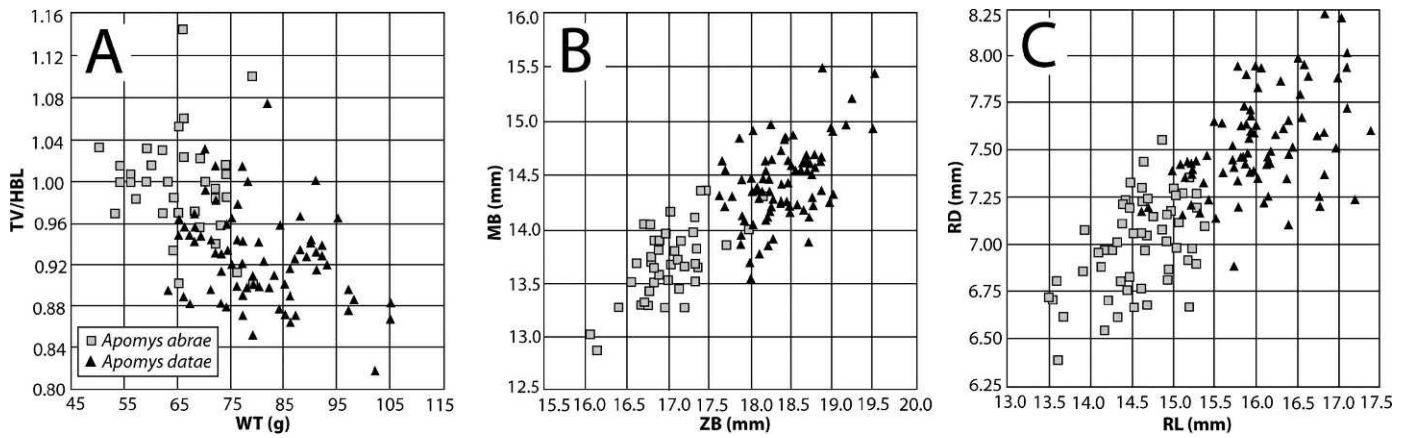


FIG. 12. Bivariate plots of measurements comparing *Apomys abrae* and *A. datae*. (A) Weight (WT) and length of tail vertebrae (TV) divided by length of head and body (HBL). (B) Zygomatic breadth (ZB) and mastoid breadth (MB). (C) Rostral length (RL) and rostral depth (RD).

*Apomys sacobianus* differs from *A. datae* in having shorter, relatively grayer dorsal pelage (vs. longer, softer, denser, and dark brown), with entirely white fur on the dorsal surface of the hind feet (vs. brown on the proximal portion). The tail is both absolutely (Fig. 21A) and proportionately longer (106% vs. 89–95%), and more sharply bicolored than is typical for *A. datae*. The length of the hind foot is greater than recorded for any *A. datae* (Fig. 21A). *Apomys sacobianus* has the carotid circulatory pattern of *A. abrae*, lacking a foramen in the bulla for a stapedia artery. The length of the incisive foramina is at the upper end of the range for *A. datae* (5.8 vs. ca. 4.6–5.8 mm), and the incisive foramina (Fig. 20B) are slightly narrower than is typical for *A. datae*. The length of the nasals is near the bottom of the range for *A. datae* (13.9 vs. 13.6–15.3 mm). The rostrum is deeper than all but the largest *A. datae* (Fig. 21B), but the rostral length is less than all but the smallest *A. datae*. Braincase height is less than in most *A. datae* (Fig. 21B), and diastema length is less than in all *A. datae* (Fig. 21C). The

lingual breadth of palate at  $M^3$  is also substantially less than in *A. datae* (Fig. 21C). Most other cranial measurements fall within the range for *A. datae*. The shape of the interparietal bone in the two species appears similar. The mandible (Fig. 20C) is similar to that of *A. datae*, although slightly more robust and with slightly shorter and more robust coronoid and angular processes.

*Apomys sacobianus* differs from *A. abrae* in being larger in all respects, with virtually no overlap (Tables 2, 3). The pelage is longer and denser in *A. abrae*, with more extensive brown tints. They have tails of similar proportional length (106% vs. 90–115% of head and body length). The tail and hind foot are longer in *A. sacobianus* than in *A. abrae* (Fig. 21A). Both have white fur on the dorsal surface of the hind feet, but on the dorsal surface of the forefeet, *A. sacobianus* has a narrow line of dark hairs reaching from the forearm to the base of the toes, whereas the forefeet of *A. abrae* are entirely white. The cranium is larger and more robust overall, with an especially more robust (deeper and wider) rostrum (Fig. 21B). The incisive foramina of the one known specimen of *A. sacobianus* are narrower, and may be longer, than is typical for *A. abrae*, and the postpalatal length is greater. The lingual breadth of palate at  $M^3$  is narrower than in *A. abrae* (Fig. 21C), which reflects the generally narrower palate of *A. sacobianus*. As noted by Musser (1982), the carotid circulation pattern in *A. sacobianus* is identical to that in *A. abrae*. The shape of the interparietal bone in the two species appears similar, although that of *A. sacobianus* is wider anteroposteriorly. The mandible of *A. sacobianus* (Fig. 20C) is larger and slightly more robust than that of *A. abrae*, with a less deeply concave posterior margin between the condylar and angular processes.

*Apomys sacobianus* differs from *A. zambalensis* sp. nov., which occurs nearby in the Zambales Mountains, in having grayish dorsal pelage (vs. rusty-orange brown) and in lacking the stapedia artery foramen in the bullae (which is present in all 53 *A. zambalensis* sp. nov. crania available). The holotype of *A. sacobianus* has a hind foot length that lies at the upper extreme of the range for *A. zambalensis* and a tail that is near the upper extreme for *A. zambalensis* sp. nov. (Fig. 22A). The crania differ conspicuously in several ways. Diastema length of *A. sacobianus* is much less than in *A. zambalensis* sp. nov., and braincase height falls near the lower extreme of the range for *A. zambalensis* sp. nov. (Fig. 22B). The length of  $M^1$  to  $M^3$  is below the lower end of the range for *A. zambalensis* sp. nov., and the lingual breadth of the palate at  $M^3$  is conspicuously

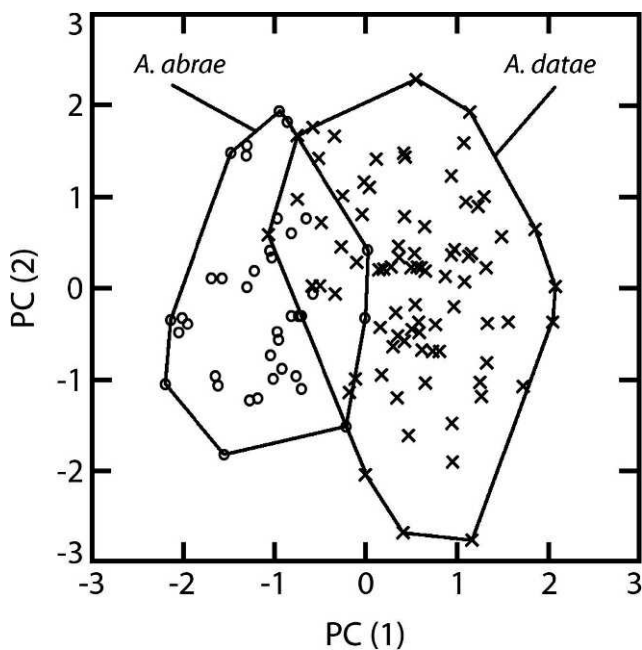


FIG. 13. Results of the principal components analysis of *Apomys datae* and *A. abrae* (see text and Table 5) based on specimens in Tables 2 and 3.

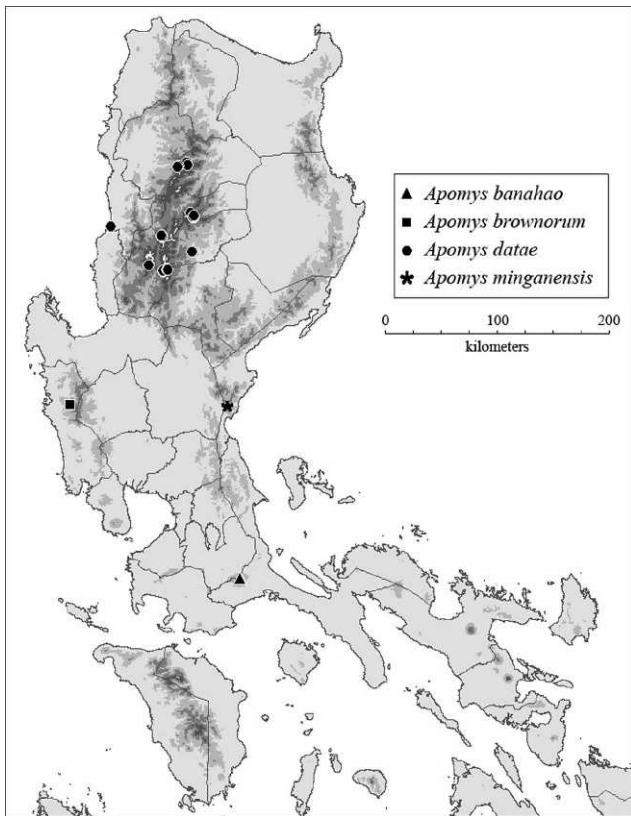


FIG. 14. Map showing the documented distribution of *Apomys banahao* sp. nov., *A. brownorum* sp. nov., *A. datae*, and *A. minganensis* sp. nov. See respective species accounts for localities. Shading on land areas, in increasingly dark tones of gray: 0–500 m elevation; 501–1000 m; 1001–1500 m; 1501–2000 m; and white above 2000 m. Provincial boundaries are shown for reference.

less (Fig. 22C). Additionally, the breadth of  $M^1$  is greater in *A. sacobianus*, although only slightly so (2.0 vs. 1.6–1.9 mm; Tables 2, 3). In other cranial measures, the holotype of *A. sacobianus* falls within the range of *A. zambalensis* sp. nov. (Tables 2, 3). The interparietal bone of *A. sacobianus* is narrower than that of *A. zambalensis* sp. nov. The mandible of *A. zambalensis* sp. nov. is similar to that of *A. sacobianus*, but the posterior margin between the condylar and angular processes is narrower and more deeply concave.

*Apomys magnus* sp. nov. is substantially larger than *A. sacobianus* in all features measured (Tables 3, 12) and differs from it in the same specific details that separate *A. sacobianus* and *A. zambalensis* sp. nov.

To further assess the extent to which *A. sacobianus* differs from *A. zambalensis* sp. nov. and *A. magnus* sp. nov., we conducted a PCA of 18 craniodontal measurements of these three species and also included *A. aurorae* sp. nov., which is geographically more distant from *A. sacobianus*, but which is a member of the same clade (Fig. 7). The first component, which accounted for 45% of the total variance, loaded heavily on all measurements except width of zygomatic plate (Table 7). The second component, which accounted for 12% of the variance, loaded heavily and positively on diastema length and postpalatal length, and heavily but negatively on interorbital breadth, palatal breadth at  $M^1$ , breadth of  $M^1$ , and width of the zygomatic plate. The remaining components had eigenvalues below 1.5 and were not interpretable. A plot of PC1 and PC2 (Fig. 23) showed the holotype (and sole

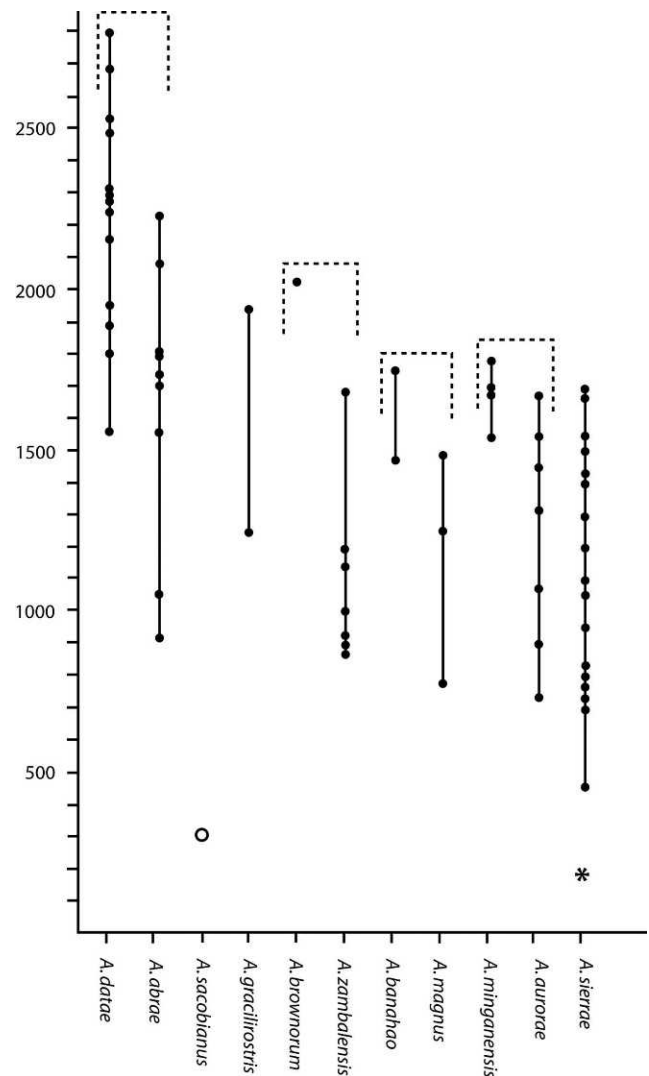


FIG. 15. Documented elevational ranges of the species of the subgenus *Megapomys* on Luzon. Brackets indicate regionally sympatric species. **Solid circle** = known elevation; **open circle** = estimated elevation (see text); **asterisk** = record from Palaui Island.

known specimen) of *A. sacobianus* with a strongly negative score on the first axis, indicating its small size relative to the other included species. It lies outside of the polygons of *A. zambalensis* sp. nov. and *A. aurorae* sp. nov., for both of which we have good samples; because the holotype is a fully adult animal, this suggests that the size difference is likely to remain consistent when more specimens are obtained. *Apomys magnus* sp. nov. has the highest scores on the first axis, reflecting its large size.

On the second component, *A. sacobianus* had an intermediate score (Fig. 23), with most specimens of *A. zambalensis* sp. nov. scoring positively and most specimens of *A. aurorae* sp. nov. scoring negatively, reflecting differences in craniodontal proportions that are more fully discussed below. *Apomys magnus* sp. nov. scored at intermediate to negative levels on this component, overlapping with *A. sacobianus* in this respect. We conclude that this analysis supports the recognition of all four of these species as being distinct from each other.

**DISTRIBUTION**—*Apomys sacobianus* is currently known only from the holotype, taken on the lower east-facing slope of the



FIG. 16. Dorsal (A), ventral (B), and lateral (D) views of the cranium and lateral view of the mandible (C) of *Apomys abrae* (FMNH 62750, holotype); scale bar = 5 mm.

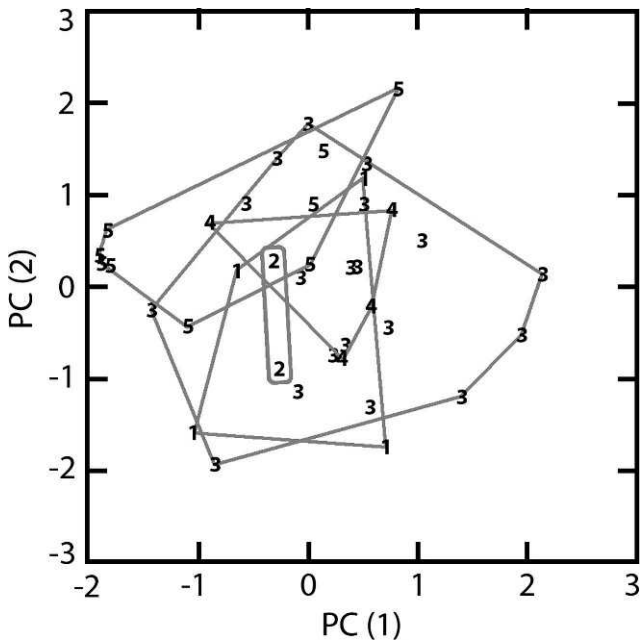


FIG. 17. Results of the principal components analysis of *Apomys abrae* (see text and Table 6) based on specimens included in Tables 2 and 3. 1 = Mt. Data, Mountain Province; 2 = Mt. Bali-it, Kalinga Province, 900 m; 3 = Mt. Bali-it, Kalinga Province, 1100 m; 4 = Mt. Bali-it, 1600 m, Kalinga Province; 5 = Mt. Amuyao, Mountain Province.

Zambales Mountains (Johnson, 1962; Fig. 18). We estimate the elevation of the type locality as roughly 300 m (Fig. 15). Because the species is known only from the holotype, the extent of the distribution is uncertain. It should be sought in the foothills of the Zambales Mountains in Pampanga, Tarlac, and Pangasinan provinces.

COMMENTS—Because *A. sacobianus* is known only from the holotype, an adult animal with moderately worn molars, the extent of variation is unknown, and no tissues are available for genetic study, making it impossible to adequately place this animal in the context of the other species treated here. Musser (1982) viewed *A. sacobianus* as a larger version of *A. abrae* but retained it as a species to emphasize the difference in size and to draw attention to the need for further study. We agree that they are similar and might be closely related, but we document here that there is indeed no overlap in cranial or external dimensions with our large sample of *A. abrae*. We also note the similarity in size with *A. zambalensis*, but the two differ in their types of carotid circulatory patterns and in numerous other cranial features, as listed above. Clearly, further study is needed, but we agree with Musser (1982) that maintaining this as a valid species is the best course of action. Further field surveys and more specimens are badly needed.

*Apomys (Megapomys) brownorum* sp. nov.

HOLOTYPE—FMNH 183524, adult male collected on 12 January 2005 by Danilo S. Balete, field number DSB 3531. A sample of muscle tissue was removed from the thigh in the



TABLE 6. Character loadings, eigenvalues, and percent variance explained on the first four components of a principal components analysis of log-transformed measurements of adult *Apomys abrae* (see Fig. 17 and Methods).

Variable	Principal component			
	1	2	3	4
Basioccipital length	0.784	0.390	0.225	0.063
Interorbital breadth	0.412	-0.285	-0.143	0.202
Zygomatic breadth	0.769	-0.077	-0.191	-0.037
Mastoid breadth	0.702	-0.264	-0.429	0.186
Nasal length	0.621	0.169	0.562	0.024
Incisive foramen length	0.362	0.470	-0.142	0.292
Rostral depth	0.832	0.107	-0.341	-0.149
Rostral length	0.620	0.352	0.453	0.146
Orbitotemporal length	0.122	0.052	0.254	0.753
Maxillary tooththrow length	0.497	-0.583	0.161	0.032
Labial palatal breadth at M <sup>1</sup>	0.547	-0.457	0.428	-0.044
Diastema length	0.391	0.755	0.034	0.118
Postpalatal length	0.763	0.159	0.005	-0.247
Lingual palatal breadth at M <sup>3</sup>	0.712	0.098	-0.245	-0.111
Braincase height	0.234	-0.496	-0.323	0.663
Breadth of M <sup>1</sup>	-0.039	-0.469	0.758	-0.011
Breadth of incisors at tip	0.726	-0.160	0.023	-0.347
Width of zygomatic plate	0.507	-0.520	-0.126	-0.175
Eigenvalue	6.105	2.613	1.979	1.457
Percent variance explained	33.92	14.52	10.99	8.096

field and preserved in ethanol before the specimen was preserved in formaldehyde. In the museum, the skull was removed and cleaned (see Methods). All parts are in good condition. This specimen will be permanently deposited at the NMP. Measurements in Table 3.

TYPE LOCALITY—Philippines: Luzon Island: Zambales Province: Palauig Munic.: Barangay Salasa: Mt. Tapulao peak, 2024 m; 15°28'54.8"N, 120°07'10.4"E (GPS reading).

PARATYPES (n = 34)—Luzon Island: Zambales Prov.: Palauig Munic.: Brgy. Salasa: Mt. Tapulao peak, 2024 m (FMNH 183494–183523, 183525–183528).

ETYMOLOGY—"brown" + "orum," meaning "of the Browns," a plural noun used in the genitive. We name this species in recognition of the long-standing support for research on mammalian diversity by Barbara and Roger Brown, without which our studies of Philippine mammals would not have been possible.

DIAGNOSIS AND DESCRIPTION—A mouse with especially soft, richly colored pelage and a relatively short tail. It is the smallest species of *Megapomys* (e.g., BOL 32.4–34.9 mm, HBL 126–140 mm; Table 3). The dorsal pelage is soft, dense, and moderately long; it is a rich dark brown, sometimes with rusty-orange tints between the eye and pinna and below the pinna and along the lower margin of the dorsal pelage (Fig. 2B). The ventral pelage is dark gray at the base, with grayish-ochraceous tips. The transition between the dorsal and ventral pelage is gradual. Dark hairs extend from the lower forelimb onto the posterior third of the forepaws, and from the lower hind leg over about four-fifths of the dorsal surface of the hind foot. The hind feet are pale ventrally, with little or no pigment (Fig. 10H). The tail is proportionately short (82–90% of HBL) and sharply bicolored, with the dorsal surface dark grayish-brown and the ventral surface nearly white. The cranium (Fig. 24; Table 3) is small, with a relatively slender rostrum and zygomatic arches and a globose braincase. The incisive foramina are short (4.8–5.2 mm) and narrow. The maxillary

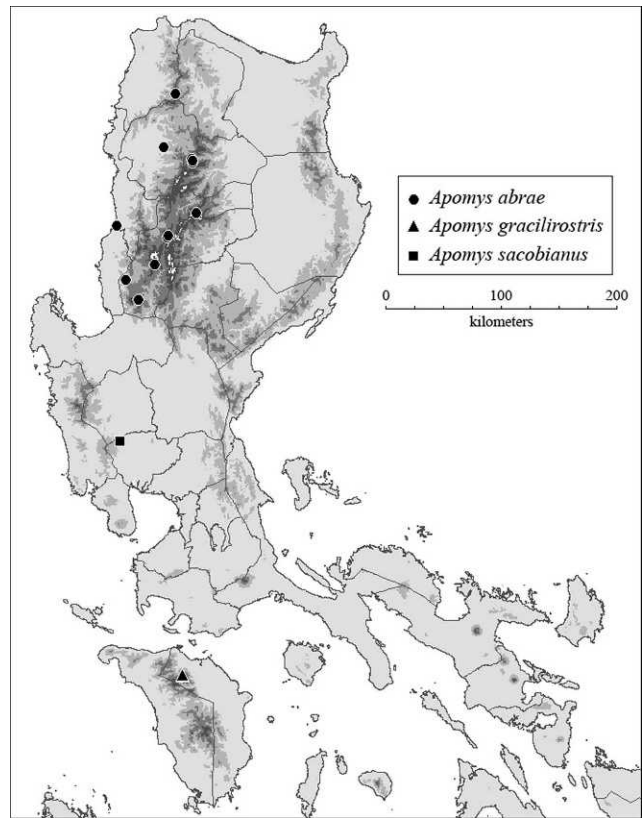


FIG. 18. Map showing the documented distribution of *Apomys abrae*, *A. gracilirostris*, and *A. sacobianus*. See respective species accounts for localities. Shading on land areas, in increasingly dark tones of gray: 0–500 m elevation; 501–1000 m; 1001–1500 m; 1501–2000 m; and white above 2000 m. Provincial boundaries are shown for reference.

molariform tooththrow is short (6.4–6.8 mm), and the tooththrow is narrow, as shown by the width of M<sup>1</sup> (1.63–1.79 mm). The maxillary tooththrows diverge slightly posteriorly, and the palate is lightly pitted and perforated. The bulla has no perforation for a stapedia artery (the "abrae pattern"; Fig. 5A). The postpalatal region is unusually short (Table 3). The interparietal bone is of moderate anteroposterior width and is usually oval in shape. The mandible (Fig. 24C) is short and rather slender, with a long, pointed coronoid process, short angular process, and a shallowly concave margin between the condylar and angular processes.

COMPARISONS—*Apomys brownorum* differs from *A. datae* in being smaller in all respects, with little overlap in any measurement (Tables 2, 3). The tail is both absolutely (110–115 vs. 121–142 mm) and proportionately (70–88% of HBL vs. 88–103%) shorter. The pelage of *A. brownorum* (Fig. 2B) is darker than that of *A. datae* (Fig. 1B), both dorsally and ventrally. The hind foot is not as dark ventrally as that of *A. datae*, with only a small amount of pigment on most individuals. The foot and toes are broader than those of *A. datae* (Fig. 10B,H). The skin of the rhinarium and lips of *A. brownorum* is less dark. The skull of *Apomys brownorum* is more slender and gracile overall, and they are easily distinguished. The braincase of *A. brownorum* (Fig. 24) is slightly more elongated and globose, the interorbital region more constricted, and the rostrum proportionately shorter and more gracile; the upper incisors are thinner in both dimensions, the incisive foramina are usually narrower, both the



FIG. 19. Dorsal (A), ventral (B), and lateral (D) views of the cranium and lateral view of the mandible (C) of *Apomys gracilirostris* (NMP 3478); scale bar = 5 mm.

zygomatic plate and the palate are absolutely and proportionately narrower, and the postpalatal region is shorter. *Apomys brownorum* has the “abrae pattern” of basicranial circulation, with no stapedia foramen in the bullae (Fig. 5A). The interparietal bones are of similar shape. The mandible (Fig. 24C) is shorter and more slender than that of *A. datae*, with a more erect and sharply pointed coronoid process, and the posterior margin between the condylar and angular processes is slightly more concave.

*Apomys brownorum* and *A. banahao* sp. nov. are generally similar but also show consistent differences. Both species have long, soft, and dense pelage dorsally that is dark brown, but that of *A. brownorum* (Fig. 2B) is slightly paler and shorter. Both species have ventral fur that is dark gray at the base and quite pale near the tips, but *A. brownorum* is washed with pale ochraceous, whereas *A. banahao* sp. nov. (Fig. 1D) is washed with ashy gray. The tail in both species is sharply dorsoventrally bicolored; neither possesses a white tip. The tail of *A. brownorum* is usually shorter than that of *A. banahao* sp. nov. both absolutely (110–115 vs. 111–133 mm) and relative to the length of head and body (70–88% vs. 87–103%; Fig. 25A). Both species have dark hairs present over much of the dorsal surface of the hind foot, but the ventral surface in *A. brownorum* is much less heavily pigmented than that of *A. banahao*, and is slightly broader (Fig. 10C,H).

The skull of *A. brownorum* is similar to that of *A. banahao* sp. nov. but is smaller overall. The braincase is slightly more elongate and globose (vs. somewhat more rectangular), the

rostrum is relatively more elongate and gracile, the incisive foramina are less broad, the zygomatic plate is narrower and the orbitotemporal fossa length is usually less (Fig. 25B), and a plot of breadth of  $M^1$  vs. labial breadth of palate at  $M^1$  shows almost no overlap (Fig. 25C); this combination of mensural characters separates all individuals. The palate of *A. banahao* sp. nov. is more heavily pitted and fenestrated. These species share the “abrae pattern” of carotid circulation, lacking a stapedia foramen in the bullae (Fig. 5A). The interparietals are similar in shape. The mandible of *A. banahao* sp. nov. is similar to that of *A. brownorum*, but the coronoid process is shorter, thinner, and directed more posteriorly, and the posterior margin between the condylar and angular processes is shallower.

A PCA of 18 craniodental measurements showed substantial differences between these two species (Fig. 26; Table 8). The first component, which accounted for 49% of the total variance, loaded strongly on all measurements, indicating that it is an indicator of size and robustness. The second component, which accounted for 11% of the total variance, was strongly dominated by high loadings on rostral and diastema length (Table 8). Subsequent components had eigenvalues of less than 2.0. Individuals of *A. brownorum* had low scores on the first component, whereas most *A. banahao* sp. nov. had higher scores, reflecting the generally greater size and robustness of the latter species. Overlap was great on the second component, although some *A. brownorum* scored low on the component, indicating their proportionately

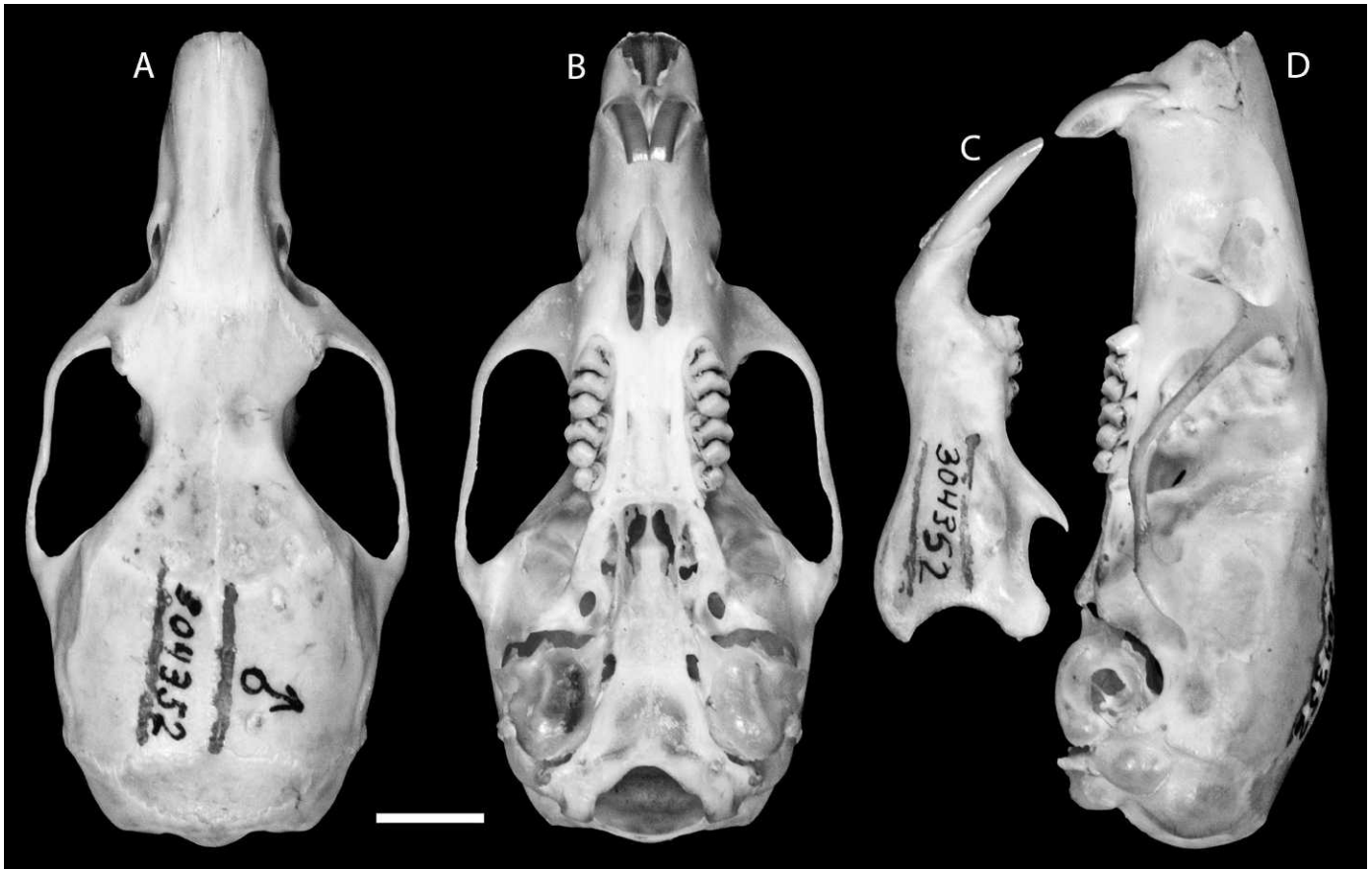


FIG. 20. Dorsal (A), ventral (B), and lateral (D) views of the cranium and lateral view of the mandible (C) of *Apomys sacobianus* (USNM 304352, holotype); scale bar = 5 mm.

long rostrum and diastema. Given the strong and consistent morphological and genetic differences that distinguish these species, we consider them to be distinct species.

*Apomys brownorum* differs in many respects from *A. zambalensis* sp. nov., which occurs on the same mountain (Mt. Tapulao) at lower elevations. Externally, there is little overlap in head and body length and no overlap in a plot of length of tail and hind foot (Fig. 27A), and most individuals of *A. zambalensis* sp. nov. are heavier (Tables 3, 15). The pelage of *A. brownorum* (Fig. 2B) is much darker dorsally and ventrally than *A. zambalensis* sp. nov. (Fig. 2A), which is a rich orange-brown dorsally and has a very pale ochraceous wash ventrally. The obvious morphological differences and genetic distance between them mark these as clearly distinct species.

*Apomys brownorum* and *A. zambalensis* sp. nov. are easily distinguished cranially, and there is no overlap in a plot of PC1 and PC2 from the PCA of cranial measurements (Fig. 6A). *Apomys brownorum* is consistently smaller in virtually all measurements (Tables 3, 15); the skull of *A. brownorum* is generally more slender, with a more globose braincase and a more delicate rostrum (vs. squarish braincase with a sturdy rostrum; Figs. 24, 46). The upper incisors are narrower and also less deep, and the incisive foramina are narrower. The palate is shorter and narrower, the molar toothrow is shorter (Fig. 27B), the zygomatic plate is narrower, and the lingual breadth at M<sup>3</sup> is usually less (Fig. 27C). *Apomys brownorum* lacks a stapedial foramen in the bullae (Fig. 5A); the foramen is present in *A. zambalensis* sp. nov. (Fig. 5B). The interparietal bone of *A. brownorum* is

of moderate anteroposterior width; that of *A. zambalensis* sp. nov. is much wider. The mandible of *A. zambalensis* sp. nov. is longer and more robust overall, with a shorter, wider, more posteriorly inclined coronoid process and a broader, longer angular process. All individuals are easily distinguished by this combination of characters.

**DISTRIBUTION**—*Apomys brownorum* is currently known only from mossy forest at a single locality near the peak of Mt. Tapulao at ca. 2024 m elevation (Figs. 3, 14). No specimens were taken at 1690 m in 391 trap-nights that yielded 50 captures of *A. zambalensis* sp. nov. or at lower elevations where *A. zambalensis* sp. nov. were equally common. We have no data from 1690 to 2024 m, so we can infer only that the lower elevational limit for the species falls somewhere within this range, perhaps at ca. 1800 m, where there is a transition from montane to mossy forest (Balet et al., 2009). Similar habitat might occur on the other high peaks of the Zambales Mountains, and this species should be sought there, especially above about 1800 m. The Zambales Mountains are isolated from other highland areas by a broad lowland plain; the Central Cordillera, which has two species of *Megapomys* (*A. abrae* and *A. datae*), is the nearest mountain range, so we doubt that *A. brownorum* occurs outside of the Zambales Mountains.

***Apomys (Megapomys) banahao* sp. nov.**

**HOLOTYPE**—FMNH 178501, adult male collected on 09 May 2004 by Eric A. Rickart, field number EAR 5279. A sample of



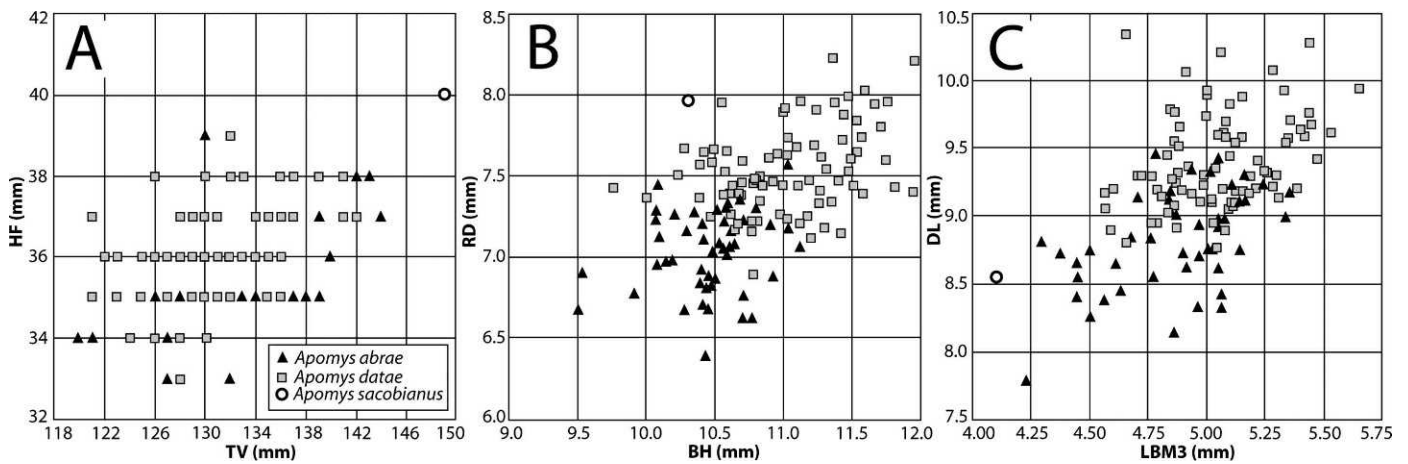


FIG. 21. Bivariate plots of measurements comparing *Apomys abrae*, *A. datae*, and *A. sacobianus*. (A) Length of tail vertebrae (TV) and length of hind foot (HF). (B) Braincase height (BH) and rostral depth (RD). (C) Lingual breadth of palate at M<sup>3</sup> (LBM<sup>3</sup>) and diastema length (DL).

muscle tissue was removed from the thigh in the field and preserved in ethanol before preserving the specimen in formaldehyde. In the museum, the skull was removed and cleaned (see Methods). All parts are in good condition. This specimen will be permanently deposited at the NMP. Measurements are in Table 9.

**TYPE LOCALITY**—Philippines: Luzon Island: Quezon Province: Mt. Banahaw; Barangay Lalo, 1465 m; 14.06635°N, 121.50855°E (from GPS).

**PARATYPES** (n = 137)—Luzon Island: Quezon Prov.: Tayabas Munic.: Brgy. Lalo: Mt. Banahaw, 1465 m (FMNH 178358, 178359, 178397, 178430–178510, 179450–179494, 179496–178500, 179502, 179507, 179508); Tayabas Munic.: Brgy. Lalo: Mt. Banahaw, 1750 m (FMNH 178511–178544, 179503–179506, 179509–179517).

**ETYMOLOGY**—From the traditional Tagalog spelling of the name of the mountain (Banahaw) where this species occurs, used as a noun in apposition.

**DIAGNOSIS AND DESCRIPTION**—A small species of the subgenus *Megapomys* (HBL 125–146 mm, BOL 33.10–35.25 mm) with a fairly short tail (86–103% of HBL). The dorsal pelage is soft, dense, and moderately long; it is dark brown, slightly paler laterally, with slight rusty tints (Fig. 1D). The ventral pelage is dark gray at the base and white washed with pale ashy-gray at the tips. The transition between the dorsal and ventral pelage is usually fairly abrupt. The ears are darkly pigmented. Dark brown fur covers the lower forelimb and about half of the posterior portion of the forepaws and is present as a dark brown area of variable size on about the center of the dorsal surface of the hind foot, with white fur both anterior and posterior. The hind feet are pigmented ventrally (Fig. 10C). The tail is sharply bicolored, with the dorsal surface dark grayish-brown and the ventral surface nearly white.

The cranium of *A. banahaw* (Fig. 28; Table 9) is small, with a moderately long, slender rostrum. The zygomatic plate is wide (2.94–3.52 mm) relative to the length of the cranium. The incisive foramina are short (4.7–5.5 mm) and moderate in width. The maxillary molariform toothrow is moderately short (6.5–7.1 mm), and the toothrow is of moderate width, as shown by the width of M<sup>1</sup> (1.77–2.05 mm). The posterior portion of the palate is more extensively pitted and perforated than any species except *A. magnus* sp. nov., which is similar in

this character. There is no perforation of the bulla for a stapedia artery (the “abrae pattern”; Fig. 5A). The mandible (Fig. 28C) is relatively small and slender, with a short, sharply pointed coronoid process, sturdy angular process, and shallow posterior margin between the condylar and angular processes.

The karyotype of *A. banahaw*, based on three males from Mt. Banahaw (FMNH 178481, 178482, 178524), is 2n = 48, FN ≥ 54 (Fig. 8D). The autosomal complement includes two pairs of small metacentric or submetacentric chromosomes and 21 pairs of telocentric or subtelocentric chromosomes. The X chromosome is large and submetacentric, and the Y is very small and acrocentric.

**COMPARISONS**—*Apomys banahaw* (Fig. 1D) is easily distinguished from *A. datae* (Fig. 1B). It is smaller in nearly all measurements (Tables 2, 9), but with some overlap. Its dorsal pelage is softer and denser and is slightly darker and less rusty-red in tone. The ears of *A. banahaw* are more darkly pigmented. The ventral pelage is paler, and there are fewer dark hairs on the dorsal surface of the hind feet. The rostrum is shorter and less robust, the braincase is more globose and less squarish, the interorbital breadth is less, the palate is narrower, and the bullae lack a foramen for the stapedia artery (“abrae type”; Fig. 5A), which is conspicuous in *A. datae* (Fig. 5B). The interparietals are similar in shape. The mandible of *A. datae* is much larger and proportionately more robust, with a longer, wider coronoid process and broader, longer angular process.

*Apomys banahaw* is equally easily distinguished from *A. magnus* sp. nov., with which it occurs syntopically at middle elevations on Mt. Banahaw. It is smaller on average in virtually all measurements, although with some overlap (Tables 9, 12). A comparison of length of head and body and length of tail distinguishes most individuals (Fig. 29A). Its dorsal pelage is longer and softer (Fig. 1D) and is less rusty than *A. magnus* sp. nov. (Fig. 1E), and it lacks the conspicuous black tips on the dorsal guard hairs of *A. magnus* sp. nov. Its fore- and hind feet have black hairs on the dorsal surface, whereas those of *A. magnus* are nearly entirely white. The ventral pelage of *A. banahaw* is dark gray at the base, with pale gray tips; that of *A. magnus* sp. nov. is pale gray at the base with white tips. Its skull is much smaller and far more gracile, usually with a narrower interorbital region (Fig. 29B). The rostrum of *A. banahaw* is shorter and less robust, and the

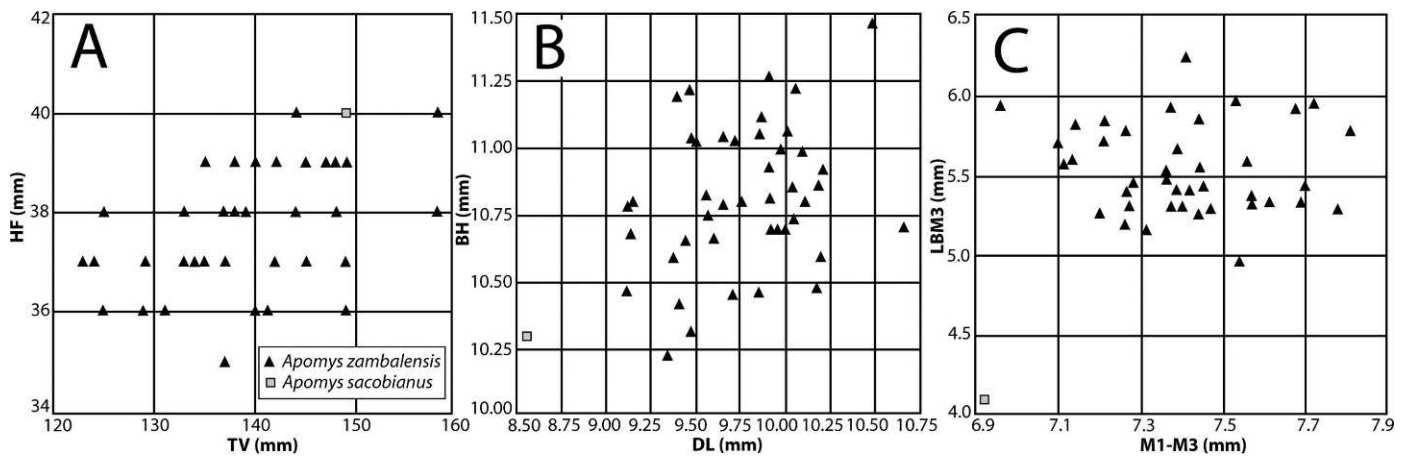


FIG. 22. Bivariate plots of measurements comparing *Apomys sacobianus* and *A. zambalensis* sp. nov. (A) Length of tail vertebrae (TV) and length of hind foot (HF). (B) Diastema length (DL) and braincase height (BH). (C) Length of maxillary molariform toothrow ( $M^1$ – $M^3$ ) and lingual breadth of palate at  $M^3$  (LBM $^3$ ).

braincase is much less square (more globose) than that of *A. magnus* sp. nov. The incisive foramina are less broad, and the zygomatic plate is narrower. The maxillary toothrow is both shorter and narrower, and the palate is narrower (Fig. 29C). The bullae lack a foramen for the stapedial artery (the “*abrae* pattern”; Fig. 5A), which is conspicuous in *A. magnus* sp. nov. (Fig. 5B). The interparietal bone of *A. banahao* is moderate in anteroposterior width; that of *A. magnus* sp. nov. is much wider. The mandible of *A. magnus* sp. nov. is larger and more robust, with a less slender coronoid process and a broader angular process. The combination of clear morphological and genetic differences strongly supports the recognition of these as distinct species.

*Apomys banahao* is generally similar to its sister-species, *A. brownorum*, but differs in having pelage that is paler and shorter, ventral fur that is washed with ashy gray (rather than a pale ochraceous wash), a relatively shorter tail, a larger cranium overall, a narrower  $M^1$  and palate, and usually narrower zygomatic plate and foramina (for details, see above). A PCA of craniodental measurements (Fig. 26; Table 8) reflected these differences, as discussed above.

**DISTRIBUTION**—*Apomys banahao* is known from 1465 to 1750 m on Mt. Banahaw (Figs. 3, 14, 15) and probably occurs from about 1400 m up to the peak at 2177 m. It should be sought on the adjacent mountain, Mt. San Cristobal, which rises to 1470 m. Because Mts. Banahaw and San Cristobal are isolated in a broad, low-elevation plain, we predict that this species will not be found in any other area. If that is the case, then its distribution is among the smallest of *Megapomys* species.

***Apomys (Megapomys) minganensis* sp. nov.**

**HOLOTYPE**—FMNH 190949, adult male collected on 05 June 2006 by Mariano Roy M. Duya, field number MRMD 416. A sample of muscle tissue was removed from the thigh in the field and preserved in ethanol before preserving the specimen in formaldehyde. In the museum, the skull was removed and cleaned (see Methods). All parts are in good condition. This specimen will be permanently deposited at the NMP. Measurements appear in Table 9.

**TYPE LOCALITY**—Philippines: Luzon: Aurora Province: Dingalan Munic.: 1.5 km S, 0.5 km W Mingan peak, 1681 m elevation, 15.46802°N, 121.40039°E (GPS reading).

**PARATYPES** (n = 97)—Luzon Island: Aurora Prov.: Dingalan Munic.: 1.7 km S, 1.3 km W Mingan Peak, 1540 m (FMNH 190941–190946, 190954, 190955); Dingalan Munic.: 1.8 km S, 1.0 km W Mingan Peak, 1677 m (FMNH 190774–190777, 190833–190845, 190847, 190848, 190936–190940); Dingalan Munic.: 1.5 km S, 0.5 km W Mingan Peak, 1681 m (FMNH 190787–190793, 190867–190886, 190947, 190948, 190950–190952, 190956–190960); Dingalan Munic.: 0.9 km S, 0.3 km W Mingan Peak, 1785 m (FMNH 190778–190786, 190849–190866, 191065).

**ETYMOLOGY**—An adjective based on the name of the mountain range (Mingan Mountains) where this species occurs.

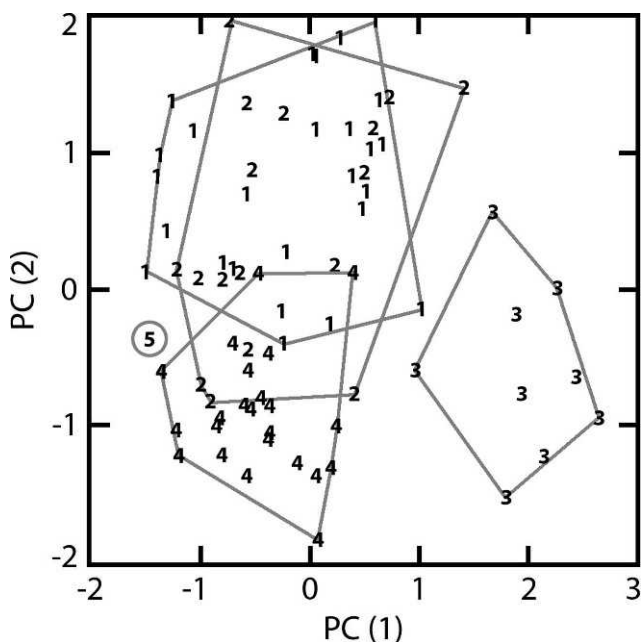


FIG. 23. Results of the principal components analysis of *Apomys aurorae* sp. nov., *A. magnus* sp. nov., *A. sacobianus*, and *A. zambalensis* sp. nov. (see text and Table 7) based on specimens included in Tables 3, 12, and 15. 1 = *A. zambalensis* from Mt. Natib, Bataan Province; 2 = *A. zambalensis* from Mt. Tapulao, Zambales Province; 3 = *A. magnus* from Quezon Province; 4 = *A. aurorae* from Aurora Province; 5 = *A. sacobianus* from Pampanga Province.

TABLE 7. Character loadings, eigenvalues, and percent variance explained on the first four components of a principal components analysis of log-transformed measurements of adult *Apomys aurorae*, *A. magnus*, *A. sacobianus*, and *A. zambalensis* (see Fig. 23 and Methods).

Variable	Principal component			
	1	2	3	4
Basioccipital length	0.894	0.309	0.116	0.126
Interorbital breadth	0.570	-0.427	-0.271	-0.245
Zygomatic breadth	0.837	-0.073	-0.102	-0.017
Mastoid breadth	0.799	-0.188	-0.020	-0.043
Nasal length	0.813	0.156	0.004	0.025
Incisive foramen length	0.515	0.123	-0.013	0.449
Rostral depth	0.721	0.289	0.057	0.098
Rostral length	0.756	0.102	-0.302	0.115
Orbitotemporal length	0.735	-0.214	0.107	0.185
Maxillary tooththrow length	0.727	-0.237	0.330	-0.054
Labial palatal breadth at M <sup>1</sup>	0.753	-0.420	0.038	-0.143
Diastema length	0.651	0.531	-0.291	0.091
Postpalatal length	0.573	0.615	0.301	0.031
Lingual palatal breadth at M <sup>3</sup>	0.540	0.155	-0.479	-0.453
Braincase height	0.564	-0.144	-0.144	-0.283
Breadth of M <sup>1</sup>	0.482	-0.743	0.270	0.043
Breadth of incisors at tip	0.624	0.072	0.409	-0.117
Width of zygomatic plate	0.086	-0.431	-0.380	0.657
Eigenvalue	8.109	2.179	1.124	1.101
Percent variance explained	45.05	12.116	6.25	6.12

DIAGNOSIS AND DESCRIPTION—A fairly small species of *Megapomys* (HBL 128–145 mm, BOL 33.2–35.0 mm; Table 9), with a tail about 94% (range 87–101%) of HBL. The dorsal pelage is dark brown with rusty-orange tips on the hairs, lying over dark gray underfur (Fig. 2E). The ventral pelage is dark gray at the base, with paler tips that usually have an ochraceous wash. On live or fresh specimens, the eyes are noticeably small. The tail is dark brown dorsally, always with some dark hairs and pigment in the scales ventrally; nearly all individuals have a small white tip, 1–4 mm long, on the tail. The dorsal surface of the hind feet is dark brown, with dark brown hairs reaching fully onto the toes; the ventral surface is lightly to heavily pigmented, except the pads, which are usually less darkly pigmented (Fig. 10F). The hallux is long, reaching to or nearly to the top of the adjacent plantar pad (Fig. 10F). The forefeet are almost entirely covered by dark fur that extends down onto the foot from the forearm. The pigmented area at the posterior tip of the scrotum of adult males is very dark brown.

The skull of *A. minganensis* (Fig. 30) is of average overall size in the subgenus *Megapomys*, with a BOL of 33.2–35.0 mm. In general configuration, the skull is similar to those of *A. aurorae* sp. nov. and *A. sierrae* sp. nov. in having a fairly globose braincase, moderately gracile rostrum, broad incisive foramina, lightly pitted palate, and the “datae pattern” of carotid circulation (Fig. 5B). The rostrum of *A. minganensis* is relatively short and narrow, and the orbitotemporal and postpalatal regions are short. The maxillary tooththrow of *A. minganensis* is unusually short, the molars are narrow, and the molar tooththrows are nearly parallel. The interparietal is variable in shape but usually is somewhat narrow in antero-posterior width. The mandible is short and slender, with a short coronoid process and relatively narrow angular process.

COMPARISONS—Compared with the sympatric *A. aurorae* sp. nov., *A. minganensis* differs externally in many respects. *Apomys minganensis* has dark dorsal fur with rusty tips and

dark gray underfur (Fig. 2E), rather than rich rusty-brown fur with medium gray underfur (Fig. 2F), and is darker ventrally, having fur that is dark gray at the base (rather than medium to pale gray), with tips with an ochraceous wash (rather than white or nearly white with a pale ochraceous wash). The hind feet of *A. minganensis* are covered by dark hairs dorsally, whereas those of *A. aurorae* sp. nov. are usually white or have scattered dark hairs that do not reach the base of the toes (i.e., the hair at the base of the toes is white). The hind feet of *A. minganensis* are typically shorter and broader than those of *A. aurorae* sp. nov., and the hallux of *A. aurorae* sp. nov. is shorter, typically reaching only the base or the middle of the adjacent plantar pad (Fig. 10G). The forefeet of *A. minganensis* have dark fur over the entire dorsal surface, but those of *A. aurorae* sp. nov. are usually white, sometimes with dark hairs over a central strip of the forefoot. The tail of *A. minganensis* is always dark dorsally and usually has substantial amounts of pigment and dark hair ventrally, whereas that of *A. aurorae* sp. nov. is dark to medium brown dorsally and either pure white or white with only some scattered dark hairs and bits of dark pigment ventrally. *Apomys minganensis* nearly always has a tiny white tip on the tail (over 95%), whereas *A. aurorae* sp. nov. rarely has such a tip (less than 3%). The tail of *A. aurorae* sp. nov. averages longer than that of *A. minganensis*, and *A. aurorae* n. sp. also averages greater in HBL, but there is considerable overlap in both of these measurements (Fig. 31A).

The skull of *A. minganensis* is also easily distinguished from that of *A. aurorae* sp. nov. There is no overlap in rostral depth, orbital length, or length of the maxillary tooththrow (Tables 9, 15; Fig. 31B,C); the M<sup>1</sup> of *A. minganensis* is narrower; and there is little overlap in lingual breadth of the palate at M<sup>3</sup> (Fig. 31C) or in postpalatal length. Overall, the skull of *A. minganensis* is slightly smaller and less elongate than that of *A. aurorae* sp. nov. The carotid circulation pattern is the same in these two species. The interparietal of *A. minganensis* is usually narrower than that of *A. aurorae* sp. nov. The mandible of *A. aurorae* sp. nov. is larger and more robust than that of *A. minganensis*, with a longer and more slender coronoid process and broader angular process.

*Apomys minganensis* is closely related to *A. sierrae* sp. nov. and also occurs nearby. These two species are easily distinguished. *Apomys minganensis* has longer, denser dorsal fur that is dark brown rather than the rusty reddish-brown of nearby populations of *A. sierrae* sp. nov. (Fig. 2E,C). The ventral fur of *A. minganensis* is usually dark gray at the base and pale gray with an ochraceous wash at the tips, whereas *A. sierrae* sp. nov. has ventral fur that is medium to pale gray at the base and either white or white washed with ochraceous at the tips. The tail of *A. minganensis* is much darker dorsally, always with scattered dark hairs and pigment ventrally; that of *A. sierrae* sp. nov. is less dark dorsally and usually unpigmented ventrally. Additionally, the tip (1–4 mm) of the tail is white dorsally and ventrally in about 95% of *A. minganensis*, whereas that of *A. sierrae* sp. nov. virtually always retains the usual dorsal and ventral color. The dorsal surface of the hind foot of *A. minganensis* is covered by dark hair, whereas that of *A. sierrae* sp. nov. has only a few scattered dark hairs among the predominantly white hair. The hallux of *A. sierrae* sp. nov. is short, reaching only to about the base of the adjacent interdigital plantar pad, whereas that of *A. minganensis* is longer, reaching to the middle or top of the adjacent pad. External measurements of these two species are generally





FIG. 24. Dorsal (A), ventral (B), and lateral (D) views of the cranium and lateral view of the mandible (C) of *Apomys brownorum* sp. nov. (FMNH 183524, holotype); scale bar = 5 mm.

similar and overlapping (Tables 9, 11, 12), but *A. sierrae* sp. nov. averages larger in most respects (e.g., ear and hind foot length; Fig. 32A).

The skull of *A. manganensis* (Fig. 30) is similar to that of *A. sierrae* sp. nov. (Fig. 34), but a number of unambiguous differences are apparent, and there is no overlap in the PC1 and PC2 of cranial measurements in the PCA that includes all *Megapomys* (Fig. 6A). Overall, the skull of *A. manganensis* is a bit shorter and more compact than that of *A. sierrae* sp. nov.,

with a distinctly less robust rostrum (no overlap in rostral depth), a shorter tooththrow with narrower molars, and a palate that is usually narrower (Fig. 32B,C). The maxillary toothrows of *A. manganensis* are nearly parallel, whereas those of *A. sierrae* sp. nov. diverge posteriorly, and the palate of *A. sierrae* sp. nov. is more heavily pitted and perforated. In *A. sierrae* sp. nov., the foramen in the bulla for the stapedia artery is absent (the “abrae pattern”; Fig. 5A), whereas in *A. manganensis*, it is always present (the “datae pattern”; Fig. 5B). The interparietal

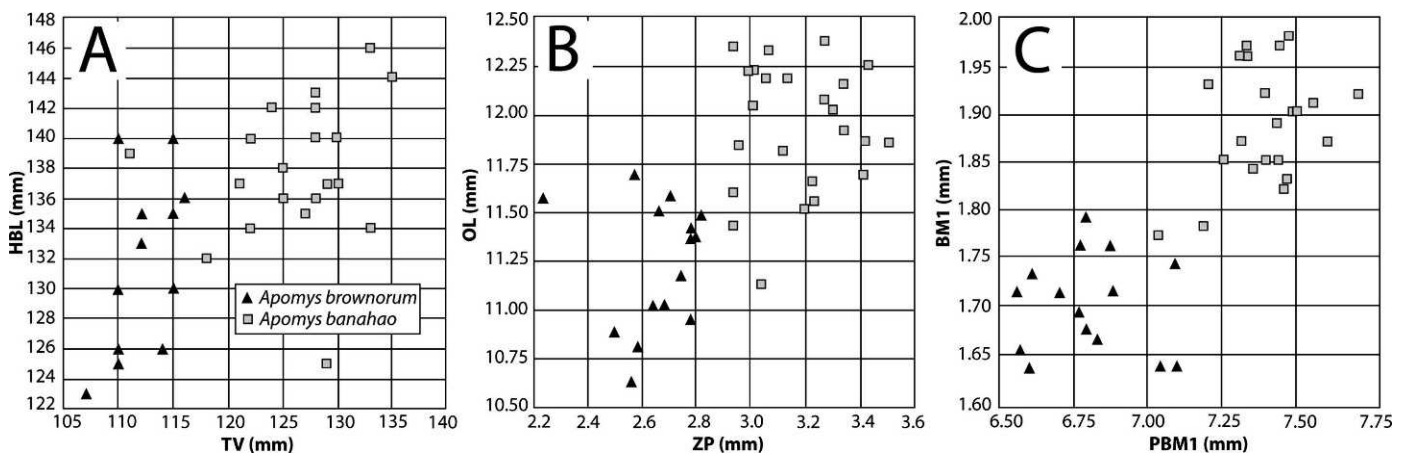


FIG. 25. Bivariate plots of measurements comparing *Apomys brownorum* and *A. banahao* spp. nov. (A) Length of tail vertebrae (TV) and length of head and body (HBL). (B) Zygomatic plate width (ZP) and orbitotemporal length (OL). (C) Labial palatal breadth at  $M^1$  ( $PBM^1$ ) and breadth of  $M^1$  ( $BM^1$ ).

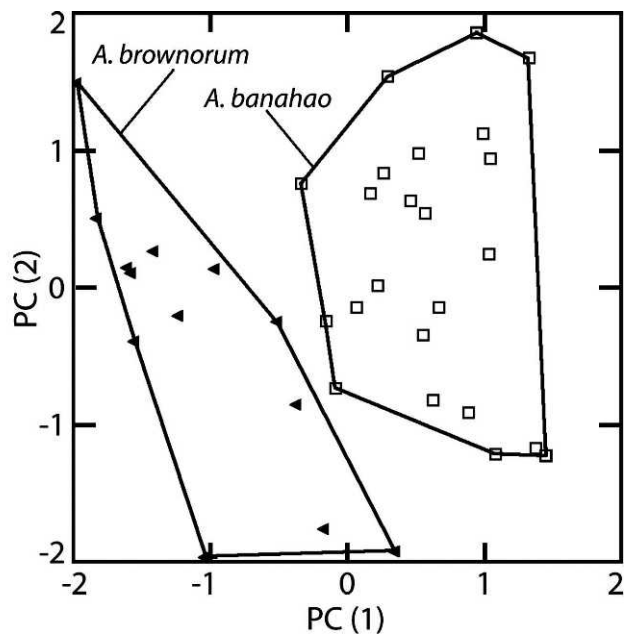


FIG. 26. Results of the principal components analysis of *Apomys brownorum* and *A. banahao* spp. nov. (see text and Table 8) based on specimens in Tables 3 and 9.

of *A. minganensis* is usually anteroposteriorly narrower than that of *A. sierrae* sp. nov. The mandibles are similar, but that of *A. minganensis* is a bit more robust, with a more deeply concave posterior margin between the condylar and angular processes.

To further assess the distinctiveness of *A. minganensis* relative to *A. aurorae* sp. nov. and *A. sierrae* sp. nov., we conducted a PCA of 18 craniodental measurements of our samples of all three species (Tables 9, 11, 12, 15). The first component, which accounted for 40% of the total variance, loaded strongly on nearly all measurements, with rostral length, diastema length, and height of braincase loading least strongly (Table 10). The second component, which accounted for 15% of the variance, loaded most strongly (and positively) on rostral and diastema length and (negatively) on length of the molar tooththrow and breadth of  $M^1$ . PC3 and PC4 had eigenvalues of less than 1.5. A plot of the first two components (Fig. 33) showed *A. minganensis* falling outside of the polygon

TABLE 8. Character loadings, eigenvalues, and percent variance explained on the first four components of a principal components analysis of log-transformed measurements of adult *Apomys banahao* and *A. brownorum* (see Fig. 26 and Methods).

Variable	Principal component			
	1	2	3	4
Basioccipital length	0.897	-0.334	-0.036	-0.004
Interorbital breadth	0.740	0.434	0.282	0.090
Zygomatic breadth	0.901	0.179	0.164	0.104
Mastoid breadth	0.668	0.274	0.447	-0.281
Nasal length	0.635	-0.433	-0.029	-0.303
Incisive foramen length	0.313	0.073	-0.659	-0.019
Rostral depth	0.906	0.114	0.162	0.059
Rostral length	0.434	-0.699	0.065	-0.187
Orbitotemporal length	0.761	0.080	-0.155	-0.331
Maxillary tooththrow length	0.634	-0.149	-0.423	-0.221
Labial palatal breadth at $M^1$	0.880	0.278	-0.217	0.171
Diastema length	0.445	-0.638	0.255	0.278
Postpalatal length	0.845	-0.344	-0.088	0.013
Lingual palatal breadth at $M^3$	0.615	-0.030	0.229	0.613
Braincase height	0.463	0.292	0.517	-0.414
Breadth of $M^1$	0.679	0.399	-0.480	-0.001
Breadth of incisors at tip	0.649	-0.035	0.195	0.046
Width of zygomatic plate	0.804	0.106	-0.267	0.186
Eigenvalue	8.904	1.991	1.754	1.077
Percent variance explained	49.47	11.06	9.75	5.99

of *A. sierrae* sp. nov. and far from that of *A. aurorae* sp. nov. Individuals of *A. minganensis* scored low on PC1, reflecting its small size relative to the other two species, although there was slight overlap at the margins of the polygons. On PC2, *A. minganensis* scored high, reflecting its long rostrum and diastema and short molar tooththrow and narrow  $M^1$ . *Apomys aurorae* sp. nov. scored low on PC2, reflecting its typically shorter rostrum and diastema and longer molar tooththrow and wider  $M^1$ , although these two species showed some overlap on this component. Individuals of *A. sierrae* sp. nov. varied greatly on PC2, overlapping extensively with *A. minganensis*, but most individuals scored lower than those of *A. minganensis*. We conclude that *A. minganensis* differs consistently from these two closely related species. Additional comparisons between *A. aurorae* sp. nov. and *A. sierrae* sp. nov., which overlap extensively on these two components, are made below.

DISTRIBUTION—We captured *A. minganensis* along our transect on the Mingan Mountains from 1540 to 1785 m

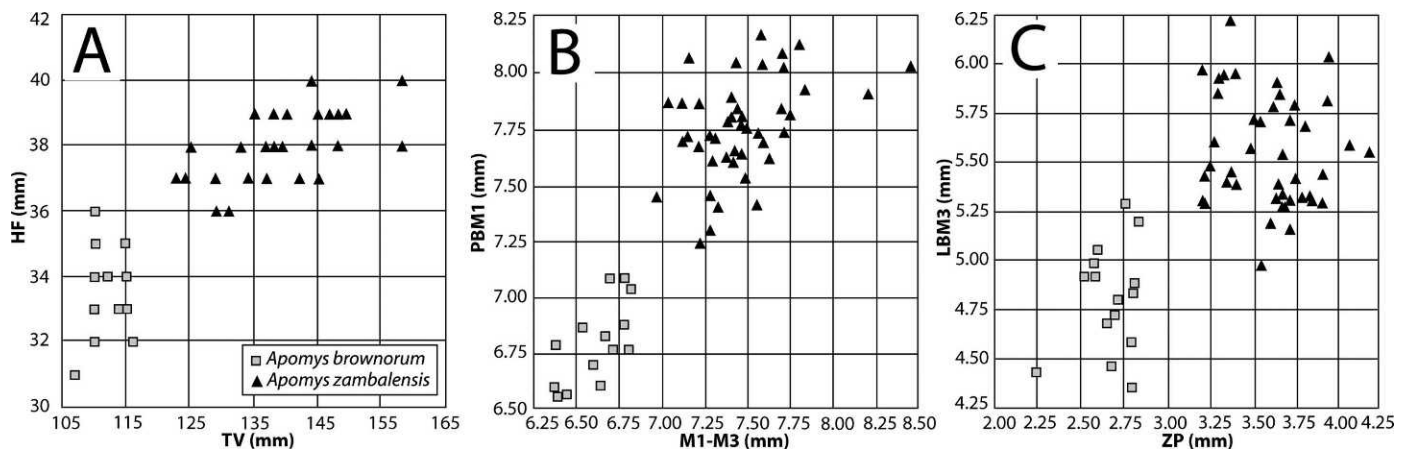


FIG. 27. Bivariate plots of measurements comparing *Apomys brownorum* and *A. zambalensis* spp. nov. (A) Length of tail vertebrae (TV) and length of hind foot (HF). (B) Length of maxillary molariform tooththrow ( $M^1$ – $M^3$ ) and labial palatal breadth at  $M^1$  (PBM $^1$ ). (C) Zygomatic plate width (ZP) and lingual breadth of palate at  $M^3$  (LBM $^3$ ).

TABLE 9. Cranial and external measurements (mean  $\pm$  1 S.D. and range) of *Apomys banahao*, *A. minganensis*, and *A. sierrae* (part).

Measurement	<i>Apomys banahao</i>			<i>Apomys minganensis</i>		
	Mt. Banahaw, 1465–1750 m, Quezon Prov.			Mingan Mtns., 1540–1785 m, Aurora Prov.		
	M-holotype FMNH 178501	M (n = 13)	F (n = 11)	M-holotype FMNH 190949	M (n = 9)	F (n = 10)
Basioccipital length	34.23	34.43 $\pm$ 0.61 (12)	34.13 $\pm$ 0.74	34.82	34.06 $\pm$ 0.47	34.02 $\pm$ 0.55
	—	33.34–35.39	33.10–35.25	—	33.42–34.82	33.16–34.97
Interorbital breadth	5.96	5.98 $\pm$ 0.28 (12)	5.88 $\pm$ 0.18	6.38	6.10 $\pm$ 0.13	6.06 $\pm$ 0.13
	—	5.47–6.33	5.58–6.15	—	5.97–6.38	5.80–6.23
Zygomatic breadth	17.96	18.21 $\pm$ 0.47 (12)	18.22 $\pm$ 0.38	18.03	17.19 $\pm$ 0.48	17.12 $\pm$ 0.23
	—	17.36–18.99	17.69–18.91	—	16.44–18.03	16.81–17.62
Mastoid breadth	14.26	14.29 $\pm$ 0.41 (12)	14.25 $\pm$ 0.28	14.47	14.20 $\pm$ 0.15 (8)	14.04 $\pm$ 0.18
	—	13.71–15.09	13.71–14.55	—	14.02–14.47	13.77–14.29
Nasal length	14.16	13.96 $\pm$ 0.47 (12)	13.99 $\pm$ 0.40	14.02	14.15 $\pm$ 0.28	14.02 $\pm$ 0.40
	—	13.06–14.64	13.40–14.81	—	13.78–14.70	13.55–14.71
Incisive foramen length	5.32	5.20 $\pm$ 0.23 (12)	5.14 $\pm$ 0.27	5.04	5.12 $\pm$ 0.12	5.01 $\pm$ 0.18
	—	4.84–5.53	4.72–5.51	—	4.92–5.30	4.60–5.23
Rostral depth	7.45	7.46 $\pm$ 0.22 (12)	7.47 $\pm$ 0.20	6.78	6.63 $\pm$ 0.13	6.71 $\pm$ 0.14
	—	7.10–7.75	7.23–7.87	—	6.40–6.78	6.43–6.86
Rostral length	14.96	14.96 $\pm$ 0.45 (12)	15.11 $\pm$ 0.36	15.72	15.37 $\pm$ 0.29	15.28 $\pm$ 0.35
	—	14.17–15.70	14.64–15.85	—	15.03–15.72	14.73–15.86
Orbitotemporal length	12.03	11.99 $\pm$ 0.27 (12)	11.88 $\pm$ 0.41	11.29	11.07 $\pm$ 0.17	10.87 $\pm$ 0.30
	—	11.56–12.38	11.13–12.35	—	10.92–11.37	10.39–11.34
Maxillary toothrow length	6.81	6.83 $\pm$ 0.21	6.78 $\pm$ 0.19	6.64	6.63 $\pm$ 0.16	6.67 $\pm$ 0.14
	—	6.47–7.19	6.52–7.09	—	6.45–6.94	6.48–6.95
Labial palatal breadth at M <sup>1</sup>	7.35	7.38 $\pm$ 0.19 (12)	7.43 $\pm$ 0.12	7.43	7.19 $\pm$ 0.18	7.28 $\pm$ 0.17
	—	7.03–7.70	7.18–7.60	—	6.90–7.43	7.05–7.55
Diastema length	9.00	9.33 $\pm$ 0.31 (12)	9.35 $\pm$ 0.36	9.80	9.57 $\pm$ 0.14	9.59 $\pm$ 0.21
	—	8.95–9.86	8.81–9.89	—	9.42–9.82	9.38–9.97
Postpalatal length	12.11	11.88 $\pm$ 0.34 (12)	11.80 $\pm$ 0.29	11.87	11.24 $\pm$ 0.34	11.15 $\pm$ 0.24
	—	11.25–12.53	11.38–12.18	—	10.88–11.87	10.81–11.50
Lingual palatal breadth at M <sup>3</sup>	4.87	4.96 $\pm$ 0.22 (12)	5.07 $\pm$ 0.22	4.90	4.86 $\pm$ 0.08	4.89 $\pm$ 0.16
	—	4.51–5.30	4.69–5.44	—	4.73–4.93	4.68–5.22
Braincase height	11.21	10.80 $\pm$ 0.39 (12)	10.88 $\pm$ 0.26	10.53	10.69 $\pm$ 0.21	10.53 $\pm$ 0.18
	—	10.02–11.44	10.55–11.35	—	10.38–10.96	10.13–10.82
Breadth of M <sup>1</sup>	1.84	1.91 $\pm$ 0.07	1.87 $\pm$ 0.06	1.82	1.80 $\pm$ 0.06	1.81 $\pm$ 0.04
	—	1.77–2.05	1.78–1.98	—	1.70–1.87	1.74–1.87
Breadth of incisors at tip	2.07	2.14 $\pm$ 0.12 (12)	2.26 $\pm$ 0.11	1.98	1.97 $\pm$ 0.05	1.99 $\pm$ 0.08
	—	1.95–2.34	2.09–2.42	—	1.91–2.05	1.85–2.10
Width of zygomatic plate	3.31	3.25 $\pm$ 0.19 (12)	3.08 $\pm$ 0.13	3.57	3.35 $\pm$ 0.15	3.40 $\pm$ 0.17
	—	2.94–3.52	2.94–3.35	—	3.15–3.57	3.09–3.67
Length of head and body	137	137.9 $\pm$ 7.5 (11)	137.3 $\pm$ 4.9 (10)	145	138.2 $\pm$ 4.4	135.3 $\pm$ 5.0 (9)
	—	125–154	128–143	—	132–145	128–141
Total length	266	265.8 $\pm$ 10.4 (11)	261.6 $\pm$ 8.0 (10)	278	269.2 $\pm$ 6.3	260.7 $\pm$ 9.1
	—	250–287	250–271	—	260–279	246–275
Length of tail vertebrae	129	127.9 $\pm$ 4.8 (11)	124.3 $\pm$ 5.9 (10)	133	131.0 $\pm$ 3.6	125.2 $\pm$ 5.9 (9)
	—	118–133	111–130	—	126–138	116–134
Length of hind foot	37	36.5 $\pm$ 0.8 (11)	35.7 $\pm$ 1.2 (10)	34	33.2 $\pm$ 1.1	33.4 $\pm$ 0.8
	—	35–37	33–37	—	31–34	32–35
Length of ear	23	23.2 $\pm$ 0.6 (12)	23.3 $\pm$ 0.7 (10)	18	18.2 $\pm$ 0.4	18.2 $\pm$ 0.4
	—	22–24	22–24	—	18–19	18–19
Weight (g)	80	78.8 $\pm$ 5.9 (12)	80.1 $\pm$ 4.3 (10)	92	76.9 $\pm$ 7.8	73.7 $\pm$ 7.0
	—	71–92	72–86	—	66–92	66–86

(Figs. 3, 14, 15; Balete et al., this volume), and we suspect that it occurs up to the top of the peak at 1910 m. At our two upper sampling areas (1681 and 1785 m), it was the only species of *Megapomys* present. At 1677 m, one of 25 specimens was an *A. aurorae* sp. nov., and at 1540 m one of nine *Megapomys* was *A. aurorae* sp. nov. At 1305, 1074, 902, and 733 m, only *A. aurorae* sp. nov. were captured. We suspect that *A. minganensis* is widespread in the Mingan Mountains above about 1500 m. Our surveys to the north of the Mingan Mountains, in the southern portions of the central Sierra Madre, yielded only specimens of *A. sierrae* sp. nov., and so we consider it unlikely that *A. minganensis* occurs there. No information on small mammals is currently available from the Dingalan Mountains, just to the south of the Mingan Mountains, or from the peaks

of the southern Sierra Madre range in Rizal and adjacent Quezon provinces; surveys there would be valuable to determine whether this species is present, or whether yet more unknown species are present. If this species is indeed confined to the high elevations of the Mingan Mountains, it has one of the smaller ranges among species of *Apomys*.

#### *Apomys (Megapomys) sierrae* sp. nov.

HOLOTYPE—FMNH 185884, adult male collected on 15 June 2005 by Mariano Roy M. Duya, field number MRMD 354B. A sample of muscle tissue was removed from the thigh in the field and preserved in ethanol before preserving the specimen



TABLE 9. *Extended.*

<i>Apomys sierrae</i>				
Mt. Cetaceo, 1300–1400 m, Cagayan Prov.				
M-holotype FMNH 185884	M (n = 8)	F (n = 4)	Mt. Cetaceo, 1500–1550 m, Cagayan Prov.	
			M (n = 12)	F (n = 10)
35.40	35.15 ± 0.46	35.24 ± 0.46	35.31 ± 0.57	35.30 ± 0.50
—	34.32–35.86	34.69–35.64	34.68–36.43	34.70–36.25
6.22	6.09 ± 0.13	6.06 ± 0.33	6.44 ± 0.22	6.30 ± 0.17
—	5.90–6.25	5.58–6.29	6.15–6.77	5.95–6.46
17.89	18.10 ± 0.48	18.24 ± 0.78	18.29 ± 0.48	18.21 ± 0.39
—	17.32–18.99	17.39–18.95	17.60–19.39	17.58–18.76
14.22	14.20 ± 0.27	14.29 ± 0.19	14.61 ± 0.28	14.38 ± 0.34
—	13.78–14.75	14.03–14.45	14.21–15.21	13.68–14.76
14.29	14.05 ± 0.35	13.88 ± 0.39	14.21 ± 0.59 (11)	14.15 ± 0.21
—	13.45–14.61	13.36–14.25	13.49–15.55	13.80–14.50
5.60	5.29 ± 0.45	5.33 ± 0.52	5.28 ± 0.22	5.57 ± 0.16
—	4.55–5.79	4.86–5.99	5.00–5.71	5.28–5.77
7.75	7.49 ± 0.16	7.48 ± 0.21	7.63 ± 0.21 (11)	7.51 ± 0.19
—	7.26–7.75	7.19–7.69	7.23–7.84	7.28–7.78
15.52	14.95 ± 0.48	14.86 ± 0.35	15.12 ± 0.55	15.05 ± 0.43
—	14.21–15.52	14.40–15.19	14.40–16.25	14.59–15.75
11.91	12.05 ± 0.20	11.89 ± 0.16	12.02 ± 0.24	12.13 ± 0.34
—	11.84–12.38	11.66–12.03	11.46–12.30	11.73–12.60
7.30	7.66 ± 0.26	7.55 ± 0.17	7.39 ± 0.19	7.47 ± 0.23
—	7.24–7.93	7.38–7.70	7.11–7.70	7.24–7.91
7.68	7.85 ± 0.29	7.87 ± 0.17	7.82 ± 0.39	7.77 ± 0.27
—	7.62–8.45	7.77–8.12	7.19–8.44	7.25–8.05
9.60	9.16 ± 0.36	9.10 ± 0.31	9.52 ± 0.30	9.56 ± 0.29
—	8.61–9.60	8.81–9.48	9.02–10.00	9.03–10.04
11.92	11.63 ± 0.29	11.60 ± 0.18	11.77 ± 0.28	11.76 ± 0.31
—	11.07–11.92	11.46–11.86	11.21–12.10	11.24–12.26
5.62	5.47 ± 0.21	5.46 ± 0.10	5.44 ± 0.26	5.42 ± 0.22
—	5.17–5.81	5.35–5.55	4.87–5.66	5.10–5.84
10.66	10.63 ± 0.16 (7)	10.72 ± 0.17	10.90 ± 0.31	10.80 ± 0.41
—	10.38–10.78	10.51–10.91	10.41–11.40	9.85–11.30
1.90	1.93 ± 0.09	1.89 ± 0.09	1.91 ± 0.07	1.89 ± 0.08
—	1.82–2.04	1.80–1.97	1.83–2.02	1.73–2.03
2.28	2.16 ± 0.10 (7)	2.11 ± 0.08	2.28 ± 0.09	2.30 ± 0.12
—	1.98–2.28	2.04–2.22	2.14–2.40	2.06–2.53
3.68	3.58 ± 0.26	3.67 ± 0.12	3.56 ± 0.21	3.48 ± 0.25
—	3.34–4.19	3.50–3.77	3.29–3.85	3.07–3.87
131	133.4 ± 6.4	140.8 ± 6.8	143.3 ± 8.7 (10)	140.6 ± 4.2 (9)
—	124–144	134–148	132–163	135–146
271	267.1 ± 6.2	276.3 ± 4.6	274.4 ± 12.5 (10)	272.1 ± 7.9 (9)
—	254–273	271–282	260–295	260–281
140	133.8 ± 4.4	135.5 ± 5.0	131.6 ± 6.7 (11)	131.6 ± 6.4 (9)
—	129–140	129–141	124–148	118–137
37	35.5 ± 1.0	35.1 ± 0.9	36.7 ± 1.2	35.7 ± 1.0 (9)
—	34–37	34–36	35–39	34–37
19	19.0 ± 0.9	19.6 ± 1.0	20.2 ± 0.6	19.7 ± 0.7 (9)
—	18–21	18–20	19–21	18–20
90	84.5 ± 5.9	81.5 ± 6.6	84.9 ± 9.5 (11)	77.2 ± 4.6 (9)
—	73–92	74–88	75–110	72–85

in formaldehyde. In the museum, the skull was removed and cleaned (see Methods). All parts are in good condition. This specimen will be permanently deposited at the NMP. Measurements appear in Table 9.

TYPE LOCALITY—Philippines: Luzon: Cagayan Province: 3.5 km SW Mt. Cetaceo peak, 1400 m elevation, 17.69561°N, 122.01683°E.

PARATYPES (n = 408)—Luzon Island: Cagayan Prov.: 1.5 km SW Mt. Cetaceo peak, 1550 m (FMNH 185834–185841, 185861–185880, 185900, 185946, 185961); 2.0 km SW Mt. Cetaceo peak, 1500 m (FMNH 185805, 185815–185833, 185842–185845, 185854–185860, 185896–185898, 185904, 185905, 185938–185945, 185955–185960); 3.5 km SW Mt. Cetaceo peak, 1400 m (FMNH 185803–185814, 185846–185853, 185881, 185883, 185885–185895, 185899, 185901–185903, 185906,

185936, 185937, 185947–185954, 185962–185970); Baggao Munic.: Barrio Via, Sitio Hot Springs, W Foothills Sierra Madre Mtns., 760–800 m (USNM 574889); Callao Munic.: Mt. Cetaceo, 1450 m (FMNH 147166–147169); Gonzaga Munic.: Brgy. Magrafil: Sitio Masok: Mt. Cagua, 800 m (FMNH 176562–176576); Penablanca Munic.: Brgy. Lapi: Sitio Baua: Mt. Cetaceo, 1300 m (FMNH 180298–180364); Penablanca Munic.: Brgy. Mangga: Sitio Lowak: Mt. Cetaceo, 1100 m (FMNH 176552–176558).

Isabela Prov.: Los Dos Cuernos, E of Tuguegarao (FMNH 142060); Mt. Dipalayag, E of San Mariano (FMNH 142061, 142062).

Nueva Vizcaya Prov.: Quezon Munic.: 0.8 km N, 0.55 km E Mt. Palali peak, 1420 m (FMNH 186726–186760, 186778, 186786, 186820–186825, 194934–194947); Quezon Munic.:

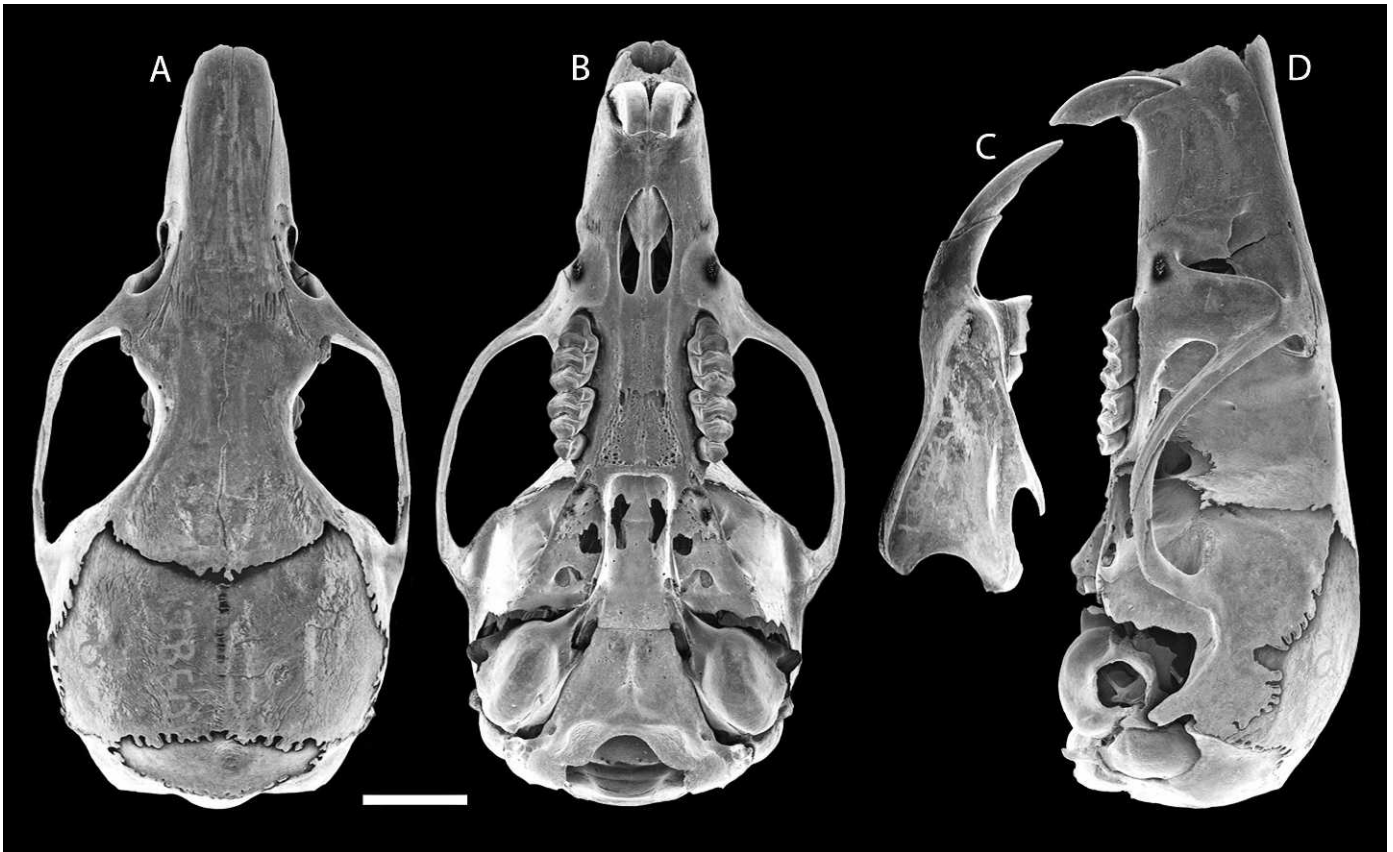


FIG. 28. Dorsal (A), ventral (B), and lateral (D) views of the cranium and lateral view of the mandible (C) of *Apomys banahao* sp. nov. (FMNH 178501, holotype); scale bar = 5 mm.

1.75 km N, 0.1 km E Mt. Palali peak, 1300 m (FMNH 194948–194961); Quezon Munic.: 2.75 km N, 0.3 km W Mt. Palali peak, 1040 m (FMNH 194962–194977); Quezon Munic.: 3.05 km N, 0.1 km E Mt. Palali peak, 900 m (FMNH 194978–194998); Quezon Munic.: 3.35 km N, 0.5 km W Mt. Palali peak, 780 m (FMNH 194999–195015); Quezon Munic.: Mt. Palali peak, 1700 m (FMNH 186761–186777, 186779–186785, 186826, 186827, 194923–194933).

Quirino Prov.: Nagtipunan Munic.: Brgy. Disimungal: Sitio Km 18: Mt. Lataan, 1200 m (FMNH 176559–176561);

Nagtipunan Munic.: Brgy. Matmad: Sitio Mangitagud: Mungiao Mtns., 450 m (FMNH 180365–180373).

Palau Island: Cagayan Prov.: Sta. Ana Munic.: Brgy. San Vicente: 4.25 km S of Cape Engano Lighthouse, 153 m (FMNH 191232–191237).

ETYMOLOGY—From the name of the mountain range (Sierra Madre) where most of the specimens of this species originated, used as a noun in the genitive case.

DIAGNOSIS AND DESCRIPTION—A species of the subgenus *Megapomys* of average size (HBL 124–171 mm, averaging

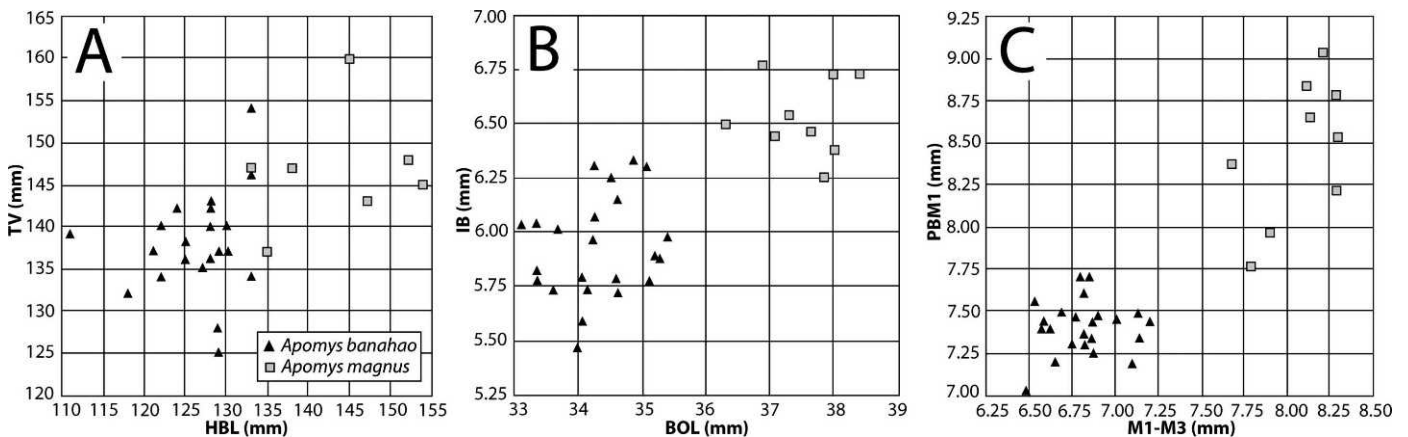


FIG. 29. Bivariate plots of measurements comparing *Apomys banahao* and *A. magnus* spp. nov. (A) Head and body length (HBL) and length of tail vertebrae (TV). (B) Basioccipital length (BOL) and interorbital breadth (IB). (C) Length of maxillary molariform tooththrow ( $M^1$ – $M^3$ ) and labial palatal breadth at  $M^1$  (PBM $^1$ ).



FIG. 30. Dorsal (A), ventral (B), and lateral (D) views of the cranium and lateral view of the mandible (C) of *Apomys manganensis* sp. nov. (FMNH 190949, holotype); scale bar = 5 mm.

133–150 mm; weight 73–111 g, averaging 79–88 g), with a tail that is about equal to the HBL (85–111%, averaging 95–102%). In the Sierra Madre range, the dorsal pelage is dark brown with conspicuous rusty-reddish tints (Fig. 2C); on Mt. Palali in the Caraballo Mountains, the dorsal pelage is a medium brown with yellow tint, and the skin of the ears and feet are paler than in individuals from the Sierra Madre (Fig. 2D). The ventral pelage is medium to pale gray at the

base and white or white washed with pale ochraceous at the tips. The tail is sharply bicolored, dark brown dorsally (somewhat paler on individuals from Mt. Palali) and usually white (unpigmented) ventrally. As with most species of *Apomys*, a few individuals (less than 5%) have a white tip on the tail. The dorsal surface of the hind foot of *A. sierrae* is mostly white, with only a few scattered dark hairs. The ventral surface is moderately to darkly pigmented (darker on those

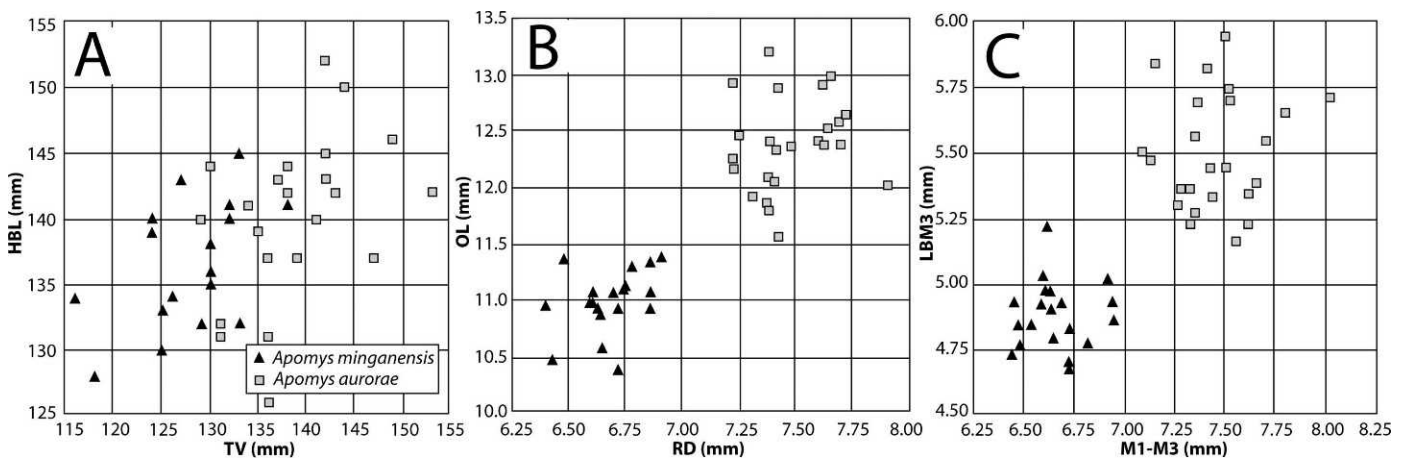


FIG. 31. Bivariate plots of measurements comparing *Apomys manganensis* and *A. aurorae* spp. nov. (A) Length of tail vertebrae (TV) and length of head and body (HBL). (B) Rostral depth (RD) and orbitotemporal length (OL). (C) Length of maxillary molariform tooththrow ( $M^1$ – $M^3$ ) and lingual breadth of palate at  $M^3$  (LBM $^3$ ).



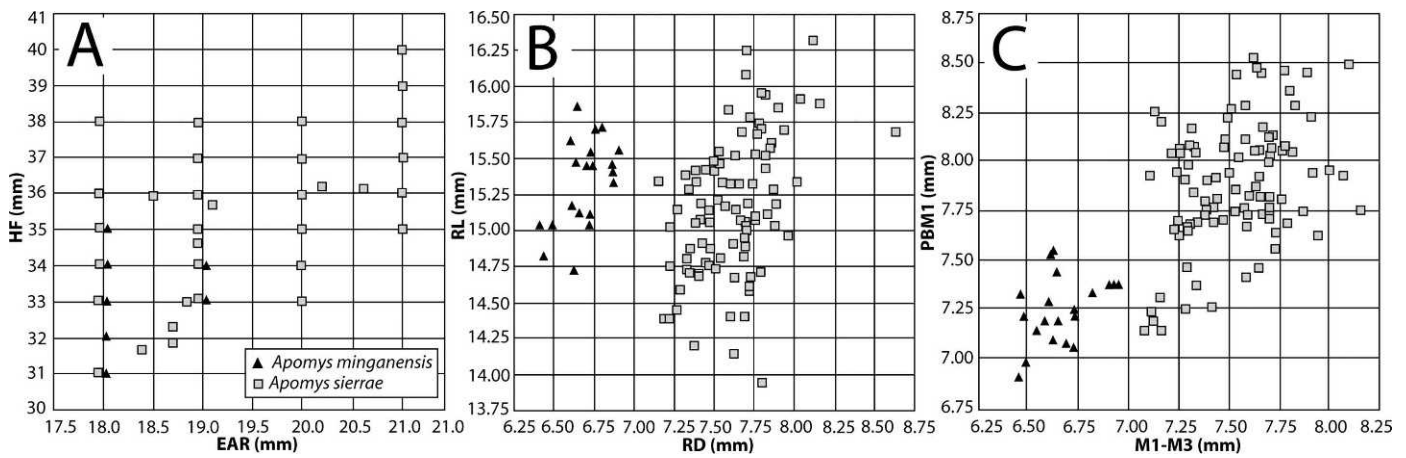


FIG. 32. Bivariate plots of measurements comparing *Apomys minganensis* and *A. sierrae* spp. nov. (A) Length of ear (EAR) and length of hind foot (HF). (B) Rostral depth (RD) and rostral length (RL). (C) Length of the maxillary tooththrow ( $M^1-M^3$ ) and labial palatal breadth at  $M^1$  (PBM $^1$ ).

from the Sierra Madre than from Mt. Palali), with relatively small plantar pads, and the hallux is short, usually extending only to about the base of the adjacent interdigital plantar pad (Fig. 10E).

The skull of *A. sierrae* (Fig. 34) is of average size within *Megapomys* (BOL 33.5–37.5 mm, with individual populations averaging 35.1–36.1 mm; Tables 9, 11, 12). It is most similar overall to several of the species to which it is most closely related: *A. aurorae* sp. nov., *A. minganensis*, and *A. zambalensis* sp. nov. (*Apomys magnus* sp. nov. is much larger and differs in other respects.) The rostrum is rather long and slender, and the braincase is globose and slightly elongated. The maxillary molar teeth are rather narrow, and the tooththrows diverge posteriorly. The palate is unusually heavily perforated and pitted, and the postpalatal region is of average length. The foramen for the stapedia artery in the bulla is absent (the “abrae pattern”; Fig. 5A). The interparietal is

usually anteroposteriorly wide. The mandible (Fig. 34C) is rather slender. The coronoid process is relatively erect (less posteriorly directed) and sharply pointed, the angular process is relatively narrow, and the posterior margin between the condylar and angular processes is deeply concave.

As noted above, our samples from Cagayan, Quirino, and Nueva Vizcaya provinces show no geographic pattern of genetic relatedness, even though they come from distant mountains and from Palau Island (Figs. 3, 7, 35). Our sample from Palau Island showed slight genetic differentiation (Fig. 7), and cranial measurements are slightly smaller than those on the nearby mainland (Tables 9, 11, 12), but the latter is explained in part by the fact that all three Palau Island specimens were young animals with partially open cranial sutures and had not completed growth. Specimens from Nueva Vizcaya have paler fur than those from Cagayan and Quirino but are otherwise externally indistinguishable. Comparison of measurements (Tables 9, 11, 12) shows extensive overlap of individuals from all of our samples, and we have noted no discrete cranial differences among them.

To further investigate possible divergence within the set of populations here referred to *A. sierrae*, we conducted a PCA of 18 craniodental measurements of the individuals included in Tables 9, 11, and 12. In this analysis, we broke our samples not only into those from each geographic locality, but also designated them by groups on the basis of elevation along the Mt. Cetaceo and Mt. Palali transects because often two species of *Megapomys* are present at different elevations on Luzon mountains (see Discussion). The first PC, which accounted for 34% of the total variance, loaded heavily on all measurements except length of upper molar tooththrow, breadth of  $M^1$ , and height of braincase (Table 13), thus generally indicating size and robustness. The second component, which accounted for 14% of the variance, loaded heavily on length of upper molar tooththrow, palatal breadth at  $M^1$ , and breadth of  $M^1$ ; diastema length and postpalatal length loaded negatively. Subsequent components had eigenvalues of less than 1.5.

Inspection of the scores of individuals on the first two components (Fig. 36) shows nearly complete overlap on the first component, with six individuals from Mt. Palali scoring outside of the primary range of values (i.e., scoring higher than 1.5 on PC1). These individuals (FMNH 186777, 194926, 194970,

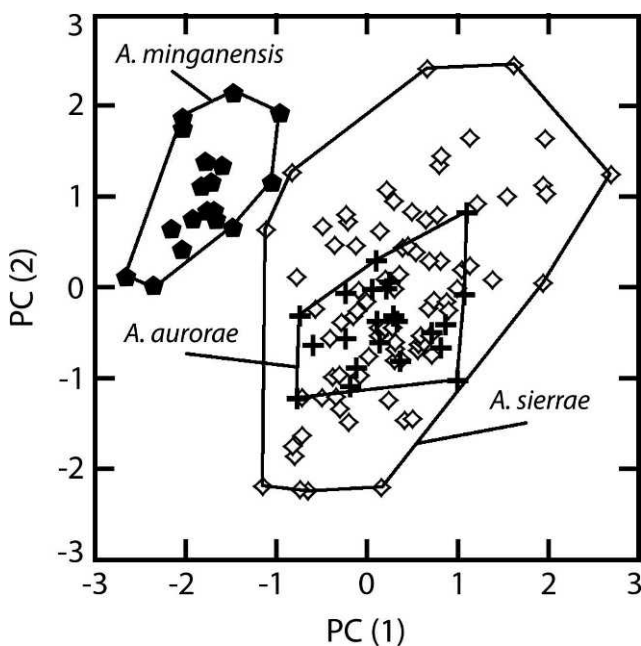


FIG. 33. Results of the principal components analysis of *Apomys aurorae*, *A. minganensis*, and *A. sierrae* spp. nov. (see text and Table 10) based on specimens in Tables 9, 11, 12, and 15.

TABLE 10. Character loadings, eigenvalues, and percent variance explained on the first four components of a principal components analysis of log-transformed measurements of adult *Apomys aurorae*, *A. minganensis*, and *A. sierrae* (see Fig. 33 and Methods).

Variable	Principal component			
	1	2	3	4
Basioccipital length	0.828	0.332	-0.092	0.261
Interorbital breadth	0.427	0.490	-0.325	-0.276
Zygomatic breadth	0.836	-0.005	0.050	-0.130
Mastoid breadth	0.619	0.245	0.041	-0.333
Nasal length	0.487	0.459	0.343	-0.242
Incisive foramen length	0.566	0.019	0.192	0.228
Rostral depth	0.854	-0.165	0.049	0.072
Rostral length	0.330	0.698	0.334	-0.180
Orbitotemporal length	0.823	-0.156	-0.131	0.239
Maxillary toothrow length	0.692	-0.576	-0.071	0.036
Labial palatal breadth at M <sup>1</sup>	0.829	-0.276	0.266	-0.203
Diastema length	0.245	0.758	0.073	0.224
Postpalatal length	0.592	0.386	-0.303	0.344
Lingual palatal breadth at M <sup>3</sup>	0.753	-0.222	0.153	0.008
Braincase height	0.321	0.035	-0.666	-0.477
Breadth of M <sup>1</sup>	0.520	-0.529	0.229	-0.291
Breadth of incisors at tip	0.676	-0.160	-0.320	0.110
Width of zygomatic plate	0.439	-0.172	0.031	0.262
Eigenvalue	7.191	2.679	1.200	1.081
Percent variance explained	39.95	14.88	6.67	6.01

195007, 195014, 195015) have unusually heavily worn teeth and skulls that are more robust than usual; they appear simply to be “old adults” that are otherwise not distinguishable from other individuals from Mt. Palali. On PC2, individuals from Palau Island, two from Mt. Cagua (which is the sample on mainland Luzon nearest to Palau Island; Figs. 3, 35) and four from Mt. Cetaceo, score near one another, outside of the primary range of values (i.e., they have scores lower than -1.5). As noted above, the three from Palau Island are young adults that have not fully completed growth; the same is true for the two from Cagua and four from Cetaceo that have low scores. The differences in measurements are largely those associated with unworn teeth. We note no differences in the crania that are not associated with their young age.

Aside from variation associated with these outliers, which we ascribe to age-related differences, all individuals assigned here to *A. sierrae* fall in a tight area of overlap in the plot of PC1 vs. PC2, and we conclude that craniodental morphometric variation is slight. Because the extent of geographic variation in *cyt b* also is slight, we hypothesize that all of these populations represent a single, widespread species.

COMPARISONS—*Apomys sierrae* is easily distinguished from its close relative *A. minganensis*, as described in detail above (Fig. 32); *A. minganensis* has longer, denser, and darker dorsal fur and many dark hairs on the dorsal surface of the hind foot, and the hallux is long, reaching nearly to the top of the adjacent plantar pad, rather than reaching only to the bottom of the pad as in *A. sierrae*. The skull has a shorter toothrow with narrower molars and a foramen in the bulla for the stapedial artery that is relatively large and conspicuous, rather than absent (Fig. 5). A PCA of craniodental measurements comparing *A. sierrae* with *A. minganensis* also showed discrete differences (Fig. 33; Table 10; see *A. minganensis* account, above).

*Apomys sierrae* differs from *A. magnus* sp. nov., to which it is closely related, by usually being smaller (e.g., HBL averaging 133–150 mm vs. 145–148 mm, BOL 35.1–36.1 mm

vs. 37.0–37.7 mm). The dorsal pelage of *A. sierrae* (Fig. 2C,D) is dark brown with rusty reddish tones or a rich rusty orange-brown, whereas that of *A. magnus* (Fig. 1E) is dark brown with prominent black guard hairs and virtually no reddish tones. Ventrally, *A. sierrae* has fur that is dark gray at the base and pale gray at the tip with an ochraceous wash, whereas that of *A. magnus* sp. nov. is somewhat paler gray at the base and nearly white at the tip. The ventral surface of the hind foot is usually darkly pigmented in both species, but the hallux of *A. magnus* sp. nov. is longer, reaching nearly to the top of the adjacent plantar pad, rather than only to its base (Fig. 10D,E). A comparison of hind foot length against weight for the two species shows little overlap (Fig. 37A).

The crania of *A. sierrae* and *A. magnus* sp. nov. differ conspicuously. That of *A. magnus* is generally larger and more robust, with little overlap in basioccipital length, interorbital breadth, zygomatic breadth, mastoid breadth, nasal length, length of the incisive foramina, length of the maxillary toothrows, and palatal breadth. Plots of orbital length against postpalatal length, and of rostral length against depth, show good but not complete separation among nearly all individuals (Fig. 37B,C); additionally, the stapedial foramen in the bulla is large and conspicuous in *A. magnus* (the “datae pattern”; Fig. 5B) but absent in *A. sierrae* (the “abrae pattern”; Fig. 5A), allowing easy identification of skulls.

To further investigate differences between *A. sierrae* and *A. magnus* sp. nov. and the closely related *A. zambalensis* sp. nov., we conducted a PCA of 18 craniodental measurements. The first principal component (PC1), which accounted for 40% of the total variance, loaded heavily on nearly all measurements, indicating that this is largely an indicator of size and robustness; only width of zygomatic plate and breadth of M<sup>1</sup> loaded less strongly (Table 14). PC2 loaded strongly (and positively) on length of the upper molar toothrow, palatal breadth at M<sup>1</sup>, and breadth of M<sup>1</sup> and strongly (but negatively) on diastema length and postpalatal length. Subsequent components had eigenvalues less than 1.2. A plot of PC1 and PC2 (Fig. 38) shows that *A. magnus* sp. nov. scored higher than *A. sierrae* on PC1 with limited overlap, confirming its generally large size. There was complete overlap on PC2. As noted below, *A. sierrae* is easily distinguished from *A. zambalensis* sp. nov. with the use of qualitative features and some craniodental features; this morphometric analysis shows that they do not differ in overall size, but they generally differ on PC2, although with overlap, confirming the utility of dental measurements, diastema length, and postpalatal length in distinguishing most individuals, as discussed below. Given the extent of morphological and genetic differences among these species, we regard each as distinct from the others.

*Apomys sierrae* differs from *A. aurorae* sp. nov., its closest geographic neighbor, usually in subtle ways, reflecting the relatively close phylogenetic relationship evident in Figure 7. Their external dimensions are similar; *A. sierrae* tends to have a longer hind foot, but the means of other measurements are similar (Fig. 39A; Tables 9, 11, 12, 15). The dorsal pelage is rusty brown on both species, but has more of a yellow tint in *A. aurorae* sp. nov. (Fig. 2F) and a more reddish tint in *A. sierrae* (Fig. 2C). The ventral pelage of the two species is similar. Dark hairs extend down further on the forelimbs of *A. sierrae*, reaching the base of the paws, whereas there is only white fur on the lower forelimbs and forepaws of *A. aurorae* sp. nov. The dorsal surface of the hind foot of *A. sierrae* is

TABLE 11. Cranial and external measurements (mean  $\pm$  1 S.D. and range) of *Apomys sierrae* (part).

Measurement	<i>Apomys sierrae</i>					
	Mt. Cagua, 800 m, Cagayan Prov.		Mt. Lataan, 1200 m, Quirino Prov.		Mungiao Mtns., 450 m, Quirino Prov.	
	M (n = 4)	F (n = 1)	M (n = 1)	F (n = 2)	M (n = 2)	F (n = 3)
Basioccipital length	35.70 $\pm$ 1.44 (3) 34.67–37.35	35.98 —	— —	35.18 $\pm$ 1.09 34.41–35.95	34.60 (1) —	34.73 $\pm$ 0.75 (2) 34.20–35.26
Interorbital breadth	6.17 $\pm$ 0.26 5.82–6.41	6.30 —	— —	5.98 $\pm$ 0.11 5.90–6.05	6.15 $\pm$ 0.25 5.97–6.32	6.15 $\pm$ 0.04 (2) 6.12–6.18
Zygomatic breadth	17.52 $\pm$ 0.42 16.97–17.96	17.66 —	— —	17.93 $\pm$ 0.89 17.30–18.56	18.24 $\pm$ 0.47 17.90–18.57	18.06 $\pm$ 0.23 (2) 17.89–18.22
Mastoid breadth	14.14 $\pm$ 0.18 14.02–14.41	14.23 —	— —	13.68 $\pm$ 0.35 13.43–13.93	14.27 $\pm$ 0.13 14.18–14.36	14.06 $\pm$ 0.69 (2) 13.57–14.54
Nasal length	14.67 $\pm$ 0.50 (3) 14.36–15.24	15.12 —	— —	14.49 $\pm$ 0.17 14.37–14.61	14.36 (1) —	14.27 $\pm$ 0.02 (2) 14.25–14.28
Incisive foramen length	5.30 $\pm$ 0.08 (3) 5.23–5.39	5.87 —	— —	4.96 $\pm$ 0.06 4.91–5.00	5.24 (1) —	5.73 $\pm$ 0.01 (2) 5.72–5.73
Rostral depth	7.57 $\pm$ 0.19 (3) 7.42–7.78	7.70 —	— —	7.55 $\pm$ 0.47 7.22–7.88	7.40 (1) —	7.79 $\pm$ 0.11 (2) 7.71–7.86
Rostral length	15.45 $\pm$ 0.27 (3) 15.19–15.72	15.19 —	— —	15.03 $\pm$ 0.01 15.02–15.03	14.70 (1) —	14.95 $\pm$ 0.49 (2) 14.60–15.29
Orbitotemporal length	12.16 $\pm$ 0.32 11.76–12.48	12.84 —	— —	12.21 $\pm$ 0.32 11.98–12.43	12.13 $\pm$ 0.71 11.63–12.63	12.14 $\pm$ 0.09 (2) 12.08–12.20
Maxillary tooththrow length	7.41 $\pm$ 0.22 7.15–7.60	7.29 —	7.69 —	7.64 $\pm$ 0.01 7.63–7.65	7.72 $\pm$ 0.27 7.53–7.91	8.01 $\pm$ 0.17 7.82–8.15
Labial palatal breadth at M <sup>1</sup>	7.57 $\pm$ 0.23 7.31–7.83	7.98 —	7.81 —	7.76 $\pm$ 0.42 7.46–8.05	8.05 $\pm$ 0.26 7.86–8.23	7.98 $\pm$ 0.26 7.75–8.27
Diastema length	9.62 $\pm$ 0.69 (3) 8.83–10.12	9.99 —	— —	9.52 $\pm$ 0.50 9.17–9.87	9.06 (1) —	9.13 $\pm$ 0.21 (2) 8.98–9.27
Postpalatal length	11.88 $\pm$ 0.62 11.50–12.81	11.82 —	— —	11.70 $\pm$ 0.51 11.34–12.06	11.81 $\pm$ 0.29 11.60–12.01	11.19 $\pm$ 0.25 (2) 11.01–11.36
Lingual palatal breadth at M <sup>3</sup>	5.24 $\pm$ 0.04 5.20–5.30	5.33 —	— —	5.42 $\pm$ 0.34 5.18–5.66	5.37 $\pm$ 0.33 5.13–5.60	5.49 $\pm$ 0.33 (2) 5.26–5.72
Braincase height	10.99 $\pm$ 0.33 10.63–11.35	10.45 —	— —	10.54 $\pm$ 0.62 10.10–10.97	10.81 $\pm$ 0.72 10.30–11.32	10.64 $\pm$ 0.16 (2) 10.52–10.75
Breadth of M <sup>1</sup>	1.81 $\pm$ 0.11 1.70–1.93	1.94 —	1.97 —	1.99 $\pm$ 0.00 1.99	2.04 $\pm$ 0.04 2.01–2.07	2.03 $\pm$ 0.07 1.95–2.08
Breadth of incisors at tip	2.19 $\pm$ 0.07 (3) 2.12–2.26	2.30 —	— —	2.34 $\pm$ 0.02 2.32–2.35	2.19 (1) —	2.24 $\pm$ 0.06 (2) 2.19–2.28
Width of zygomatic plate	3.50 $\pm$ 0.20 3.22–3.69	3.59 —	— —	3.79 $\pm$ 0.01 3.78–3.80	3.85 $\pm$ 0.00 3.85	3.61 $\pm$ 0.22 (2) 3.45–3.76
Length of head and body	132.4 $\pm$ 9.4 (3) 122–141	— —	133 —	149 (1) —	143.0 $\pm$ 8.5 137–149	134.7 $\pm$ 4.0 131–139
Total length	271.0 $\pm$ 19.3 (3) 250–288	277 —	262 —	296 (1) —	286.5 $\pm$ 19.1 273–300	274.0 $\pm$ 12.3 265–288
Length of tail vertebrae	138.6 $\pm$ 9.9 (3) 128–147	— —	129 —	139.3 $\pm$ 10.3 132–147	143.5 $\pm$ 10.6 136–151	139.3 $\pm$ 8.4 134–149
Length of hind foot	33.2 $\pm$ 1.8 32–36	32 —	33 —	34.0 $\pm$ 0.0 34	36.5 $\pm$ 2.1 35–38	35.0 $\pm$ 2.0 33–37
Length of ear	18.8 $\pm$ 0.3 18–19	19 —	20 —	20.0 $\pm$ 0.0 20	21.0 $\pm$ 0.0 21	20.0 $\pm$ 1.0 19–21
Weight (g)	84.3 $\pm$ 8.3 78–96	106 —	66 —	79.0 $\pm$ 17.0 67–91	86.0 $\pm$ 14.1 76–96	79.3 $\pm$ 13.6 64–90

primarily white, with a few scattered dark hairs, whereas that of *A. aurorae* sp. nov. is either white or has scattered dark hairs, except for having pure white adjacent to and on the toes. Both species have a short hallux that reaches only about to the bottom of the adjacent plantar pad. The two species are most readily distinguished on the basis of the basicranial carotid circulatory pattern. In *A. sierrae*, the foramen for the stapedia artery in the bulla is absent (the “abrae pattern”; Fig. 5A), whereas in *A. aurorae* sp. nov., it is small but always present (the “datae pattern”; Fig. 5B). The configuration of the skulls is similar, and the PCA of cranial measurements shows that individuals of *A. aurorae* sp. nov. fall entirely within the plots of *A. sierrae* (Fig. 33; Table 10). However, close inspection

shows the skull of *A. sierrae* is slightly more elongate, usually with a slightly shorter rostrum and orbitotemporal fossa (Fig. 39C), and a braincase that is less broad. The maxillary tooththrows of *A. sierrae* usually are slightly narrower and they diverge posteriorly to a greater degree than in *A. aurorae* sp. nov. The zygomatic plate of *A. sierrae* tends to be narrower than that of *A. aurorae* sp. nov. (Figs. 34, 39B). The interparietal bones of the two species are variable, but usually similar in width. The mandible of *A. aurorae* sp. nov. is slightly deeper, and the posterior margin between the condylar and angular processes is less concave. Although most differences are slight, the discrete difference in the form of the carotid circulatory system and the genetic monophyly of the two



TABLE 11. *Extended.*

<i>Apomys sierrae</i>					
Mt. Palali, 700–839 m, Nueva Vizcaya Prov.		Mt. Palali, 1052–1259 m, Nueva Vizcaya Prov.		Mt. Palali, 1434–1443 m, Nueva Vizcaya Prov.	
M (n = 7)	F (n = 2)	M (n = 2)	F (n = 4)	M (n = 8)	F (n = 12)
36.13 ± 0.78 (6)	35.25 ± 0.40	35.19 ± 2.01	34.57 ± 0.70	34.68 ± 0.75	35.07 ± 0.70
35.52–37.52	34.97–35.53	33.77–36.61	33.55–35.12	33.49–35.63	34.44–36.80
6.23 ± 0.19 (6)	6.24 ± 0.21	6.13 ± 0.46	6.13 ± 0.38	6.05 ± 0.19	5.91 ± 0.16
6.05–6.54	6.09–6.38	5.80–6.45	5.57–6.38	5.76–6.32	5.64–6.22
18.76 ± 0.50 (6)	17.75 ± 0.26	18.47 ± 0.71	18.34 ± 0.80	18.18 ± 0.22	18.36 ± 0.55
18.05–19.55	17.56–17.93	17.96–18.97	17.45–19.18	17.84–18.58	17.42–19.48
14.83 ± 0.59 (6)	14.21 ± 0.27	14.78 ± 0.21	14.30 ± 0.48	14.43 ± 0.16	14.45 ± 0.38
13.99–15.36	14.02–14.40	14.63–14.92	13.97–15.01	14.28–14.73	13.88–15.35
15.15 ± 0.29 (6)	15.03 ± 0.40	14.44 ± 0.73	14.03 ± 0.53	14.26 ± 0.41	14.43 ± 0.37
14.70–15.46	14.75–15.31	13.92–14.95	13.58–14.73	13.49–14.83	13.76–15.03
5.98 ± 0.27 (6)	5.35 ± 0.08	5.47 ± 0.06	5.35 ± 0.26	5.41 ± 0.34	5.40 ± 0.31
5.57–6.34	5.29–5.40	5.43–5.51	5.02–5.57	4.68–5.78	4.78–5.84
8.03 ± 0.35 (6)	7.74 ± 0.27	7.75 ± 0.40	7.50 ± 0.20	7.57 ± 0.19	7.55 ± 0.16
7.68–8.63	7.55–7.93	7.46–8.03	7.21–7.68	7.26–7.80	7.32–7.81
15.98 ± 0.21 (6)	15.53 ± 0.26	15.34 ± 0.82	15.07 ± 0.61	14.87 ± 0.53	15.06 ± 0.39
15.70–16.32	15.35–15.71	14.76–15.92	14.40–15.84	13.95–15.34	14.40–15.69
12.43 ± 0.31 (6)	12.11 ± 0.40	11.95 ± 0.74	12.05 ± 0.32	11.84 ± 0.43	12.07 ± 0.33
12.13–13.03	11.82–12.39	11.43–12.47	11.58–12.30	11.10–12.17	11.39–12.65
7.52 ± 0.31	7.29 ± 0.02	7.51 ± 0.16	7.36 ± 0.18	7.62 ± 0.17	7.61 ± 0.22
7.21–8.09	7.27–7.30	7.39–7.62	7.16–7.60	7.25–7.81	7.13–8.00
8.16 ± 0.29 (6)	7.99 ± 0.11	8.21 ± 0.44	7.97 ± 0.26	7.88 ± 0.18 (7)	7.88 ± 0.20
7.73–8.49	7.91–8.07	7.90–8.52	7.73–8.21	7.62–8.05	7.55–8.25
9.78 ± 0.43 (6)	9.47 ± 0.30	9.09 ± 1.02	9.41 ± 0.50	9.23 ± 0.41	9.33 ± 0.34
9.39–10.51	9.25–9.68	8.37–9.81	8.89–10.09	8.55–9.99	8.97–10.17
11.94 ± 0.59 (6)	11.67 ± 0.21	11.66 ± 0.79	11.29 ± 0.36	11.27 ± 0.47	11.56 ± 0.36
11.35–13.08	11.52–11.82	11.10–12.22	10.80–11.67	10.43–11.89	11.00–12.34
5.55 ± 0.25 (6)	5.57 ± 0.07	5.67 ± 0.46	5.61 ± 0.45	5.51 ± 0.19 (7)	5.39 ± 0.17
5.06–5.77	5.52–5.62	5.34–5.99	5.08–6.15	5.32–5.84	5.10–5.68
10.64 ± 0.39 (6)	10.89 ± 0.06	11.12 ± 0.37	10.50 ± 0.43	10.72 ± 0.22	10.77 ± 0.22
10.07–10.99	10.85–10.93	10.86–11.38	10.01–11.02	10.52–11.10	10.31–11.11
1.96 ± 0.09	1.95 ± 0.12	1.93 ± 0.09	1.93 ± 0.05	1.97 ± 0.04	1.99 ± 0.09
1.87–2.14	1.86–2.03	1.87–1.99	1.87–1.98	1.91–2.04	1.84–2.10
2.17 ± 0.13 (6)	2.12 ± 0.03	2.10 ± 0.32	2.09 ± 0.11	2.13 ± 0.06 (7)	2.30 ± 0.09 (11)
2.05–2.40	2.10–2.14	1.87–2.32	2.02–2.25	2.06–2.22	2.12–2.51
3.65 ± 0.13 (6)	3.35 ± 0.02	3.52 ± 0.45	3.46 ± 0.15	3.50 ± 0.19	3.45 ± 0.27
3.49–3.79	3.33–3.36	3.20–3.83	3.32–3.65	3.18–3.69	2.85–4.05
150.0 ± 11.5 (6)	142.5 ± 0.7	141.5 ± 7.8	138.0 ± 2.2	138.3 ± 6.3	139.1 ± 6.0 (11)
136–171	142–143	136–147	136–141	128–147	130–149
291.7 ± 11.5 (6)	275.0 ± 0.0	278.5 ± 21.9	278.3 ± 7.4	271.0 ± 10.4	276.9 ± 9.9 (11)
275–304	275	263–294	270–287	254–283	254–285
141.7 ± 12.1 (6)	132.5 ± 0.7	137.0 ± 14.1	140.3 ± 5.3	132.8 ± 7.3	137.8 ± 7.0 (11)
124–154	132–133	127–147	134–146	123–146	124–147
36.0 ± 1.8 (6)	36.5 ± 2.1	36.0 ± 0.0	35.8 ± 1.0	35.4 ± 2.1	35.8 ± 1.5
34–39	35–38	36	35–37	31–38	33–38
20.2 ± 1.0 (6)	19.0 ± 1.4	19.0 ± 0.0	19.7 ± 1.2 (3)	19.4 ± 0.9	19.3 ± 0.8
19–21	18–20	19	19–21	18–21	18–20
91.6 ± 12.3 (5)	86.5 ± 10.6	85.0 ± 12.7	74.5 ± 6.4	79.6 ± 7.6	86.8 ± 8.2
80–111	79–94	76–94	70–84	64–90	72–100

groups leads us to hypothesize that they are discrete species, and we treat them as such.

*Apomys sierrae* is easily distinguished from *A. zambalensis* sp. nov., to which it is also closely related (Fig. 7). *Apomys sierrae* averages smaller in nearly all respects; a plot of ear length and hind foot length shows limited overlap (Fig. 40A). The dorsal pelage of *A. zambalensis* sp. nov. is a rather bright rusty umber (Fig. 2A), whereas that of *A. sierrae* is either a dark, slightly reddish brown (in the Sierra Madre; Fig. 2C) or a somewhat tawny brown (on Mt. Palali; Fig. 2D). The fore- and hind feet of *A. zambalensis* sp. nov. have almost no dark hairs on the dorsal surface, whereas *A. sierrae* virtually always has at least some dark hairs. The ventral surface of the hind foot of *A. zambalensis* sp. nov. is typically only moderately

pigmented and has large plantar pads, whereas *A. sierrae* typically is heavily pigmented and has smaller pads. The hallux of *A. sierrae* is short, reaching only to the bottom of the adjacent plantar pad, whereas that of *A. zambalensis* sp. nov. is long, reaching about to the top of the pad (Fig. 10E,I). The cranium of *A. zambalensis* sp. nov. is larger than that of *A. sierrae*, with a more robust rostrum, broader and more squarish braincase, broader incisive foramina, narrower M<sup>1</sup>, less divergent maxillary toothrows, less heavily pitted and perforated palate, and longer postpalatal region. Bivariate plots of postpalatal length vs. breadth of M<sup>1</sup> (Fig. 40B) and rostral depth vs. diastema length (Fig. 40C) taken in combination allow separation of most individuals. The interparietal bones in the two species are variable in shape

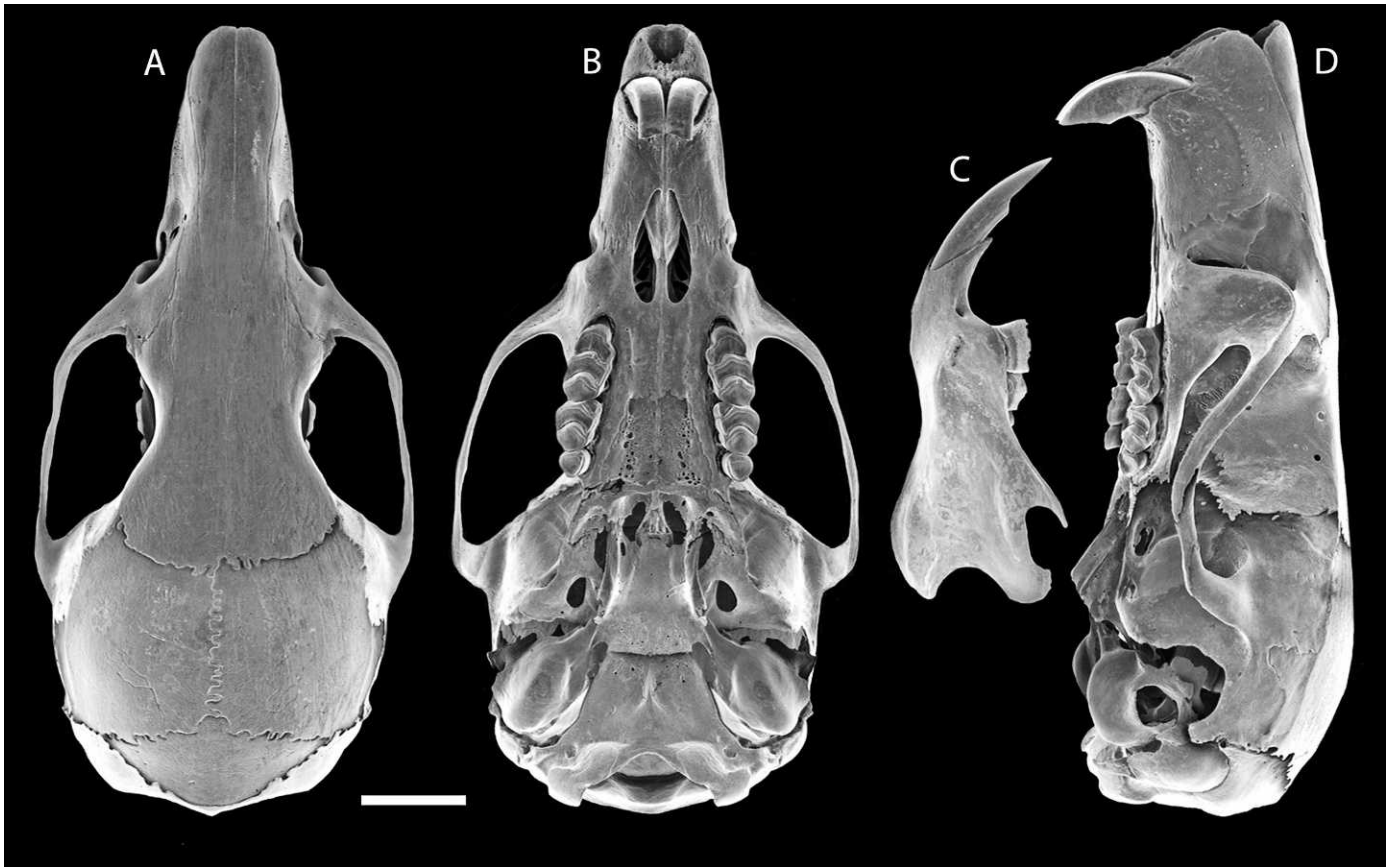


FIG. 34. Dorsal (A), ventral (B), and lateral (D) views of the cranium and lateral view of the mandible (C) of *Apomys sierrae* sp. nov. (FMNH 185884, holotype); scale bar = 5 mm.

but usually similar in width. The mandible of *A. zambalensis* sp. nov. is deeper, with a somewhat more robust coronoid process, broader angular process, and broader and slightly less concave posterior margin between the condylar and angular processes. The PCA described above (Fig. 38; Table 14) shows no difference in size (PC1) but overlaps with substantially different averages along PC2, which loads heavily on the dental features, diastema length, and postpalatal length that are individually apparent as differences. These metric differences, combined with the difference in carotid circulatory pattern and clear genetic monophyly, lead us to conclude that these are different species.

**DISTRIBUTION**—Specimens referred to this species have a wide distribution, from Palau Island off the NE tip of Luzon, south through the main mass of the Sierra Madre mountain range in Cagayan Province to Mt. Lataan and the Mungiao Mountains in Quirino Province (Figs. 3, 35). We also refer specimens from Mt. Palali, in the Caraballo Mountains of Nueva Viscaya, to this species because they are genetically and morphologically highly similar, except for having paler pelage. *Apomys sierrae* probably has the broadest geographic range of any species of *Megapomys*, although the ranges of *A. abrae* and *A. datae* are nearly as large. The report by Danielsen et al. (1994) of large *Apomys* tentatively referred to *A. datae* actually refers to this species. The documented elevational range of the species on Luzon is from ca. 475 to 1700 m, one of the greatest among *Apomys* (Fig. 15), but we also recorded it at 153 m on Palau Island, which has a maximum elevation of about 300 m. The distribution of this species and *A. abrae*, and possibly *A. datae*, might overlap in the area where the Caraballo

Mountains and the Central Cordillera come into contact in southwestern Nueva Viscaya; surveys in that area should produce interesting information about comparative habitat use by these species.

*Apomys (Megapomys) magnus* sp. nov.

**HOLOTYPE**—FMNH 183574, adult female collected on 23 February 2005 by Danilo S. Balete, field number DSB 3606. A sample of muscle tissue was removed from the thigh in the field and preserved in ethanol before the specimen was preserved in formaldehyde. In the museum, the skull was removed and cleaned (see Methods). Palate damaged by perforation, pterygoid process broken off and lost from left side; otherwise, in good condition. This specimen will be permanently deposited at the NMP. Measurements appear in Table 12.

**TYPE LOCALITY**—Philippines: Luzon Island: Quezon Province: Tayabas Munic.: Barangay Lalo: Mt. Banahaw, Hasaan, 1250 m; 14°3'44"N, 121°31'8"E (from GPS).

**PARATYPES** (n = 12)—Luzon Island: Quezon Prov.: Tayabas Munic.: Brgy. Lalo: Idoro: Mt. Banahaw, 765 m (FMNH 183569–183572); Tayabas Munic.: Brgy. Lalo: Hasaan: Mt. Banahaw, 1250 m (FMNH 183573, 183575–183579); Tayabas Munic.: Brgy. Lalo: Mt. Banahaw, 1465 m (FMNH 178395–178396).

**ETYMOLOGY**—An adjective from the Latin *magnus*, meaning “large,” in recognition that it is the largest species of *Apomys* currently known.

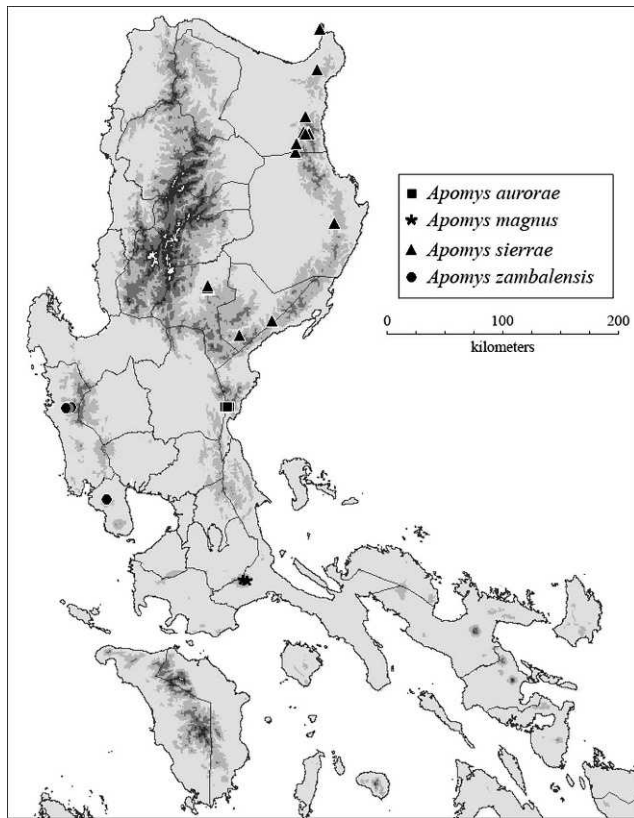


FIG. 35. Map showing the documented distribution of *Apomys aurorae*, *A. magnus*, *A. sierrae*, and *A. zambalensis* spp. nov. See respective species accounts for localities. Shading on land areas, in increasingly dark tones of gray: 0–500 m elevation; 501–1000 m; 1001–1500 m; 1501–2000 m; and white above 2000 m. Provincial boundaries are shown for reference.

**DIAGNOSIS AND DESCRIPTION**—The largest species of *Megapomys*, with HBL averaging about 147 mm, and weight usually 98–108 g; some individuals weighed up to 128 g. The length of the tail is typically 96–99% of the length of HBL. *Apomys magnus* has dorsal fur of moderate length; it is dark brown with conspicuous dark tips, with little evidence of orange or yellow highlights (Fig. 1E). The ventral fur is medium gray at the base, and white at the tips. The tail is unpigmented ventrally and dark brown dorsally. The hind foot is the longest of any *Megapomys*, averaging 39–40 mm; it is broad relative to its length, the plantar pads are of moderate size, and the ventral surface is moderately to heavily pigmented, with the exception of the thenar pad (Fig. 10D). The toes are robust, with the hallux reaching to about the top of the adjacent interdigital plantar pad, and digit 5 reaching nearly to the base of digit 4. The fur on the dorsal surface of the hind foot is white or pale cream. On the forefoot, a stripe of dark hairs extends along the median from the forearm to (or near to) the base of the toes.

The cranium of *A. magnus* (Fig. 41) is the largest among *Megapomys*, averaging about 37.4 mm in basioccipital length and 19.3 in zygomatic width (Table 12). The rostrum is robust and fairly long, and the incisive foramina are unusually long. The braincase is broad and sturdy, and the zygomatic arches are robust and flare to the sides. The maxillary tooththrow is long, and  $M^1$  is especially wide. The bony palate is broad and the posterior portion has many small pits and perforations. The postpalatal region is of average length. The basicranial

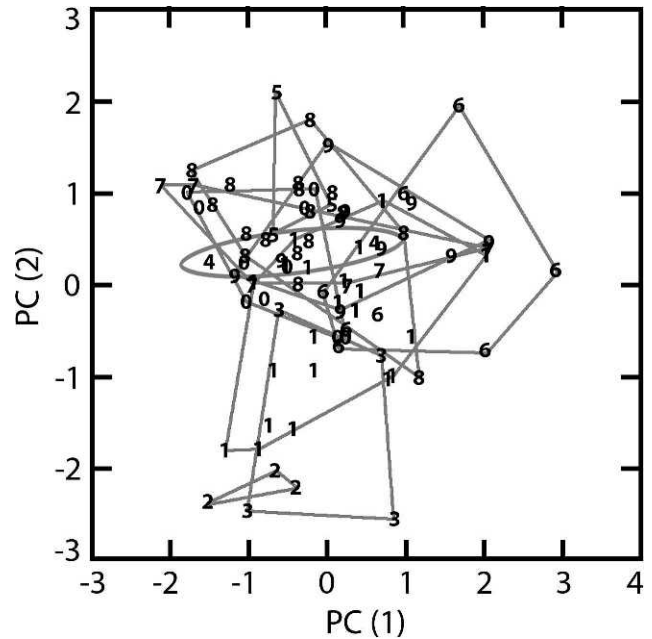


FIG. 36. Results of the principal components analysis of *Apomys sierrae* sp. nov. (see text and Table 13) based on specimens in Tables 9, 11, and 12. 0 = Mt. Cetaceo, Cagayan Province, ca. 1300 m; 1 = Mt. Cetaceo, Cagayan Province, ca. 1500 m; 2 = Palau Island, Cagayan Province; 3 = Mt. Cagua, Cagayan Province; 4 = Mt. Lataan, Quirino Province; 5 = Mungiao Mtns., Quirino Province; 6 = Mt. Palali, Nueva Vizcaya Province, ca. 800 m; 7 = Mt. Palali, Nueva Vizcaya Province, ca. 1100 m; 8 = Mt. Palali, Nueva Vizcaya Province, ca. 1440 m; 9 = Mt. Palali, Nueva Vizcaya Province, 1700 m.

circulation is of the “datae pattern” (Fig. 5B). The interparietal is variable in shape but is usually anteroposteriorly wide. The mandible (Fig. 41C) is robust, with a coronoid process of average length, a broad angular process, and a shallow concave edge between the condylar and angular processes.

**COMPARISONS**—*Apomys magnus* differs from *A. banahao* in the ways described above for that species, which occurs largely above it in elevation on Mt. Banahaw, but occasionally in sympatry (Fig. 15). In general, *A. banahao* has longer, softer pelage, the hallux is short, the maxillary tooththrow is shorter and narrower, the palate is narrower (Fig. 29C), and the bullae lack a foramen for the stapedial artery. Our genetic data show them to be distantly related, confirming them as distinct species.

*Apomys magnus* differs from *A. sierrae* as described above; *A. sierrae* averages smaller, with little overlap in most external and cranial measurements (Fig. 37), has dorsal fur that is dark brown with rusty reddish tones and ventral fur that is dark gray at the base and pale gray at the tip with an ochraceous wash. The hallux of *A. magnus* is long, and that of *A. sierrae* is short. The crania are usually easily distinguished using a combination of several measurements (Fig. 37B,C), and the stapedial foramen is large and conspicuous in *A. magnus* but absent in *A. sierrae*. The metric differences are apparent in a PCA that includes *A. magnus*, *A. sierrae*, and *A. zambalensis*, discussed in the *A. sierrae* species account (Fig. 38; Table 14).

*Apomys magnus* differs from *A. aurorae* sp. nov., one of its closest relatives, in being much larger in all external and cranial measurements, often with little overlap (Fig. 42). The dorsal fur of *A. aurorae* sp. nov. (Fig. 2F) is not as dark and has a yellow tint that is absent in *A. magnus* (Fig. 1E), and *A.*



TABLE 12. Cranial and external measurements (mean  $\pm$  1 S.D. and range) of *Apomys sierrae* (part) and *A. magnus*.

Measurement	<i>Apomys sierrae</i>			<i>Apomys magnus</i>		
	Mt. Palali, 1680–1700 m, Nueva Vizcaya Prov.		Palau Island, Cagayan Prov.	Mt. Banahaw, 765–1465 m, Quezon Prov. F-holotype FMNH 183574	Mt. Banahaw, 765–1465 m, Quezon Prov.	
	M (n = 8)	F (n = 3)	M (n = 3)		M (n = 3)	F (n = 6)
Basioccipital length	35.44 $\pm$ 0.96 33.65–36.34	35.21 $\pm$ 0.18 35.02–35.36	35.14 $\pm$ 0.33 34.76–35.33	37.04 —	37.06 $\pm$ 0.86 36.30–38.00	37.70 $\pm$ 0.49 37.04–38.39
Interorbital breadth	6.31 $\pm$ 0.20 6.09–6.68	6.17 $\pm$ 0.09 6.08–6.25	6.16 $\pm$ 0.25 5.90–6.40	6.44 —	6.55 $\pm$ 0.19 6.38–6.76	6.53 $\pm$ 0.19 6.25–6.73
Zygomatic breadth	18.76 $\pm$ 0.69 17.65–19.63	18.89 $\pm$ 0.10 18.78–18.95	17.59 $\pm$ 0.73 16.96–18.39	19.40 —	19.18 $\pm$ 0.64 18.47–19.73	19.38 $\pm$ 0.35 18.79–19.84
Mastoid breadth	14.67 $\pm$ 0.17 (7) 14.50–14.96	14.43 $\pm$ 0.27 14.20–14.72	14.11 $\pm$ 0.23 13.84–14.26	15.15 —	14.88 $\pm$ 0.27 14.70–15.19	15.08 $\pm$ 0.27 14.62–15.37
Nasal length	14.60 $\pm$ 0.58 13.84–15.50	14.54 $\pm$ 0.13 14.39–14.64	14.29 $\pm$ 0.55 13.66–14.63	15.25 —	15.01 $\pm$ 0.37 14.59–15.24	15.56 $\pm$ 0.61 14.81–16.35
Incisive foramen length	5.61 $\pm$ 0.45 5.07–6.34	5.63 $\pm$ 0.50 5.10–6.09	5.39 $\pm$ 0.29 5.07–5.63	5.34 —	5.79 $\pm$ 0.18 5.65–5.99	5.75 $\pm$ 0.34 5.34–6.12
Rostral depth	7.72 $\pm$ 0.26 7.15–7.96	7.80 $\pm$ 0.28 7.49–8.02	7.52 $\pm$ 0.18 7.33–7.68	7.80 —	8.11 $\pm$ 0.35 7.82–8.49	8.34 $\pm$ 0.30 7.80–8.62
Rostral length	15.43 $\pm$ 0.30 14.97–15.86	15.34 $\pm$ 0.15 15.19–15.49	14.94 $\pm$ 0.10 14.83–15.01	16.40 —	15.64 $\pm$ 0.30 15.30–15.82	16.51 $\pm$ 0.53 15.91–17.42
Orbitotemporal length	12.31 $\pm$ 0.70 11.33–13.12	12.44 $\pm$ 0.33 12.08–12.73	12.09 $\pm$ 0.35 11.71–12.40	13.09 —	13.25 $\pm$ 0.17 13.07–13.41	13.13 $\pm$ 0.18 12.82–13.35
Maxillary toothrow length	7.61 $\pm$ 0.17 7.29–7.80	7.42 $\pm$ 0.12 7.29–7.50	7.07 $\pm$ 0.05 7.03–7.13	8.13 —	7.95 $\pm$ 0.31 7.67–8.28	8.13 $\pm$ 0.19 7.78–8.28
Labial palatal breadth at M <sup>1</sup>	8.14 $\pm$ 0.30 7.67–8.46	7.99 $\pm$ 0.30 7.65–8.22	7.09 $\pm$ 0.13 6.95–7.20	8.65 —	8.28 $\pm$ 0.29 7.96–8.52	8.54 $\pm$ 0.47 7.76–9.03
Diastema length	9.54 $\pm$ 0.30 9.08–10.01	9.35 $\pm$ 0.42 8.86–9.60	9.37 $\pm$ 0.21 9.24–9.62	9.73 —	9.95 $\pm$ 0.20 9.75–10.15	10.06 $\pm$ 0.34 9.73–10.50
Postpalatal length	11.43 $\pm$ 0.37 (7) 10.97–11.94	11.14 $\pm$ 0.25 10.85–11.29	11.88 $\pm$ 0.14 11.73–12.01	12.39 —	12.56 $\pm$ 0.38 12.19–12.95	12.45 $\pm$ 0.41 12.10–13.21
Lingual palatal breadth at M <sup>3</sup>	5.60 $\pm$ 0.15 5.40–5.78	5.40 $\pm$ 0.24 5.13–5.57	4.91 $\pm$ 0.31 4.63–5.24	6.04 —	5.86 $\pm$ 0.31 5.64–6.21	5.96 $\pm$ 0.29 5.73–6.51
Braincase height	10.91 $\pm$ 0.43 (7) 10.31–11.57	11.04 $\pm$ 0.52 10.68–11.63	10.48 $\pm$ 0.04 10.44–10.51	11.57 —	11.15 $\pm$ 0.29 10.82–11.37	11.36 $\pm$ 0.25 11.06–11.65
Breadth of M <sup>1</sup>	1.97 $\pm$ 0.05 1.91–2.05	1.90 $\pm$ 0.15 1.76–2.05	1.78 $\pm$ 0.04 1.73–1.81	2.19 —	2.09 $\pm$ 0.10 2.01–2.21	2.10 $\pm$ 0.07 2.01–2.19
Breadth of incisors at tip	2.22 $\pm$ 0.07 2.10–2.33	2.30 $\pm$ 0.18 2.13–2.49	2.18 $\pm$ 0.08 2.09–2.24	2.24 —	2.41 $\pm$ 0.12 2.31–2.54	2.38 $\pm$ 0.12 2.24–2.55
Width of zygomatic plate	3.47 $\pm$ 0.08 3.35–3.58	3.57 $\pm$ 0.24 3.29–3.75	3.50 $\pm$ 0.08 3.41–3.55	3.62 —	3.42 $\pm$ 0.04 3.40–3.46	3.59 $\pm$ 0.14 3.43–3.81
Length of head and body	143.1 $\pm$ 7.3 132–151	144.3 $\pm$ 2.1 142–146	142.0 $\pm$ 7.2 134–148	137 —	147.5 $\pm$ 0.7 (2) 147–148	146.4 $\pm$ 8.5 (5) 137–160
Total length	279.1 $\pm$ 13.4 261–295	280.7 $\pm$ 2.1 279–283	279.7 $\pm$ 8.5 271–288	272 —	292.5 $\pm$ 10.6 (2) 285–300	289.2 $\pm$ 13.5 (5) 272–305
Length of tail vertebrae	136.0 $\pm$ 9.5 121–149	136.3 $\pm$ 4.0 134–141	137.7 $\pm$ 2.1 136–140	135 —	145.0 $\pm$ 9.9 (2) 138–152	142.8 $\pm$ 8.7 (5) 133–154
Length of hind foot	36.6 $\pm$ 1.6 35–40	34.7 $\pm$ 1.2 34–36	35.3 $\pm$ 0.6 35–36	39 —	40.3 $\pm$ 0.6 40–41	38.8 $\pm$ 1.2 37–40
Length of ear	20.0 $\pm$ 0.8 19–21	19.3 $\pm$ 0.6 19–20	20.0 $\pm$ 1.0 19–21	22 —	22.7 $\pm$ 0.6 22–23	21.8 $\pm$ 0.4 (5) 21–22
Weight (g)	78.6 $\pm$ 7.3 69–90	92.0 $\pm$ 13.9 84–108	83.3 $\pm$ 11.0 72–94	98 —	98.7 $\pm$ 6.5 92–105	108.6 $\pm$ 14.4 (5) 93–128

*aurorae* sp. nov. lacks the dark tips on dorsal hairs that are conspicuous on *A. magnus*. The ventral surface of the foot is much darker on *A. magnus* than on *A. aurorae* sp. nov., and the hallux of *A. magnus* reaches to about the top of the adjacent interdigital plantar pad, whereas that of *A. aurorae* sp. nov. reaches only to the base of the pad (Fig. 10G). Bivariate plots of basioccipital length and interorbital breadth, and of nasal length and rostral depth, show no overlap between these species (Fig. 42B,C). The interparietal of *A. magnus* is variable in shape but usually somewhat wider anteroposteriorly than that of *A. aurorae* sp. nov. As described in the species account for *A. sacobianus*, a PCA of that species

plus *A. aurorae* sp. nov., *A. magnus*, and *A. zambalensis* sp. nov. showed complete separation of *A. magnus* and *A. aurorae* sp. nov. on a plot of PC1 and PC2, primarily reflecting their consistent difference in overall size (Fig. 23; Table 7). This difference, combined with their genetic monophyly, leads us to treat them as different species.

*Apomys magnus* differs from *A. zambalensis* sp. nov., another close relative, in having longer dorsal fur with black tips; *A. zambalensis* sp. nov. has fur that is a brighter, rusty orange with only barely evident black tips. The ventral fur of *A. magnus* is gray at the base and nearly white at the tips; that of *A. zambalensis* sp. nov. is a paler gray at the base and white

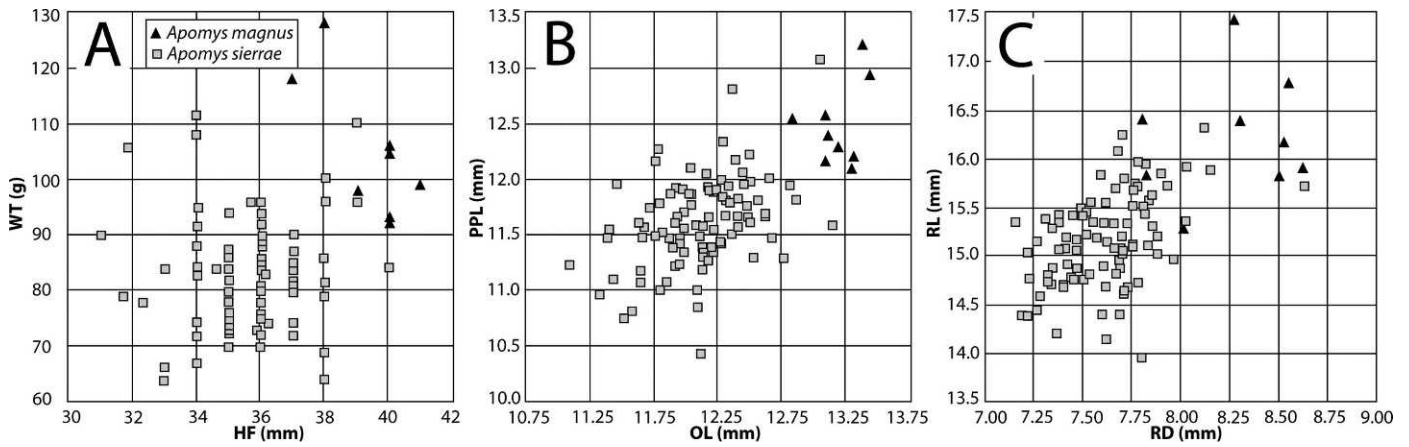


FIG. 37. Bivariate plots of measurements comparing *Apomys sierrae* and *A. magnus* spp. nov. (A) Length of hind foot (HF) and weight (WT). (B) Orbitotemporal length (OL) and postpalatal length (PPL). (C) Rostral depth (RD) and rostral length (RL).

at the tips with an ochraceous wash. The hind feet are similar, but those of *A. zambalensis* sp. nov. are slightly smaller (39–40 vs. 37–38 mm) and less heavily pigmented (Fig. 10I). A plot of weight vs. total length (Fig. 43A) shows that *A. magnus* is usually longer and heavier, but there is overlap. A plot of the width of  $M^1$  vs. breadth of incisors at the tip shows no overlap (Fig. 43B), and length of the maxillary tooththrow vs. labial palatal breadth at  $M^1$  shows little overlap (Fig. 43C); *A. magnus* is the larger in all of these measures. These metric differences are apparent in a PCA that includes *A. magnus*, *A. sierrae*, and *A. zambalensis*, discussed in the *A. sierrae* species account, which shows no overlap between *A. magnus* and *A. zambalensis* sp. nov. on the plot of PC1 vs. PC2 (Fig. 38; Table 14). The combination of discrete morphological features, multivariate morphometric differences, and genetic monophyly lead us to consider these to be clearly distinct species.

**DISTRIBUTION**—Our elevational transect on Mt. Banahaw documented this species from 765 to 1465 m in lowland and montane rainforest (Figs. 15, 35). Extensive trapping at 620 m failed to detect this species, and we doubt that it occurs below about 700 m. We suspect that it occurs on Mt. Banahaw and the adjacent Mt. San Cristobal (in Laguna and Quezon provinces) from about 700 to about 1465 m elevation, in any forested area. Above about 1465 m, we captured large numbers of *A. banahao*, so we expect *A. magnus* to be absent from high-elevation areas. Mts. Banahaw and San Cristobal sit on a flat, low-elevation (below 300 m) plain, with scattered peaks, largely below 1000 m, within 50 km in any direction. We predict that this species will not be found in any other areas, but surveys of the peaks in the general vicinity (Batangas, Cavite, Laguna, and southern Quezon provinces) would be worthwhile, especially at elevations above 700 m.

*Apomys (Megapomys) aurorae* sp. nov.

**HOLOTYPE**—FMNH 190812, adult male collected on 15 June 2006 by Phillip A. Alviola, field number PAA 864. A sample of muscle tissue was removed from the thigh in the field and preserved in ethanol before preserving the specimen in formaldehyde. In the museum, the skull was removed and cleaned (see Methods). All parts are in good condition. This

specimen will be permanently deposited at the NMP. Measurements appear in Table 15.

**TYPE LOCALITY**—Philippines: Luzon Id: Aurora Province: Dingalan Munic.: 2 km S, 2 km W Mingan peak, 1305 m, 15.46456°N, 121.38421°E (from GPS).

**PARATYPES** (n = 98)—Luzon Island: Aurora Prov.: Dingalan Munic.: 2.25 km S, 3.25 km W Mingan peak, 733 m (FMNH 190933–190935); Dingalan Munic.: 2.1 km S, 2.9 km W Mingan peak, 902 m (FMNH 190825, 190918–190932); Dingalan Munic.: 1.9 km S, 2.5 km W Mingan peak, 1074 m (FMNH 190826–190832, 190925, 190929); Dingalan Munic.: 2 km S, 2 km W Mingan peak, 1305 m (FMNH 190810, 190811, 190813–190824, 190910–190917, 191067–191076); Dingalan Munic.: 1.8 km S, 1.6 km W Mingan peak, 1476 m (FMNH 190794–190809, 190887–190909, 191066); Dingalan Munic.: 1.7 km S, 1.3 km W Mingan peak, 1540 m (FMNH 190953); Dingalan

TABLE 13. Character loadings, eigenvalues, and percent variance explained on the first four components of a principal components analysis of log-transformed measurements of adult *Apomys sierrae* (see Fig. 36 and Methods).

Variable	Principal component			
	1	2	3	4
Basioccipital length	0.824	-0.266	0.099	-0.250
Interorbital breadth	0.567	-0.325	0.207	0.272
Zygomatic breadth	0.723	0.263	0.064	0.299
Mastoid breadth	0.633	0.120	0.219	0.383
Nasal length	0.705	-0.009	-0.338	-0.171
Incisive foramen length	0.460	0.010	-0.137	-0.485
Rostral depth	0.719	0.086	-0.217	-0.010
Rostral length	0.767	-0.158	-0.289	0.015
Orbitotemporal length	0.672	-0.100	0.002	-0.380
Maxillary tooththrow length	-0.009	0.701	0.328	-0.395
Labial palatal breadth at $M^1$	0.635	0.675	-0.123	0.078
Diastema length	0.696	-0.434	-0.110	0.126
Postpalatal length	0.556	-0.478	0.203	-0.305
Lingual palatal breadth at $M^3$	0.530	0.389	-0.178	0.421
Braincase height	0.290	-0.004	0.697	0.046
Breadth of $M^1$	0.127	0.782	-0.026	-0.224
Breadth of incisors at tip	0.391	0.029	0.595	-0.007
Width of zygomatic plate	0.335	0.288	0.000	0.034
Eigenvalue	6.032	2.514	1.416	1.283
Percent variance explained	33.51	13.96	7.87	7.13

TABLE 14. Character loadings, eigenvalues, and percent variance explained on the first four components of a principal components analysis of log-transformed measurements of adult *Apomys magnus*, *A. sierrae*, and *A. zambalensis* (see Fig. 38 and Methods).

Variable	Principal component			
	1	2	3	4
Basioccipital length	0.866	-0.308	-0.228	-0.071
Interorbital breadth	0.498	0.244	0.543	-0.227
Zygomatic breadth	0.785	0.213	0.203	0.071
Mastoid breadth	0.695	0.249	0.140	-0.101
Nasal length	0.745	0.032	0.170	0.205
Incisive foramen length	0.526	-0.050	-0.026	0.086
Rostral depth	0.771	-0.188	-0.022	0.167
Rostral length	0.784	-0.244	0.169	0.192
Orbitotemporal length	0.753	-0.094	-0.182	0.024
Maxillary toothrow length	0.454	0.498	-0.589	-0.075
Labial palatal breadth at M <sup>1</sup>	0.701	0.511	0.012	0.198
Diastema length	0.667	-0.582	0.092	-0.007
Postpalatal length	0.553	-0.606	-0.311	-0.188
Lingual palatal breadth at M <sup>3</sup>	0.588	-0.025	0.301	0.052
Braincase height	0.501	0.140	0.019	-0.542
Breadth of M <sup>1</sup>	0.313	0.820	-0.116	0.077
Breadth of incisors at tip	0.533	0.085	-0.222	-0.478
Width of zygomatic plate	0.298	-0.010	-0.280	0.561
Eigenvalue	7.220	2.284	1.184	1.113
Percent variance explained	40.11	12.69	6.58	6.18

Munic.: 1.8 km S, 1.0 km W Mingan peak, 1677 m (FMNH 190846).

ETYMOLOGY—From the name of the province (Aurora) where this species was captured; used as a noun in the genitive case.

DIAGNOSIS AND DESCRIPTION—One of the smaller species of *Megapomys*, although averaging only slightly larger than *A. minganensis*, *A. brownorum*, and *A. abrae* in most measurements (Tables 2, 3, 9). The dorsal pelage of *A. aurorae* is rich, rusty reddish-brown, with medium-gray underfur (Fig. 2F). The ventral pelage is somewhat paler at the base, with the tips either white or white with a pale ochraceous wash. The brown pelage extends only a short distance onto the forearms and lower hind legs, but scattered dark hairs are sometimes present on the upper surface of the forefeet and hind feet. The ventral surface of the hind feet is usually moderately darkly pigmented, often including the pads, and the hallux is short, reaching only to about the bottom of the adjacent interdigital plantar pad (Fig. 10G). The tail is sharply bicolored and long, averaging 98–100% of the length of the head and body. The ventral surface of the tail is usually white, but some individuals have scattered dark hairs and darkly pigmented scales.

The cranium (Fig. 44) has a somewhat globose braincase that is less elongate than most species, a moderately short and comparatively slender rostrum, a short diastema, and a short postpalatal region. The molar toothrows are of average length and width and diverge posteriorly, and the bony palate is moderately broad. The stapedial foramen in the bulla for the carotid artery is present in all individuals (the “datae pattern”; Fig. 5). The interparietal is variable in shape, but usually is moderately wide anteroposteriorly. The mandible (Fig. 44C) is of average depth with a relatively long and posteriorly curved coronoid process. The angular process is broad and has a blunt tip.

COMPARISONS—*Apomys aurorae* differs from *A. minganensis* as described above; *A. minganensis* is darker dorsally and

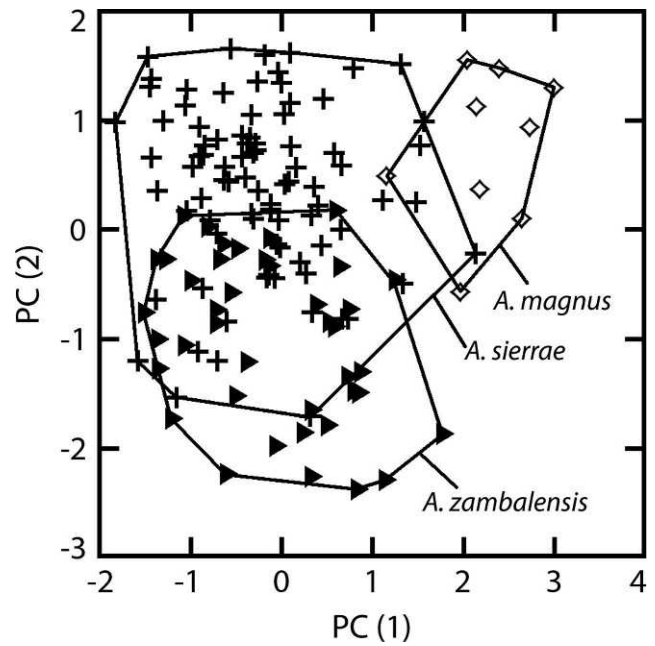


FIG. 38. Results of the principal components analysis of *Apomys sierrae*, *A. magnus*, and *A. zambalensis* spp. nov. (see text and Table 14) based on specimens in Tables 9, 11, 12, and 15.

ventrally, always has a tail with scattered dark hairs and pigment ventrally, and has dark hair on the entire dorsal surface of the hind feet. The hallux of *A. aurorae* is short, reaching only to about the bottom of the adjacent interdigital pad, whereas that of *A. minganensis* is long, reaching to about the top of the pad. There is no overlap between these species in rostral depth, orbital length, or length of the maxillary toothrow, and there is little overlap in lingual breadth of the palate at M<sup>3</sup> (Fig. 31C). As described above, a PCA of craniodental measurements that included *A. aurorae*, *A. minganensis*, and *A. sierrae* (Fig. 33; Table 10) showed no overlap in a plot of PC1 vs. PC2, with most of the differences reflecting the features shown in Figures 31B and C. On the basis of the qualitative and quantitative differences and the genetic evidence of monophyly of these two populations, we conclude that they represent distinct species.

*Apomys aurorae* differs from *A. sierrae* only in subtle ways, as described above. They are most easily distinguished by the presence of a foramen for the stapedial artery in the bullae of *A. aurorae* (the “datae pattern”; Fig. 5B) and its absence in *A. sierrae* (the “abrae pattern”; Fig. 5A). A PCA of craniodental measurements (Fig. 33; Table 10), discussed above, showed complete overlap on the two interpretable components, but the difference in the stapedial foramen and the genetic evidence of monophyly leads us to view these as distinct species.

*Apomys aurorae* differs from *A. magnus* in being consistently smaller in all external and cranial measurements, so it is easily distinguished (Fig. 42). The carotid circulation pattern is the same (the “datae pattern”; Fig. 5B) in these two species. The dorsal fur of *A. aurorae* (Fig. 2F) is not as dark and has a yellow tint that is absent in *A. magnus* (Fig. 1E), and *A. aurorae* lacks the dark tips on dorsal hairs that are conspicuous on *A. magnus*. *Apomys magnus* has few or no dark hairs on the dorsal surface of the hind foot, but some individuals of *A. aurorae* have scattered dark hairs. Further-



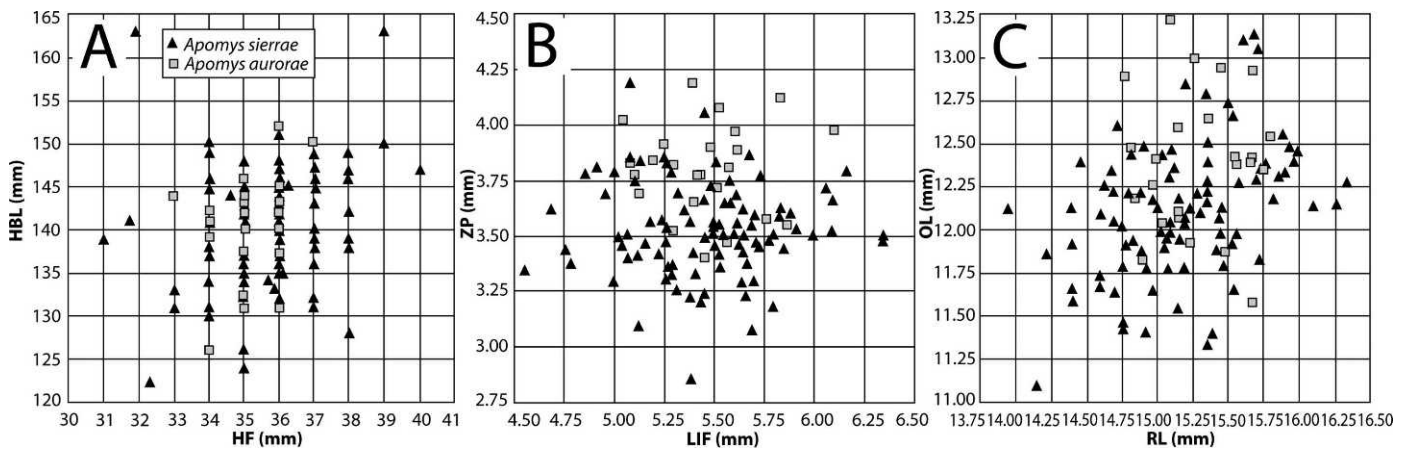


FIG. 39. Bivariate plots of measurements comparing *Apomys sierrae* and *A. aurorae* spp. nov. (A) Length of hind foot (HF) and length of head and body (HBL). (B) Length of incisive foramen (LIF) and width of zygomatic plate (ZP). (C) Rostral length (RL) and orbitotemporal length (OL).

more, the ventral surface of the foot is much darker on *A. magnus* than on *A. aurorae*, and the hallux of *A. aurorae* is short, reaching only to the bottom of the adjacent plantar pad (Fig. 10G), whereas that of *A. magnus* is long, reaching to about the top of the pad (Fig. 10D). Bivariate plots of basioccipital length and interorbital breadth, and of nasal length and rostral depth, show no overlap between these species (Fig. 42B,C). The interparietal of *A. aurorae* is usually somewhat smaller than that of *A. magnus*. A PCA of craniodental measurements (Fig. 23; Table 7), discussed above, showed no overlap on the first component, which reinforces the consistent difference in size. Combined with the qualitative features summarized here and the genetic evidence of monophyly (Fig. 7), we conclude that these are distinct species.

*Apomys aurorae* is similar in size to *A. zambalensis* sp. nov. in some respects, but other features differ with little overlap. The dorsal pelage of *A. aurorae* is darker brown (Fig. 2F), whereas that of *A. zambalensis* sp. nov. is bright rusty orange (Fig. 2A); the ventral fur of *A. zambalensis* sp. nov. has a moderate to heavy ochraceous wash, whereas *A. aurorae* has less of the ochraceous wash. The hind foot of *A. zambalensis*

sp. nov. is usually longer (Fig. 45A) and the ventral surface less heavily pigmented, with a longer hallux than that of *A. aurorae* (Fig. 10G,I). The cranium of *A. zambalensis* sp. nov. is usually larger overall, with a deeper rostrum and longer postpalatal region (Fig. 45B) and narrower  $M^1$ , although there is some overlap. A PCA of craniodental measurements (Fig. 23; Table 7), discussed above, showed complete overlap on the first component, which reinforces the overall similarity in size. On the second component, which loaded heavily (and positively) on diastema length and postpalatal length and (negatively) on interorbital breadth, palatal breadth at  $M^1$ , and width of the zygomatic plate, the overlap between these species was limited. Combined with the qualitative differences summarized here and the genetic evidence of monophyly (Fig. 7), we conclude that these are closely related but distinct species.

**DISTRIBUTION**—Our elevational transect of the Mingan Mountains documented this species from 733 to 1677 m (Figs. 3, 15, 35; Balete et al., this volume). It was the most abundant species along the transect from 902 to 1476 m. At the low end of the transect, we captured none at our 559-m sampling area, and at the high end, we captured only one at

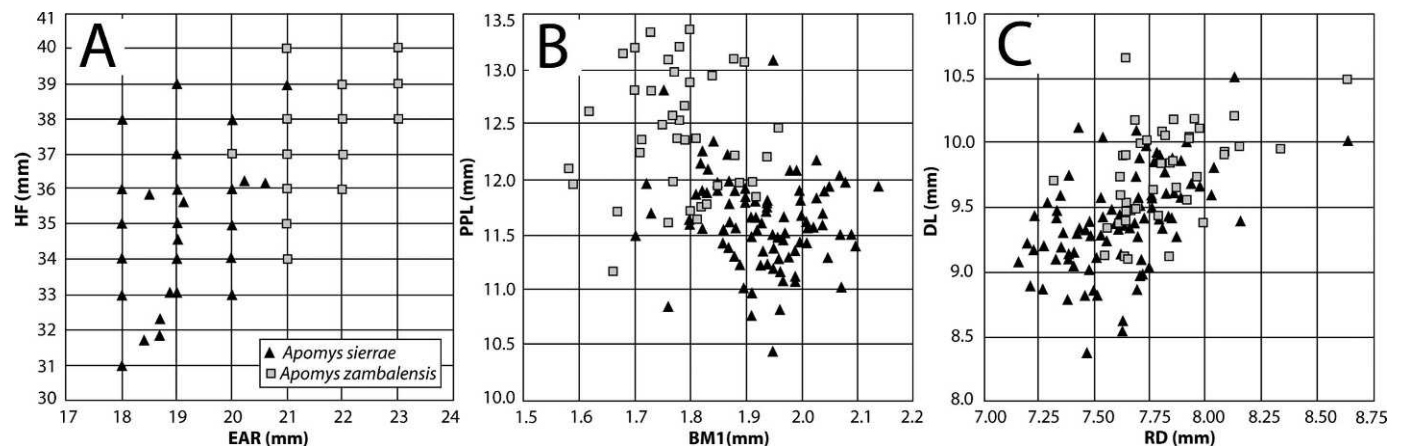


FIG. 40. Bivariate plots of measurements comparing *Apomys sierrae* and *A. zambalensis* spp. nov. (A) Length of ear (EAR) and length of hind foot (HF). (B) Breadth of  $M^1$  ( $BM^1$ ) and postpalatal length (PPL). (C) Rostral depth (RD) and diastema length (DL).



FIG. 41. Dorsal (A), ventral (B), and lateral (D) views of the cranium and lateral view of the mandible (C) of *Apomys magnus* sp. nov. (FMNH 183574, holotype); scale bar = 5 mm.

1540 m (plus 8 *A. minganensis*), one at 1677 m (plus 24 *A. minganensis*), and none at 1681 or 1785 m (where *A. minganensis* was common). We infer that this species may be expected throughout the Mingan Mountains from about 700 to 1675 m, with no *Megapomys* below 700 m and only *A. minganensis* above about 1700 m.

No specimens of *A. aurorae* are currently available other than from our transect (Fig. 35), so the extent of its distribution is uncertain. The Mingan Mountains lie in the central portion of Aurora Province and the adjacent area of Nueva Ecija Province (Fig. 3). Areas of low elevation lie to the north and to the south of the Mingan Mountains, with passes at ca. 250 and 300 m, respectively, which is well below the

lower elevational limit currently documented for this species; thus, the Mingan Mountains appear to function as a habitat island for this species. There are specimens of *A. sierrae* from northern Aurora Province and from Nueva Vizcaya, just to the north of the Mingan Mountains (Fig. 35), so we predict that *A. aurorae* will not be found to the north of the Mingan Mountains (i.e., not north of the road that goes from Bongabon, Nueva Ecija, to Baler, Aurora). Beyond the low pass to the south (south of Gabaldon, Nueva Ecija, and Dingalan, Aurora), there are no known specimens of *Megapomys* from a long, rugged section of the southern Sierra Madre that has Mt. Irid and Mt. Angilo as the high points (in Rizal and nearby Quezon provinces; Fig. 3). Since

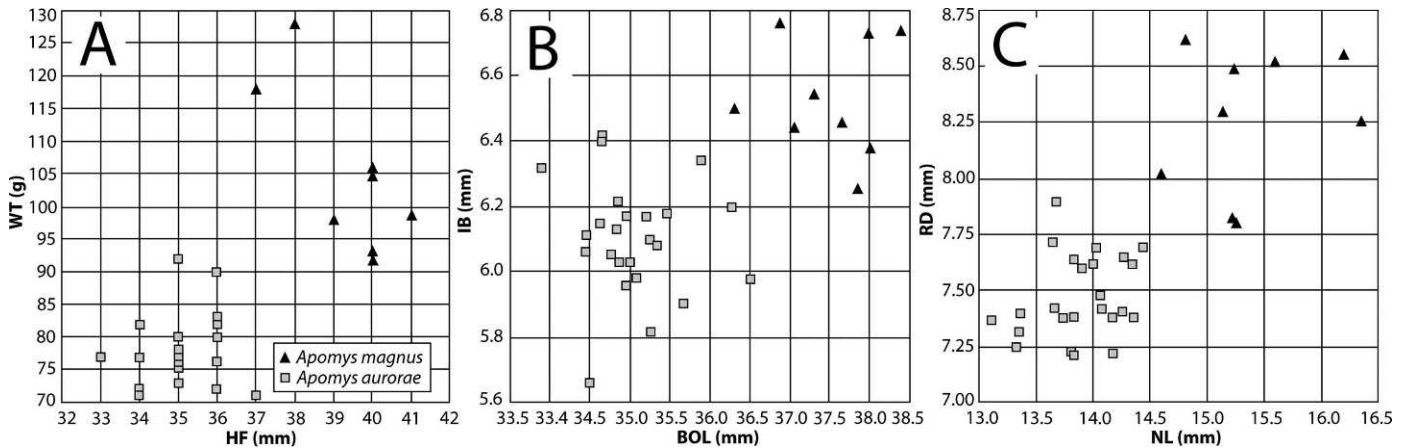


FIG. 42. Bivariate plots of measurements comparing *Apomys magnus* and *A. aurorae* spp. nov. (A) Length of hind foot (HF) and weight (WT). (B) Basioccipital length (BOL) and interorbital breadth (IB). (C) Nasal length (NL) and rostral depth (RD).

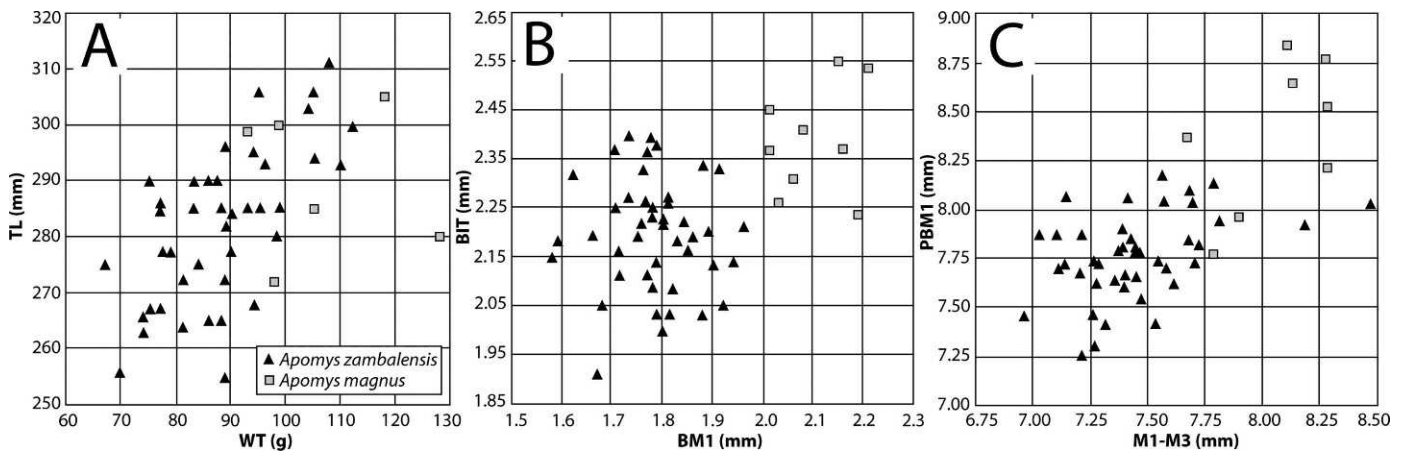


FIG. 43. Bivariate plots of measurements comparing *Apomys magnus* and *A. zambalensis* spp. nov. (A) Weight (WT) and total length (TL). (B) Breadth of  $M^1$  ( $BM^1$ ) and breadth of incisors at tip (BIT). (C) Length of maxillary molariform toothrow ( $M^1$ – $M^3$ ) and labial palatal breadth at  $M^1$  ( $PBM^1$ ).

the peaks in this region reach well over 1000 m, *Megapomys* should be present and should be sought to determine whether *A. aurora* occurs there, or whether yet another, currently unknown species of *Megapomys* is present.

*Apomys (Megapomys) zambalensis* sp. nov.

HOLOTYPE—FMNH 183420, adult female collected on 25 March 2005 by Lawrence R. Heaney, field number LRH 7339.

A sample of muscle tissue was removed from the thigh in the field and preserved in ethanol before preserving the specimen in formaldehyde. In the museum, the skull was removed and cleaned (see Methods). All parts are in good condition. This specimen will be permanently deposited at the NMP. Measurements in Table 15.

TYPE LOCALITY—Philippines: Luzon Id.: Bataan Province: 0.1 km N Mt. Natib peak, 1150 m, 14.71513°N, 120.39892°E (GPS reading).



FIG. 44. Dorsal (A), ventral (B), and lateral (D) views of the cranium and lateral view of the mandible (C) of *Apomys aurora* sp. nov. (FMNH 190812, holotype); scale bar = 5 mm.



TABLE 15. Cranial and external measurements (mean  $\pm$  1 S.D. and range) of *Apomys aurorae* and *A. zambalensis*.

Measurement	<i>Apomys aurorae</i>			<i>Apomys zambalensis</i>				
	Mingan Mtns., 733–1677 m, Aurora Prov.			Mt. Natib, Bataan Prov.			Mt. Tapulao, 860–1690 m, Zambales Prov.	
	M-holotype	M	F	F-holotype	M	F	M	F
	FMNH 190812	(n = 12)	(n = 12)	FMNH 183420	(n = 12)	(n = 13)	(n = 10)	(n = 8)
Basioccipital length	35.25	35.23 $\pm$ 0.49	34.87 $\pm$ 0.65	36.99	35.78 $\pm$ 1.16	36.04 $\pm$ 0.99	35.43 $\pm$ 0.95	35.46 $\pm$ 1.18
Interorbital breadth	5.81	6.08 $\pm$ 0.15	6.12 $\pm$ 0.20	6.29	5.92 $\pm$ 0.13	5.82 $\pm$ 0.20	6.14 $\pm$ 0.20	5.94 $\pm$ 0.20
Zygomatic breadth	18.15	18.09 $\pm$ 0.33 (11)	18.13 $\pm$ 0.57	18.13	17.95 $\pm$ 0.43	18.15 $\pm$ 0.58	18.30 $\pm$ 0.52	18.27 $\pm$ 0.42
Mastoid breadth	14.40	14.25 $\pm$ 0.17	14.35 $\pm$ 0.20	14.74	14.35 $\pm$ 0.35	14.40 $\pm$ 0.33	14.10 $\pm$ 0.23	14.13 $\pm$ 0.39
Nasal length	14.18	14.03 $\pm$ 0.31	13.76 $\pm$ 0.34	14.26	14.11 $\pm$ 0.45	14.22 $\pm$ 0.41	14.29 $\pm$ 0.46	14.27 $\pm$ 0.52
Incisive foramen length	5.57	5.49 $\pm$ 0.31	5.41 $\pm$ 0.21	5.67	5.45 $\pm$ 0.29	5.36 $\pm$ 0.31	5.30 $\pm$ 0.29	5.63 $\pm$ 0.40
Rostral depth	7.38	7.40 $\pm$ 0.14	7.53 $\pm$ 0.18	7.81	7.72 $\pm$ 0.16	7.80 $\pm$ 0.23	7.90 $\pm$ 0.29	7.81 $\pm$ 0.24
Rostral length	15.00	15.22 $\pm$ 0.36	15.40 $\pm$ 0.27	15.64	15.41 $\pm$ 0.58	15.31 $\pm$ 0.59	15.69 $\pm$ 0.43	15.51 $\pm$ 0.64
Orbitotemporal length	12.41	12.47 $\pm$ 0.48	12.31 $\pm$ 0.33	12.36	12.20 $\pm$ 0.46	12.08 $\pm$ 0.41	12.40 $\pm$ 0.27	12.54 $\pm$ 0.52
Maxillary toothrow length	7.42	7.52 $\pm$ 0.16	7.39 $\pm$ 0.25	7.41	7.46 $\pm$ 0.24	7.53 $\pm$ 0.40	7.38 $\pm$ 0.19	7.40 $\pm$ 0.16
Labial palatal breadth at M <sup>1</sup>	8.04	7.88 $\pm$ 0.19	7.84 $\pm$ 0.21	8.05	7.78 $\pm$ 0.20	7.81 $\pm$ 0.26	7.71 $\pm$ 0.12	7.68 $\pm$ 0.28
Diastema length	9.37	9.43 $\pm$ 0.23	9.42 $\pm$ 0.37	10.05	9.74 $\pm$ 0.42	9.77 $\pm$ 0.32	9.78 $\pm$ 0.44	9.80 $\pm$ 0.32
Postpalatal length	11.52	11.62 $\pm$ 0.31	11.43 $\pm$ 0.32	13.20	12.59 $\pm$ 0.52	12.62 $\pm$ 0.48	12.18 $\pm$ 0.49 (8)	12.04 $\pm$ 0.59
Lingual palatal breadth at M <sup>3</sup>	5.44	5.41 $\pm$ 0.21	5.59 $\pm$ 0.19	6.23	5.49 $\pm$ 0.26	5.61 $\pm$ 0.31	5.44 $\pm$ 0.30 (9)	5.62 $\pm$ 0.19
Braincase height	10.65	10.78 $\pm$ 0.40	10.78 $\pm$ 0.37	11.22	10.82 $\pm$ 0.31	10.84 $\pm$ 0.20	10.86 $\pm$ 0.30	10.72 $\pm$ 0.28
Breadth of M <sup>1</sup>	1.96	1.95 $\pm$ 0.07	1.88 $\pm$ 0.05	1.70	1.82 $\pm$ 0.07	1.76 $\pm$ 0.09	1.81 $\pm$ 0.09	1.74 $\pm$ 0.10
Breadth of incisors at tip	2.36	2.20 $\pm$ 0.10	2.14 $\pm$ 0.10	2.25	2.22 $\pm$ 0.10	2.22 $\pm$ 0.14	2.15 $\pm$ 0.10	2.19 $\pm$ 0.10
Width of zygomatic plate	3.81	3.80 $\pm$ 0.16	3.80 $\pm$ 0.25	3.34	3.56 $\pm$ 0.24	3.53 $\pm$ 0.20	3.52 $\pm$ 0.21	3.64 $\pm$ 0.35
Length of head and body	145	143.5 $\pm$ 4.7 (11)	136.9 $\pm$ 6.0 (11)	158	145.3 $\pm$ 6.7	147.7 $\pm$ 9.0 (12)	139.6 $\pm$ 6.5 (9)	139.6 $\pm$ 6.9 (7)
Total length	287	285.2 $\pm$ 8.2 (11)	272.7 $\pm$ 9.0 (11)	306	283.9 $\pm$ 13.7	286.9 $\pm$ 15.8 (12)	278.9 $\pm$ 11.6 (9)	277.9 $\pm$ 10.3 (7)
Length of tail vertebrae	142	141.7 $\pm$ 5.3 (11)	135.5 $\pm$ 5.7	148	138.7 $\pm$ 9.8	139.3 $\pm$ 8.8 (12)	141.2 $\pm$ 9.2	138.3 $\pm$ 5.3 (7)
Length of hind foot	36	35.6 $\pm$ 0.8	34.7 $\pm$ 0.9	39	38.1 $\pm$ 1.3	38.0 $\pm$ 0.9	37.1 $\pm$ 1.2	36.8 $\pm$ 0.9
Length of ear	20	19.8 $\pm$ 0.8	20.0 $\pm$ 0.7 (9)	22	21.8 $\pm$ 0.9	21.9 $\pm$ 0.8 (11)	21.1 $\pm$ 0.6 (9)	21.6 $\pm$ 0.5 (7)
Weight (g)	80	81.2 $\pm$ 5.9 (11)	73.8 $\pm$ 6.3 (11)	105	88.7 $\pm$ 12.9	93.4 $\pm$ 10.6	84.2 $\pm$ 11.1	87.4 $\pm$ 9.1

PARATYPES (n = 231)—Luzon Island: Bataan Prov.: 0.1 km N Mt. Natib peak, 1150 m (FMNH 183389, 183391, 183392, 183414–183416, 183418, 183421–183424); 0.3 km N, 0.1 km W Mt. Natib peak, 1000 m (FMNH 183382–183386, 183388, 183390, 183405–183413, 183417, 183419, 183425); 0.7 km N, 0.2 km W Mt. Natib peak, 900 m (FMNH 183341–183381, 183387, 183393–183404).

Zambales Prov.: Palauig Munic.: Brgy. Salasa, Mt. Tapulao, 860 m (FMNH 178310, 178326–178330); Palauig Munic.: Brgy. Salasa, Mt. Tapulao, 925 m (FMNH 183529–183545); Palauig Munic.: Brgy. Salasa, Mt. Tapulao, 1200 m (FMNH

178276–178292, 178331–178333, 178338–178343, 179434–179442); Palauig Munic.: Brgy. Salasa, Mt. Tapulao, 1690 m (FMNH 178293–178309, 178311–178325, 178334–178337, 178344–178357).

ETYMOLOGY—An adjective from the name of the province, Zambales, from which the majority of the specimens originated, and the name of the geological region (the Zambales Range) that includes the type locality.

DIAGNOSIS AND DESCRIPTION—*Apomys zambalensis* is the second largest known species of *Megapomys*, with a total length averaging 278–289 mm and weight averaging 84–94 g

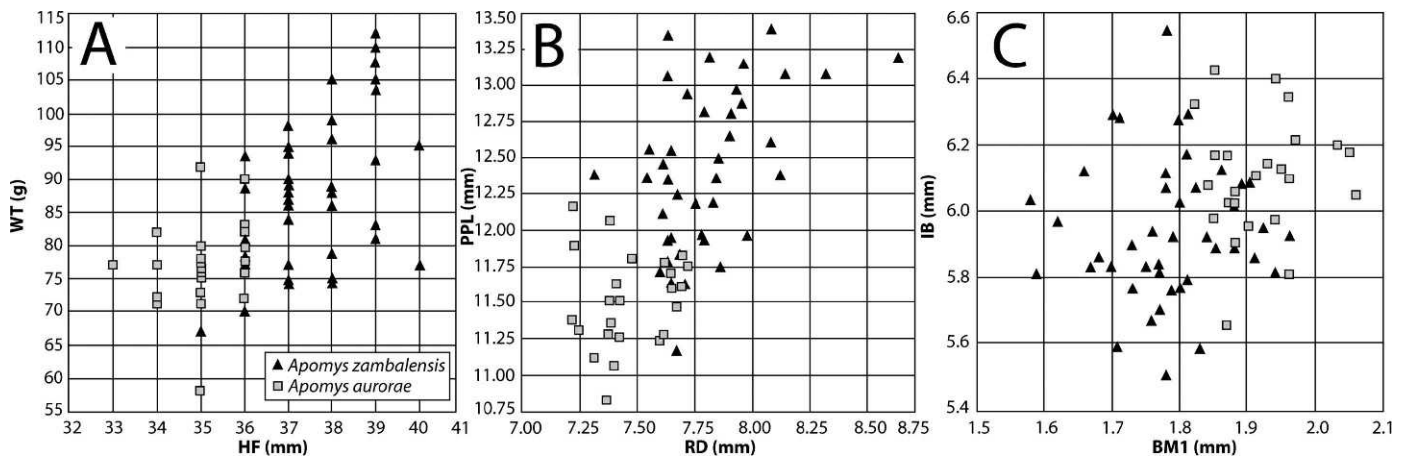


FIG. 45. Bivariate plots of measurements comparing *Apomys aurorae* and *A. zambalensis* spp. nov. (A) Length of hind foot (HF) and weight (WT). (B) Rostral depth (RD) and postpalatal length (PPL). (C) Breadth of M<sup>1</sup> (BM<sup>1</sup>) and interorbital breadth (IB).

(Table 15). The tail is typically 94–100% of the length of the head and body, making it one of the longest-tailed species in the subgenus. The dorsal fur is shorter and paler than that of most species, with a bright rusty-orange appearance (Fig. 2A). The ventral fur is pale to medium gray at the base, and white with an ochraceous wash at the tips that varies between individuals from slight to heavy. The ears are large, usually 22–23 mm, and less heavily pigmented than those of most other *Megapomys*. The tail is sharply bicolored, heavily pigmented dorsally but nearly white ventrally. The rusty-brown dorsal color extends onto the forelimb in a dark stripe

that is bounded by pale orange, barely reaching to the base of the foot. The hind foot is long (usually 36–39 mm) and broad, with digit 5 reaching nearly to the middle joint of digit 4. It is nearly white dorsally, sometimes with a few dark hairs. The ventral side of the hind foot is lightly pigmented, with some pigment on interdigital pad 4 and the hypothenar. The hallux is long, reaching about to the top of the adjacent interdigital pad (Fig. 10I).

The skull of *A. zambalensis* (Fig. 46) is large, with basioccipital length averaging 34–38 mm (Table 15); only that of *A. magnus* is larger overall. The rostrum is long and robust,



FIG. 46. Dorsal (A), ventral (B), and lateral (D) views of the cranium and lateral view of the mandible (C) of *Apomys zambalensis* sp. nov. (FMNH 183420, holotype); scale bar = 5 mm.

and the braincase is sturdy and somewhat elongate and flattened. The incisive foramina are unusually broad, especially in the posterior portions. The bony palate is of typical width and is moderately heavily pitted over its posterior portion. The maxillary toothrows are of roughly average length and width and diverge slightly posteriorly. The postpalatal region is elongated. The foramen in the bulla for the stapedia artery is relatively large and conspicuous (the “datae pattern”; Fig. 5B). The interparietal is variable in shape but usually is wide anteroposteriorly. The mandible (Fig. 46C) is average in depth, with a shorter than average coronoid process, average angular process, and rather deep concavity between the condylar and angular processes.

As noted above, the analysis of mitochondrial DNA shows only slight divergence between our two samples from Mt. Tapulao and Mt. Natib (Fig. 7). A PCA of craniodontal measurements, discussed above (Fig. 23; Table 7) that included the closely related *A. aurorae* and *A. magnus*, as well as the holotype of the geographically adjacent *A. sacobianus*, showed virtually complete overlap of individuals from these two mountains on both the first component, which primarily indicated size, and the second component, which loaded heavily (and positively) on diastema length and postpalatal length and (negatively) on interorbital breadth, palatal breadth at M<sup>1</sup>, and width of the zygomatic plate. Additionally, we are unable to detect any discrete cranial features to separate these samples. On the basis of these genetic and morphological data, we consider these populations to represent a single species, and we predict that individuals from geographically intermediate populations will bridge the current slight genetic gap between northern and southern populations.

The karyotype of *A. zambalensis* on the basis of eight males and seven females from Mt. Natib, Bataan Province (FMNH 183361, 183362, 183364, 183367, 183368, 183370–183373, 183376–183379, 183387, 183391), has  $2n = 44$ ,  $FN \geq 58$  (Fig. 8C). The autosomal complement consists of two pairs of large submetacentric, two pairs of medium-sized subtelocentric, two pairs of very small metacentric or submetacentric, and 15 pairs of small to large-sized telocentric or subtelocentric elements. The X chromosome is medium-sized and submetacentric, and the Y chromosome is small and telocentric.

COMPARISONS—*Apomys zambalensis* is easily distinguished externally from other *Megapomys* by its large size, comparatively pale, bright rusty-brown fur, and pale ears and ventral surface of the hind feet. Similarly, the skull is easily distinguished by its large size, exceeding all species except *A. magnus*. *Apomys zambalensis* is easily distinguished from its closest relative, *A. aurorae*, as described above; *A. aurorae* is smaller, with darker brown dorsal fur, dark hairs on the dorsal side of the hind foot and more heavily pigmented soles, a short hallux, a longer and more robust rostrum and braincase (Fig. 45), and a larger stapedia foramen in the bulla. As reflected in the PCA (Fig. 23; Table 7) of *A. zambalensis*, *A. aurorae*, *A. magnus*, and *A. sacobianus*, *A. zambalensis* typically differs from *A. aurorae* in having a narrower M<sup>1</sup> and low braincase, but longer diastema, incisive foramina, and postpalatal region (Fig. 45). The hallux of *A. zambalensis* is long, whereas that of *A. aurorae* is short (Fig. 10G). Both *A. zambalensis* and *A. aurorae* possess the “datae pattern” of basicranial circulation (Fig. 5B), but *A. aurorae* has a smaller stapedia foramen than *A. zambalensis*.

*Apomys zambalensis* differs from *A. magnus*, also closely related, as described above under that species; *A. magnus* is slightly larger and generally darker, with dark ears and dark soles on the hind feet, with a broader M<sup>1</sup>, longer maxillary toothrow, and broader palate (Fig. 43). These differences are clearly apparent in a PCA of craniodontal measurements (Fig. 23; Table 7).

As described above, *A. sierrae* is somewhat smaller than *A. zambalensis* in external features and is much darker dorsally and ventrally, with much dark hair on the dorsal surface of the hind foot and dark pigment on the ventral surface, and it has a short hallux. *Apomys sierrae* has the “abrae pattern” of basicranial carotid circulation (Fig. 5A) and is smaller in breadth of M<sup>1</sup>, postpalatal length, and diastema length (Fig. 40). The PCA of craniodontal measurements described above (Fig. 38; Table 14) shows no difference in size (PC1); there is overlap, but with substantially different averages along PC2, which loads heavily on the dental features, diastema length, and postpalatal length that are individually apparent as differences. Given these morphological differences and the clear evidence of genetic monophyly and intervening species in the phylogeny, we conclude that they represent distinct species.

DISTRIBUTION—We have documented *A. zambalensis* along our elevational transects on Mt. Tapulao from 860 to 1690 m and on Mt. Natib from 900 to 1150 m (Figs. 15, 35; Balet et al., 2009). We had no sampling areas below these elevations on either transect, so we do not know the lower limit of the species’ distribution with certainty; because it was common at our lowest sites, we suspect that it also occurs somewhat lower. The upper boundary is also uncertain, because we have no data between 1690 and 2024 m, but we suspect that it lies near 1800 m, the elevation at which primary mossy forest begins (Balet et al., 2009). We lack data from other mountains in this region, but the presence of *A. zambalensis* on Mts. Tapulao and Natib (Figs. 3, 35) leads us to suspect that it occurs throughout the Zambales Mountains and on Mt. Mariveles on the Bataan Peninsula at elevations above about 700 m. If this is so, it makes *A. zambalensis* one of the more widely distributed species of *Megapomys*.

## Discussion

### The Status of Discovery of Philippine Mammalian Diversity

The discovery and description of seven previously unknown species of mammals may surprise some people, especially since all but one come from within 150 km of Manila (Fig. 3), a metropolitan area with roughly 15 million people, and especially in the current millennium, when it is widely assumed that, although some less conspicuous organisms are poorly known, mammals have generally been well documented. Our studies in the field and museum show that this widespread assumption is not well-founded. With one species of *Archboldomys* (Balet et al., 2006), two species of *Rhynchomys* (Balet et al., 2007), and a new genus and species of mouse (*Musseromys gulantang*; Heaney et al., 2009) already described from the same areas on Luzon, as well as our ongoing studies indicating that many additional new species in other genera were obtained in the same surveys, it is clear that a great deal of the mammalian diversity on Luzon, and perhaps in the Philippines as a whole, has been unknown to the scientific and



conservation communities in the past, and it is likely that many species remain unknown.

One might ask how long this poor state of knowledge will persist in the future. Our studies of Luzon mammals have been conducted in the context of predictive biogeographic models and thus have been focused on those places most likely to result in the discovery of new biological diversity. We predict that locally endemic mammals will be found on individual mountains or on mountain ranges that reach above 1000 m elevation and are isolated from other such mountainous areas by elevations below 300 m that are at least 10 km wide (Heaney & Rickart, 1990; Heaney et al., 2000; Heaney, 2001, 2004; Rickart et al., 2010). Although our field surveys are not yet complete, we predict that within a few more years, few scientifically unknown mammals will remain on Luzon, with one exception. Because our models are discrete and predictive, they can be (and are being) tested, and so our prediction of a declining curve of discovery will soon be either validated or falsified. Thus, on the basis of current and planned surveys, we will soon know whether mammalian diversity on Luzon is well documented or whether our models were incorrect, and therefore an unknown, but potentially great, number of species remains to be found.

The one exception noted above refers to insectivorous bats. This group is notoriously difficult to capture using our standard sampling procedure, the use of mist nets, and we know that some “species” are actually groups of cryptic species (e.g., Ingle & Heaney, 1992; Sedlock & Weyandt, 2009). We explicitly acknowledge that we have not documented this group adequately and look forward to the results of the increased use of alternative methods (such as bat traps, V-nets, and tunnel traps; e.g., Alviola, 2008; Sedlock et al., 2008, this volume; Alviola et al., this volume; Balete et al., this volume) and evaluations using molecular genetics.

This discussion has referred only to the mammals of Luzon Island. The predictive biogeographic models that we have developed (Heaney & Rickart, 1990; Heaney, 2000, 2001, 2004; Rickart et al., 2011) refer to geographic features (e.g., elevational patterns of distribution, elevation of mountains, degree of isolation of mountains, etc.) that are relevant to other still very incompletely surveyed areas in the Philippines. Our discovery of a previously unknown species of *Batomys* from southeastern Mindanao (Balete et al., 2008) is consistent with the patterns we have noted on Luzon, and it implies that many subcenters of mammalian endemism, and therefore many currently unknown species of mammals, remain to be documented on Mindanao. The recent description of *Crociodura panayensis* from Panay Island (Hutterer, 2007) implies to us that similar conditions exist on the islands that formed large aggregate islands during Pleistocene periods of low sea level and suggests that similarly intensive surveys of mammalian diversity on those islands are warranted.

### Geographic Distribution Patterns in *Megapomys*

The distribution of species in the subgenus *Megapomys* is distinctly nonrandom, with six patterns that can be readily identified at this time.

- 1) Species of *Megapomys* extend from northernmost Luzon to Mt. Banahaw, but no further south on Luzon (Fig. 3). Intensive surveys of small mammals on the Bicol Peninsula of southern Luzon, on Mt. Labo, Saddle Peak,

Mt. Isarog, Mt. Malinao, and Mt. Bulusan, using the same techniques that easily capture them in central and northern Luzon, have failed to capture any *Megapomys*, although the smaller species of *Apomys* are often present and common (Rickart et al., 1991; Balete & Heaney, 1997; Heaney et al., 1999; L. R. Heaney, unpubl. data and specimens, FMNH). The elevation of the highest point connecting the Bicol Peninsula and central Luzon is only about 4 m above sea level, and this area of low elevation is extensive, thus significantly isolating the mountains of southern Luzon from those of central and northern Luzon.

- 2) All of the species of *Megapomys* occur on Luzon only at elevations above 450 m, with few records below 800 m (Fig. 15), even in areas of dense sampling effort where forest is present (e.g., the Sierra Madre; Duya et al., 2007). The one possible exception is *A. sacobianus*, known from a single specimen taken near the Sacobia River “just above the point where it emerges from the foothills of the Zambales Mountains onto the plains of Pampanga” (Johnson, 1962). From maps of the area, we estimate this to be 300 m. Each of the mountain masses has one or more species of *Megapomys* from this lower point up to the highest peak of the mountain. These data suggest that the large areas of Luzon below 450 m do not, and did not before deforestation, support populations of *Megapomys* (except perhaps rarely between 450 and 300 m). On the other hand, every mountain mass with a peak above about 1000 m that has been intensively surveyed has at least one species present. Clearly, the species of *Megapomys* are principally animals of montane and mossy forest. We note, however, that *A. sierrae* has been documented on Palau Island, a small island off the NE tip of Luzon, at ca. 150 m. Specimens of *A. sierrae* have been taken only above about 750 m in the adjacent areas of Cagayan Province on Luzon Island. We suspect the lower elevational range is associated with the fact that Palau is a small island with reduced species richness, as seen among small mammals on Dinagat and Siargao islands, which lie off the NE coast of Mindanao (Heaney and Rabor, 1982; Heaney et al., 1998); further study is needed.
- 3) Each species of *Megapomys* is associated with a single mountain range or individual mountain that is isolated from other such mountains by lowland areas at 300 m or lower. Each such mountainous area is thus an island of montane or mossy forest habitat in a “sea” of lowland forest (or, in recent centuries, agricultural lands). In cases in which the mountain range is very extensive, as with the Central Cordillera and the Sierra Madre, the species are similarly widespread (i.e., *A. abrae*, *A. datae*, and *A. sierrae*). In cases in which the mountain range is somewhat smaller, such as the Zambales Mountains (which in this case we define to include the mountains of the Bataan Peninsula), the range is smaller (i.e., *A. zambalensis*). In cases in which the mountain range is very small, the range of the species is very small (e.g., *A. manganensis* and *A. aurorae* in the Mangan Mountains and *A. banahaw* and *A. magnus* on Mt. Banahaw). The only exception to this pattern currently evident is the occurrence of *A. zambalensis* on Mt. Natib (on the Bataan Peninsula) and on the Zambales Mountains, which are separated from one another by a lowland area that drops to about 200 m. However, the distance along the highest ridge connecting Mt. Natib to Zambales that is below 450 m is less than

10 km wide and is made up of fairly steep, rugged slopes, not flat lowlands. This might provide some clue as to the precise conditions that prevent the movement of *Megapomys* from one mountain mass to another.

- 4) Two species of *Megapomys* occur on mountains over most of central and northern Luzon, although which species are present varies between mountain masses (Fig. 15). In the Central Cordillera, *A. abrae* occurs from about 900 to 2200 m, and *A. datae* from about 1500 m to higher than 2800 m. The former occurs most often in relatively open (often disturbed) and drier habitats, and the latter in more mature, moister forest (Rickart et al., 2011). On Mt. Banahaw, *A. magnus* occurs from about 800 to 1465 m, and *A. banahao* from 1465 m up to at least 1800 m. In the Mingan Mountains, *A. aurorae* occurs from about 750 to ca. 1550 m, and *A. minganensis* from 1550 to 1750 m. In the Zambales Mountains, *A. zambalensis* occurs from about 850 to about 1750 m, and *A. brownorum* near the peak at about 2050 m. These data show that over most of central and northern Luzon, two species of *Megapomys* usually occur on any given mountain mass, with one species occurring from the lower limits of montane forest elements (which begin to appear at about 500 m, but often are sparse and widely scattered below 800 m) up to the beginnings of prime mossy forest at about 1500 m, and the other species occurring in mossy forest from about 1500 m up to the peak. Current data are limited, but they suggest that the species at the lower elevation will often occur in more open and drier habitat at the upper edge of their ranges and that syntopy between individuals of the two species will be present but not extensive.
- 5) Species that occur within the same mountain mass are not sister-species and most often are rather distantly related (Fig. 7). For example, on Mt. Banahaw (*A. banahao* and *A. magnus*) and the Zambales Mountains (*A. brownorum* and *A. zambalensis*), the co-occurring pairs are distantly related to one another. In the Mingan Mountains, *A. aurorae* and *A. minganensis* are more closely related, but they are still separated by considerable genetic distance and several nodes in the phylogenetic tree. Only in the Central Cordillera is this pattern not directly supported: *A. abrae* and *A. datae* appear to be sister-taxa on the basis of Figure 5, but we question the accuracy of the mitochondrial data in this case because our preliminary nuclear sequence data indicate that they are more distantly related (S. J. Stepan, unpubl. data). Instead of close relatives occupying nearby localities in the same mountain region, they occupy similar elevations in different mountains.
- 6) There appears to be considerable ecological conservatism, with all but one (*A. abrae*) of the species in clades B and C (Fig. 7) occurring in high-elevation mossy forest and all but one (*A. minganensis*) of the species in clade D occurring in montane forest, primarily below 1500 m. This pattern suggests diversification among *Megapomys* within particular portions of the elevational gradient throughout northern and central Luzon.

Taken together, these six patterns imply a long history of diversification within the subgenus *Megapomys*, with diversification processes that usually involved ecological (habitat and climate) and geographic (topographic and geological) components. Furthermore, our ongoing studies of other endemic

Philippine murid genera on Luzon (*Archboldomys*, *Batomys*, *Chrotomys*, *Musseromys*, and *Rhynchomys*) suggest that these genera also have undergone extensive diversification. These patterns and processes will be considered in detail elsewhere following the necessary taxonomic studies.

## Acknowledgments

This study has been made possible by the Philippine Department of Environment and Natural Resources, which has provided not only permits but logistical and administrative support. We especially thank the staff of the Protected Areas and Wildlife Bureau, especially T. M. Lim, A. Manila, J. DeLeon, M. Mendoza, C. Custodio, and A. Tagtag, for their continuing encouragement and support. We are grateful to the Regional Executive Directors and their staffs for Regions 3, 4-A, and 5, the Cordillera Autonomous Region, and the National Capital Region for their patience in dealing with the many permits that they have issued to us.

Funding for this project has been generously provided by the Barbara A. Brown Fund for Mammal Research, the Ellen Thorne Smith Fund, and the Marshall Field Fund of the Field Museum; by the Grainger Foundation and the Negaunee Foundation; and NSF DEB-0238837, 0454673, and 0841447 to Scott Stepan. Their long-term support is deeply appreciated. The Field Museum, Utah Museum of Natural History, Conservation International–Philippines, and National Museum of the Philippines have all provided logistical support and permitted us to pursue our research on Philippine biodiversity, for which we are deeply grateful.

At the Field Museum, this work would not have been possible without the hard work, meticulous attention to detail, and patience of Bill Stanley, Michi Schulenberg, John Phelps, and Tracy Damitz. The many beautiful illustrations here were prepared by Lisa Kanellos, Andria Niedzielski, Clara Richardson, Betty Strack, and Velizar Simeonovski. Tricia DeCoster has devoted many long hours to preparing data and conducting analyses, developing maps, and attending to dozens of details, always with the highest of standards. We thank Michael Reno and Rebecca Justiniano for assisting with PCR and sequencing. We thank Richard Thorington and Jennifer R. Miller for photographing the skull of the holotype of *A. sacobianus*. We also thank the staff of the Division of Mammals at the U.S. National Museum of Natural History, especially Richard Thorington, Michael Carleton, Linda Gordon, David Schmidt, and Helen Kafka, for their hospitality and support over many years, without which this and many other research projects would not have been possible. In the field, we have been ably assisted by Joel Sarmiento, Nonito Antoque, Cardo Buenviaje, and many others, whose patience, skill, and persistence have been key to any success that we have achieved. This manuscript has benefited from thoughtful, detailed reviews of an earlier draft by Michael Carleton, Guy Musser, Margaret Thayer, and an anonymous reviewer.

Finally, we offer our most sincere thanks to the people in the many areas where we have conducted our field work, who have taken us into their homes, fed us, guided us into the forest, worked hard on our behalf, and kept us from harm. Their efforts and their friendship have made this project not only possible but a deep and genuine pleasure.

## Literature Cited

- ALVIOLA, P. A. 2008. Distribution patterns of microchiropterans along different elevational gradients in the Mt. Makiling Forest Reserve, Philippines. Unpublished M.S. thesis, University of the Philippines at Los Baños.
- ALVIOLA, P. A., M. R. M. DUYA, M. V. DUYA, L. R. HEANEY, AND E. A. RICKART. 2011. Mammalian diversity patterns on Mount Palali, Caraballo Mountains, Luzon, pp. 61–74. *In* Heaney, L. R., ed., *Discovering Diversity: Studies of the Mammals of Luzon Island, Philippines*. Fieldiana: Life and Earth Sciences, **2**.
- BALETE, D. S., AND L. R. HEANEY. 1997. Density, biomass, and movement estimates for murid rodents in mossy forest on Mount Isarog, southern Luzon, Philippines. *Ecotropica*, **3**: 91–100.
- BALETE, D. S., L. R. HEANEY, P. A. ALVIOLA, M. R. M. DUYA, M. V. DUYA, AND E. A. RICKART. 2011. The mammals of the Mingan Mountains, Luzon: Evidence for a new center of mammalian endemism, pp. 75–87. *In* Heaney, L. R., ed., *Discovering Diversity: Studies of the Mammals of Luzon Island, Philippines*. Fieldiana: Life and Earth Sciences, **2**.
- BALETE, D. S., L. R. HEANEY, E. A. RICKART, R. S. QUIDLAT, AND J. C. IBANEZ. 2008. A new species of *Batomys* (Muridae: Murinae) from eastern Mindanao Island, Philippines. *Proceedings of the Biological Society of Washington*, **121**: 411–428.
- BALETE, D. S., L. R. HEANEY, M. J. VELUZ, AND E. A. RICKART. 2009. Diversity patterns of small mammals in the Zambales Mts., Luzon, Philippines. *Mammalian Biology*, **74**: 456–466.
- BALETE, D. S., E. A. RICKART, AND L. R. HEANEY. 2006. A new species of the shrew-mouse, *Archboldomys* (Rodentia: Muridae: Murinae) from the Philippines. *Systematics and Biodiversity*, **4**: 489–501.
- BALETE, D. S., E. A. RICKART, R. G. B. ROSELL-AMBAL, S. JANS, AND L. R. HEANEY. 2007. Descriptions of two new species of *Rhynchomys* Thomas (Rodentia: Muridae: Murinae), from Luzon Island, Philippines. *Journal of Mammalogy*, **88**: 287–301.
- CATIBOG-SINHA, C., AND L. R. HEANEY. 2006. Philippine Biodiversity, Principles and Practice. Haribon Foundation for the Conservation of Natural Resources Inc., Quezon City, Philippines.
- DANIELSEN, E., D. S. BALETE, T. D. CHRISTENSEN, M. HEEGAARD, O. F. JAKOBSEN, A. JENSEN, T. LUND, AND M. K. POULSEN. 1994. Conservation of Biological Diversity in the Sierra Madre Mountains of Isabela and Southern Cagayan Province, the Philippines. BirdLife International, Manila and Copenhagen.
- DUYA, M. R. M., P. A. ALVIOLA, M. V. DUYA, D. S. BALETE, AND L. R. HEANEY. 2007. Report on a survey of the mammals of the Sierra Madre Range, Luzon Island, Philippines. *Banwa*, **4**: 41–68.
- DUYA, M. R. M., M. V. DUYA, P. A. ALVIOLA, D. S. BALETE, AND L. R. HEANEY. 2011. Diversity of small mammals in montane and mossy forests on Mount Cetaceo, Cagayan Province, Luzon, pp. 88–95. *In* Heaney, L. R., ed., *Discovering Diversity: Studies of the Mammals of Luzon Island, Philippines*. Fieldiana: Life and Earth Sciences, **2**.
- ELLERMAN, J. R. 1941. The Families and Genera of Living Rodents, Vol. II. Family Muridae. British Museum (Natural History), London.
- FELSENSTEIN, J. 1985. Confidence limits on phylogenies: An approach using the bootstrap. *Evolution*, **39**: 783–791.
- GOOD, J. M., S. HIRD, J. R. DEMBOSKI, S. J. STEPPAN, T. R. MARTIN-NIMS, AND J. SULLIVAN. 2008. Ancient hybridization and mitochondrial capture between two distantly related species of chipmunks (*Tamias*: Rodentia). *Molecular Ecology*, **17**: 1313–1327.
- HEANEY, L. R. 1985. Zoogeographic evidence for Middle and Late Pleistocene land bridges to the Philippine Islands. *Modern Quaternary Research in Southeast Asia*, **9**: 127–143.
- . 1986. Biogeography of mammals in Southeast Asia: Estimates of rates of colonization, extinction, and speciation. *Biological Journal of the Linnean Society*, **28**: 127–165.
- . 2000. Dynamic disequilibrium: A long-term, large-scale perspective on the equilibrium model of island biogeography. *Global Ecology and Biogeography*, **9**: 59–74.
- . 2001. Small mammal diversity along elevational gradients in the Philippines: An assessment of patterns and hypotheses. *Global Ecology and Biogeography*, **10**: 15–39.
- . 2004. Conservation biogeography in oceanic archipelagoes, pp. 345–360. *In* Lomolino, M. V., and L. R. Heaney, eds., *Frontiers of Biogeography, New Directions in the Geography of Nature*. Sinauer Associates, Sunderland, MA.
- HEANEY, L. R., D. S. BALETE, M. L. DOLAR, A. C. ALCALA, A. T. L. DANS, P. C. GONZALES, N. R. INGLE, M. V. LEPITEN, W. L. R. OLIVER, P. S. ONG, E. A. RICKART, B. R. TABARANZA, JR., AND R. C. B. UTZURRUM. 1998. A synopsis of the mammalian fauna of the Philippine Islands. *Fieldiana: Zoology*, n.s., **88**: 1–61.
- HEANEY, L. R., D. S. BALETE, G. V. GEE, M. V. LEPITEN-TABAO, E. A. RICKART, AND B. R. TABARANZA, JR. 2003. Preliminary report on the mammals of Balbalasang, Kalinga Province, Luzon. *Sylvatrop*, **13**: 51–62.
- HEANEY, L. R., D. S. BALETE, E. A. RICKART, R. C. B. UTZURRUM, AND P. C. GONZALES. 1999. Mammalian diversity on Mt. Isarog, a threatened center of endemism on southern Luzon Island, Philippines. *Fieldiana: Zoology*, n.s., **95**: 1–62.
- HEANEY, L. R., D. S. BALETE, E. A. RICKART, M. J. VELUZ, AND S. JANS. 2009. A new genus and species of small “tree mouse” (Rodentia, Muridae) related to the Philippine giant cloud-rats. *Bulletin of the American Museum of Natural History*, **331**: 215–229.
- HEANEY, L. R., P. D. HEIDEMAN, E. A. RICKART, R. C. B. UTZURRUM, AND J. S. H. KLOMPEN. 1989. Elevational zonation of mammals in the central Philippines. *Journal of Tropical Ecology*, **5**: 259–280.
- HEANEY, L. R., AND D. S. RABOR. 1982. Mammals of Dinagat and Siargao Islands, Philippines. Occasional papers of the Museum of Zoology. University of Michigan, **699**: 1–30.
- HEANEY, L. R., AND E. A. RICKART. 1990. Correlations of clades and clines: Geographic, elevational, and phylogenetic distribution patterns among Philippine mammals, pp. 321–332. *In* Peters, G., and R. Hutterer, eds., *Vertebrates in the Tropics*. Museum Alexander Koenig, Bonn, Germany.
- HEANEY, L. R., AND B. R. TABARANZA, JR. 2006. A new species of forest mouse, genus *Apomys* (Mammalia: Rodentia: Muridae) from Camiguin Island, Philippines. *Fieldiana: Zoology*, n.s., **106**: 14–27.
- HEANEY, L. R., B. R. TABARANZA, JR., D. S. BALETE, AND N. RIGERTAS. 2006a. Synopsis and biogeography of the mammals of Camiguin Island, Philippines. *Fieldiana: Zoology*, n.s., **106**: 28–48.
- HEANEY, L. R., B. R. TABARANZA, JR., E. A. RICKART, D. S. BALETE, AND N. R. INGLE. 2006b. The mammals of Mt. Kitanglad Nature Park, Mindanao, Philippines. *Fieldiana: Zoology*, n.s., **112**: 1–63.
- HEANEY, L. R., E. K. WALKER, B. R. TABARANZA, JR., AND N. R. INGLE. 2000. Mammalian diversity in the Philippines: An assessment of the adequacy of current data. *Sylvatrop*, **10**: 6–27.
- HUELSENBECK, J. P., AND F. RONQUIST. 2003. MrBayes 3: Bayesian phylogenetic inference under mixed models. *Bioinformatics*, **19**: 1572–1574.
- HUTTERER, R. 2007. Records of shrews from Panay and Palawan, Philippines, with the description of two new species of *Crociodura* (Mammalia: Soricidae). *Lynx*, **38**: 5–20.
- INGLE, N. R., AND L. R. HEANEY. 1992. A key to the bats of the Philippine Islands. *Fieldiana: Zoology*, n.s., **69**: 1–44.
- JANS, S., K. BARKER, AND L. R. HEANEY. 2006. The pattern and timing of diversification of Philippine endemic rodents: Evidence from mitochondrial and nuclear gene sequences. *Systematic Biology*, **55**: 73–88.
- JOHNSON, D. H. 1962. Two new murine rodents. *Proceedings of the Biological Society of Washington*, **75**: 317–319.
- KUCH, M., N. ROHLAND, J. BETANCOURT, C. LATTORE, S. J. STEPPAN, AND H. N. POINAR. 2002. Molecular analysis of a 11,700-year-old rodent midden from the Atacama Desert, Chile. *Molecular Ecology*, **11**: 913–924.
- LECOMPTÉ, E., K. APLIN, C. DENYS, F. CATZEFLIS, M. CHADES, AND P. CHEVRET. 2008. Phylogeny and biogeography of African Murinae based on mitochondrial and nuclear gene sequences, with a new tribal classification of the subfamily. *BMC Evolutionary Biology*, **8**: 199.
- MEYER, A. B. 1898–1899. Säugetiere vom Celebes—und Philippinen Archipel II. Abhandlungen und Berichte des Königl. Zoologisches Museum Dresden, series 7, **7**: viii + pp. 1–55 + 11 pls.
- MILLER, G. G. 1910. Descriptions of two new genera and sixteen new species of mammals from the Philippine Islands. *Proceedings of the United States National Museum*, **38**: 391–404.



- MUSSER, G. G. 1982. Results of the Archbold Expeditions. No. 108. The definition of *Apomys*, a native rat of the Philippine Islands. *American Museum Novitates*, **2746**: 1–43.
- MUSSER, G. G., AND M. D. CARLETON. 2005. Superfamily Muroidea, pp. 894–1531. In Wilson, D. E., and D. M. Reeder, eds., *Mammal Species of the World, A Taxonomic and Geographic Reference*. The Johns Hopkins University Press, Baltimore.
- MUSSER, G. G., AND L. R. HEANEY. 1992. Philippine rodents: Definitions of *Tarsomys* and *Limnomys* plus a preliminary assessment of phylogenetic patterns among native Philippine murines (Murinae, Muridae). *Bulletin of the American Museum of Natural History*, **211**: 1–138.
- PATTON, J. L. 1967. Chromosome studies of certain pocket mice, genus *Perognathus* (Rodentia: Heteromyidae). *Journal of Mammalogy*, **48**: 27–37.
- POINAR, H., M. KUCH, G. McDONALD, P. MARTIN, AND S. PAABO. 2003. Nuclear gene sequences from a late Pleistocene sloth coprolite. *Current Biology*, **13**: 1150–1152.
- POSADA, D., AND K. A. CRANDALL. 1998. Modeltest: Testing the model of DNA substitution. *Bioinformatics*, **14**: 817–818.
- RICKART, E. A., D. S. BALETE, AND L. R. HEANEY. 2007. Habitat disturbance and the ecology of small mammals in the Philippines. *Journal of Environmental Science and Management*, **10**: 34–41.
- RICKART, E. A., AND L. R. HEANEY. 2002. Further studies on the chromosomes of Philippine rodents (Muridae: Murinae). *Proceedings of the Biological Society of Washington*, **115**: 473–487.
- RICKART, E. A., L. R. HEANEY, D. S. BALETE, AND B. R. TABARANZA, JR. 2011. Small mammal diversity along an elevational gradient in northern Luzon, Philippines. *Mammalian Biology*, **76**: 12–21.
- RICKART, E. A., L. R. HEANEY, S. M. GOODMAN, AND S. JANSÁ. 2005. Review of the Philippine genera *Chrotomys* and *Celaenomys* (Murinae) and description of a new species. *Journal of Mammalogy*, **86**: 415–428.
- RICKART, E. A., L. R. HEANEY, P. D. HEIDEMAN, AND R. C. B. UTZURRUM. 1993. The distribution and ecology of mammals on Leyte, Biliran, and Maripipi Islands, Philippines. *Fieldiana: Zoology*, n.s., **72**: 1–62.
- RICKART, E. A., L. R. HEANEY, AND M. J. ROSENFELD. 1989. Chromosomes of ten species of Philippine fruit bats (Chiroptera: Pteropodidae). *Proceedings of the Biological Society of Washington*, **102**: 520–531.
- RICKART, E. A., L. R. HEANEY, B. R. TABARANZA, JR., AND D. S. BALETE. 1998. A review of the genera *Crunomys* and *Archboldomys* (Rodentia: Muridae: Murinae), with descriptions of two new species from the Philippines. *Fieldiana: Zoology*, n.s., **89**: 1–24.
- RICKART, E. A., L. R. HEANEY, AND R. C. B. UTZURRUM. 1991. Distribution and ecology of small mammals along an elevational transect in southeastern Luzon, Philippines. *Journal of Mammalogy*, **72**: 458–469.
- RICKART, E. A., AND G. G. MUSSEY. 1993. Philippine rodents: Chromosomal characteristics and their significance for phylogenetic inference among 13 species (Rodentia: Muridae: Murinae). *American Museum Novitates*, **3064**: 1–34.
- ROWE, K. C., M. L. RENO, D. M. RICHMOND, R. M. ADKINS, AND S. J. STEPPAN. 2008. Pliocene colonization and adaptive radiations in Australia and New Guinea (Sahul): Multilocus systematics of the old endemic rodents (Muroidea: Murinae). *Molecular Phylogenetics and Evolution*, **47**: 84–101.
- RUEDAS, L. A. 1995. Description of a new large-bodied species of *Apomys* Mearns, 1905 (Mammalia: Rodentia: Muridae) from Mindoro Island, Philippines. *Proceedings of the Biological Society of Washington*, **108**: 302–318.
- SANBORN, C. C. 1952. Philippine zoological expedition 1946–1947. *Mammals. Fieldiana: Zoology*, **33**: 87–158.
- SATHIAMURTHY, E., AND H. K. VORIS. 2006. Maps of Holocene sea level transgression and submerged lakes on the Sunda Shelf. *The Natural History Journal of Chulalongkorn University*, **2**(Supplement), 1–43.
- SEDLACK, J. L., N. R. INGLE, AND D. S. BALETE. 2011. Enhanced sampling of bat assemblages: A field test on Mount Banahaw, Luzon, pp. 96–102. In Heaney, L. R., ed., *Discovering Diversity: Studies of the Mammals of Luzon Island, Philippines*. *Fieldiana: Life and Earth Sciences*, **2**.
- SEDLACK, J. L., AND S. E. WEYANDT. 2009. Genetic divergence between morphologically and acoustically cryptic bats: Novel niche partitioning or recent contact? *Journal of Zoology*, **279**: 388–395.
- SEDLACK, J. L., S. E. WEYANDT, L. CORCORAN, M. DAMEROW, S.-H. HWA, AND B. PAULI. 2008. Bat diversity in tropical forest and agro-pastoral habitats within a protected area in the Philippines. *Acta Chiropterologica*, **10**: 349–358.
- SPSS, INC. 2000. SYSTAT 10. SPSS Inc., Chicago.
- STEPPAN, S. J., C. ZAWADSKI, AND L. R. HEANEY. 2003. Molecular phylogeny of the endemic Philippine rodent *Apomys* (Muridae) and the dynamics of diversification in an oceanic archipelago. *Biological Journal of the Linnean Society*, **80**: 699–715.
- SWOFFORD, D. L. 2002. PAUP\*. Phylogenetic analysis using parsimony (\*and other methods), Ver. 4.0 bv.10. Sinauer Associates, Sunderland, MA.
- WILGENBUSCH, J. C., D. L. WARREN, AND D. L. SWOFFORD. 2004. AWTY: A system for graphical exploration of MCMC convergence in Bayesian phylogenetic inference. <http://ceb.csit.fsu.edu/awty>

## Appendix I

Location and GenBank accession numbers for sequenced individuals. Brgy., Barangay, Munic., Municipality; Prov., Province.

Genus	Species	Voucher	Island/Province	Locality	GenBank accession
<i>Apomys</i>	<i>abrae</i>	FMNH 169051	Luzon/Kalinga Prov.	Balbalan Munic.	HM371053
<i>Apomys</i>	<i>abrae</i>	FMNH 170904	Luzon/Kalinga Prov.	Balbalan Munic.	HM371054
<i>Apomys</i>	<i>abrae</i>	FMNH 170915	Luzon/Kalinga Prov.	Balbalan Munic., Balbalasang Brgy.: Mapga	HM371055
<i>Apomys</i>	<i>abrae</i>	FMNH 170929	Luzon I/Kalinga Prov.	Balbalan Munic., Balbalasang Brgy.: Mapga	HM371056
<i>Apomys</i>	<i>abrae</i>	FMNH 188293	Luzon/Mountain Prov.	Mt. Data: 1.0 km N, 1.25 km E south peak	HM371057
<i>Apomys</i>	<i>abrae</i>	FMNH 188294	Luzon/Mountain Prov.	Mt. Data: 0.9 km N, 1.75 km E south peak	HM371059
<i>Apomys</i>	<i>abrae</i>	FMNH 188297	Luzon/Mountain Prov.	Mt. Data: 0.9 km N, 1.75 km E south peak	HM371058
<i>Apomys</i>	<i>abrae</i>	FMNH 193867	Luzon/Mountain Prov.	0.4 km N Barlig Munic. Hall	HM371060
<i>Apomys</i>	<i>abrae</i>	FMNH 193872	Luzon/Mountain Prov.	0.6 km N Barlig Munic. Hall	HM371061
<i>Apomys</i>	<i>abrae</i>	FMNH 193876	Luzon/Mountain Prov.	0.6 km N Barlig Munic. Hall	HM371062
<i>Apomys</i>	<i>abrae</i>	FMNH 62724	Luzon/Mountain Prov.	Mt. Data	HM371049
<i>Apomys</i>	<i>abrae</i>	FMNH 62749	Luzon/Abra Prov.	Massiat	HM371050
<i>Apomys</i>	<i>abrae</i>	FMNH 92759	Luzon/Ilocos Norte Prov.	Mt. Simminublar (Mt. Sicapoo)	HM371051
<i>Apomys</i>	<i>abrae</i>	FMNH 92760	Luzon/Ilocos Norte Prov.	Mt. Simminublar (Mt. Sicapoo)	HM371052
<i>Apomys</i>	<i>aurorae</i>	FMNH 190919	Luzon/Aurora Prov.	Dingalan Munic.: 2.1 km S, 2.9 km W Mingan peak	HM371035
<i>Apomys</i>	<i>aurorae</i>	FMNH 190921	Luzon/Aurora Prov.	Dingalan Munic.: 2.1 km S, 2.9 km W Mingan peak	HM371036
<i>Apomys</i>	<i>aurorae</i>	FMNH 190928	Luzon/Aurora Prov.	Dingalan Munic.: 2.1 km S, 2.9 km W Mingan peak	HM371037
<i>Apomys</i>	<i>aurorae</i>	FMNH 190932	Luzon/Aurora Prov.	Dingalan Munic.: 2.1 km S, 2.9 km W Mingan peak	HM371038
<i>Apomys</i>	<i>banahao</i>	FMNH 179453	Luzon/Quezon Prov.	Mt. Banahaw, Brgy. Lalo	HM371078
<i>Apomys</i>	<i>banahao</i>	FMNH 179456	Luzon/Quezon Prov.	Mt. Banahaw, Brgy. Lalo	HM371079
<i>Apomys</i>	<i>banahao</i>	FMNH 179459	Luzon/Quezon Prov.	Mt. Banahaw, Brgy. Lalo	HM371080
<i>Apomys</i>	<i>banahao</i>	FMNH 179462	Luzon/Quezon Prov.	Mt. Banahaw, Brgy. Lalo	HM371081
<i>Apomys</i>	<i>banahao</i>	FMNH 179465	Luzon/Quezon Prov.	Mt. Banahaw, Brgy. Lalo	HM371082
<i>Apomys</i>	<i>banahao</i>	FMNH 179505	Luzon/Quezon Prov.	Mt. Banahaw, Brgy. Lalo	HM371083
<i>Apomys</i>	<i>banahao</i>	FMNH 179511	Luzon/Quezon Prov.	Mt. Banahaw, Brgy. Lalo	HM371084
<i>Apomys</i>	<i>banahao</i>	FMNH 179515	Luzon/Quezon Prov.	Mt. Banahaw, Brgy. Lalo	HM371085
<i>Apomys</i>	<i>brownorum</i>	FMNH 183495	Luzon/Zambales Prov.	Palauig Munic.: Brgy. Salasa: Mt. Tapulao	HM371086
<i>Apomys</i>	<i>brownorum</i>	FMNH 183497	Luzon/Zambales Prov.	Palauig Munic.: Brgy. Salasa: Mt. Tapulao	HM371087
<i>Apomys</i>	<i>brownorum</i>	FMNH 183499	Luzon/Zambales Prov.	Palauig Munic.: Brgy. Salasa: Mt. Tapulao	HM371088
<i>Apomys</i>	<i>brownorum</i>	FMNH 183501	Luzon/Zambales Prov.	Palauig Munic.: Brgy. Salasa: Mt. Tapulao	HM371089
<i>Apomys</i>	<i>brownorum</i>	FMNH 183503	Luzon/Zambales Prov.	Palauig Munic.: Brgy. Salasa: Mt. Tapulao	HM371090
<i>Apomys</i>	<i>camiguinensis</i>	FMNH 154816	Camiguin	Mt. Timpoong, 2 km N, 6.5 km W Mahinog	AY324476
<i>Apomys</i>	<i>camiguinensis</i>	FMNH 154854	Camiguin	Mt. Timpoong, 2 km N, 6.5 km W Mahinog	AY324477
<i>Apomys</i>	<i>datae</i>	FMNH 167243	Luzon/Kalinga Prov.	Balbalan Munic., Balbalasang: Magdalo	AY324463
<i>Apomys</i>	<i>datae</i>	FMNH 167358	Luzon/Kalinga Prov.	Balbalan Munic., Balbalasang: Magdalo	AY324464
<i>Apomys</i>	<i>datae</i>	FMNH 169098	Luzon/Kalinga Prov.	Balbalan Munic., Balbalasang Brgy.: Am-licao	HM371064
<i>Apomys</i>	<i>datae</i>	FMNH 169103	Luzon/Kalinga Prov.	Balbalan Munic., Balbalasang Brgy.: Am-licao	HM371065
<i>Apomys</i>	<i>datae</i>	FMNH 169108	Luzon/Kalinga Prov.	Balbalan Munic., Balbalasang Brgy.: Am-licao	HM371066
<i>Apomys</i>	<i>datae</i>	FMNH 169110	Luzon/Kalinga Prov.	Balbalan Munic., Balbalasang Brgy.: Am-licao	HM371067
<i>Apomys</i>	<i>datae</i>	FMNH 169120	Luzon/Kalinga Prov.	Balbalan Munic., Balbalasang Brgy.: Am-licao	HM371068

**Appendix I**  
Continued.

Genus	Species	Voucher	Island/Province	Locality	GenBank accession
<i>Apomys</i>	<i>datae</i>	FMNH 175682	Luzon/Kalinga Prov.	Balbalan Munic., Balbalasang Brgy.: Mt. Bali-it	HM371069
<i>Apomys</i>	<i>datae</i>	FMNH 175683	Luzon/Kalinga Prov.	Balbalan Munic., Balbalasang Brgy.: Mt. Bali-it	HM371070
<i>Apomys</i>	<i>datae</i>	FMNH 175708	Luzon/Kalinga Prov.	Balbalan Munic., Balbalasang Brgy.: Mt. Bali-it	HM371071
<i>Apomys</i>	<i>datae</i>	FMNH 188298	Luzon/Mountain Prov.	Mt. Data: 0.1 km E south peak	HM371072
<i>Apomys</i>	<i>datae</i>	FMNH 188300	Luzon/Mountain Prov.	Mt. Data: 0.1 km E south peak	HM371073
<i>Apomys</i>	<i>datae</i>	FMNH 188305	Luzon/Mountain Prov.	Mt. Data: 0.1 km E south peak	HM371074
<i>Apomys</i>	<i>datae</i>	FMNH 193554	Luzon/Mountain Prov.	0.5 km N, 0.5 W Mt. Amuyao peak	HM371075
<i>Apomys</i>	<i>datae</i>	FMNH 193655	Luzon/Mountain Prov.	1.0 km N, 1.0 km W Mt. Amuyao peak	HM371076
<i>Apomys</i>	<i>datae</i>	FMNH 193877	Luzon/Mountain Prov.	0.6 km N Bartlig Munic. Hall	HM371077
<i>Apomys</i>	<i>datae</i>	FMNH 62709	Luzon/Mountain Prov.	Mt. Data	HM371063
<i>Apomys</i>	<i>gracitirostris</i>	CMNH 646	Mindoro/Mindoro Oriental Prov.	North ridge approach to Mt. Halcon, Hanglo	AY324465
<i>Apomys</i>	<i>gracitirostris</i>	CMNH 648	Mindoro/Mindoro Oriental Prov.	North ridge approach to Mt. Halcon, Hanglo	AY324466
<i>Apomys</i>	<i>hylocoetes</i>	FMNH 147871	Mindanao/Bukidnon Prov.	Mt. Katanglad range, 16.5 km S, 4 km E Camp Phillips	AY324467
<i>Apomys</i>	<i>hylocoetes</i>	FMNH 147914	Mindanao/Bukidnon Prov.	Mt. Katanglad range, 16.5 km S, 4 km E Camp Phillips	AY324468
<i>Apomys</i>	<i>hylocoetes</i>	FMNH 148149	Mindanao/Bukidnon Prov.	Mt. Katanglad range, 16.5 km S, 4 km E Camp Phillips	AY324469
<i>Apomys</i>	<i>insignis</i>	FMNH 147911	Mindanao/Bukidnon Prov.	Mt. Katanglad range, 16.5 km S, 4 km E Camp Phillips	AY324470
<i>Apomys</i>	<i>insignis</i>	FMNH 147915	Mindanao/Bukidnon Prov.	Mt. Katanglad range, 16.5 km S, 4 km E Camp Phillips	AY324471
<i>Apomys</i>	<i>insignis</i>	FMNH 147924	Mindanao/Bukidnon Prov.	Mt. Katanglad range, 16.5 km S, 4 km E Camp Phillips	AY324473
<i>Apomys</i>	<i>insignis</i>	FMNH 148160	Mindanao/Bukidnon Prov.	Mt. Katanglad range, 16.5 km S, 4 km E Camp Phillips	AY324472
<i>Apomys</i>	<i>magnus</i>	FMNH 178395	Luzon/Quezon Prov.	Mt. Banahaw, Brgy. Lalo	HM371039
<i>Apomys</i>	<i>magnus</i>	FMNH 178396	Luzon/Quezon Prov.	Mt. Banahaw, Brgy. Lalo	HM371040
<i>Apomys</i>	<i>magnus</i>	FMNH 183569	Luzon/Quezon Prov.	Taya bas Munic.: Brgy. Lalo: Mt. Banahaw, Ido	HM371041
<i>Apomys</i>	<i>magnus</i>	FMNH 183570	Luzon/Quezon Prov.	Taya bas Munic.: Brgy. Lalo: Mt. Banahaw, Ido	HM371042
<i>Apomys</i>	<i>magnus</i>	FMNH 183573	Luzon/Quezon Prov.	Taya bas Munic.: Brgy. Lalo: Mt. Banahaw, Hasa-an	HM371043
<i>Apomys</i>	<i>magnus</i>	FMNH 183574	Luzon/Quezon Prov.	Taya bas Munic.: Brgy. Lalo: Mt. Banahaw, Hasa-an	HM371044
<i>Apomys</i>	<i>microdon</i>	FMNH 167241	Luzon/Kalinga Prov.	Balbalan Munic., Balbalasang: Magdalo	AY324478
<i>Apomys</i>	<i>microdon</i>	FMNH 167242	Luzon/Kalinga Prov.	Balbalan Munic., Balbalasang: Magdalo	AY324479
<i>Apomys</i>	<i>microdon</i>	USNM 458907	Luzon/Camarines Sur Prov.	Mt. Isarog	AY324480
<i>Apomys</i>	<i>microdon</i>	USNM 458919	Luzon/Camarines Sur Prov.	Mt. Isarog	AY324481
<i>Apomys</i>	<i>minganensis</i>	FMNH 190778	Luzon/Aurora Prov.	Dingalan Munic.: 0.9 km S, 0.3 km W Mangan peak	HM371045
<i>Apomys</i>	<i>minganensis</i>	FMNH 190781	Luzon/Aurora Prov.	Dingalan Munic.: 0.9 km S, 0.3 km W Mangan peak	HM371046
<i>Apomys</i>	<i>minganensis</i>	FMNH 190782	Luzon/Aurora Prov.	Dingalan Munic.: 0.9 km S, 0.3 km W Mangan peak	HM371047
<i>Apomys</i>	<i>minganensis</i>	FMNH 190861	Luzon/Aurora Prov.	Dingalan Munic.: 0.9 km S, 0.3 km W Mangan peak	HM371048
<i>Apomys</i>	<i>musculus</i>	USNM 458925	Luzon/Camarines Sur Prov.	Mt. Isarog	AY324482
<i>Apomys</i>	<i>musculus</i>	USNM 458913	Luzon/Camarines Sur Prov.	Mt. Isarog	AY324483
<i>Apomys</i>	<i>sierrae</i>	FMNH 176562	Luzon/Cagayan Prov.	Gonzaga Munic., Brgy. Magrafil, Mt. Cagua, Sitio Masok	HM370984
<i>Apomys</i>	<i>sierrae</i>	FMNH 176564	Luzon/Cagayan Prov.	Gonzaga Munic., Brgy. Magrafil, Mt. Cagua, Sitio Masok	HM370985
<i>Apomys</i>	<i>sierrae</i>	FMNH 176566	Luzon/Cagayan Prov.	Gonzaga Munic., Brgy. Magrafil, Mt. Cagua, Sitio Masok	HM370986
<i>Apomys</i>	<i>sierrae</i>	FMNH 176568	Luzon/Cagayan Prov.	Gonzaga Munic., Brgy. Magrafil, Mt. Cagua, Sitio Masok	HM370987
<i>Apomys</i>	<i>sierrae</i>	FMNH 176570	Luzon/Cagayan Prov.	Gonzaga Munic., Brgy. Magrafil, Mt. Cagua, Sitio Masok	HM370988



**Appendix I**  
Continued.

Genus	Species	Voucher	Island/Province	Locality	GenBank accession
<i>Apomys</i>	<i>sierrae</i>	FMNH 180302	Luzon/Cagayan Prov.	Penablanca Munic., Brgy. Lapi, Sitio Baua, Mt. Cetaceo	HM370989
<i>Apomys</i>	<i>sierrae</i>	FMNH 180310	Luzon/Cagayan Prov.	Penablanca Munic., Brgy. Lapi, Sitio Baua, Mt. Cetaceo	HM370990
<i>Apomys</i>	<i>sierrae</i>	FMNH 180320	Luzon/Cagayan Prov.	Penablanca Munic., Brgy. Lapi, Sitio Baua, Mt. Cetaceo	HM370991
<i>Apomys</i>	<i>sierrae</i>	FMNH 180330	Luzon/Cagayan Prov.	Penablanca Munic., Brgy. Lapi, Sitio Baua, Mt. Cetaceo	HM370992
<i>Apomys</i>	<i>sierrae</i>	FMNH 180340	Luzon/Cagayan Prov.	Penablanca Munic., Brgy. Lapi, Sitio Baua, Mt. Cetaceo	HM370993
<i>Apomys</i>	<i>sierrae</i>	FMNH 180365	Luzon/Quirino Prov.	Nagtipunan Munic., Brgy. Matmad, Sitio Mangitagud, Mungiao Mtns	HM370994
<i>Apomys</i>	<i>sierrae</i>	FMNH 180367	Luzon/Quirino Prov.	Nagtipunan Munic., Brgy. Matmad, Sitio Mangitagud, Mungiao Mtns	HM370995
<i>Apomys</i>	<i>sierrae</i>	FMNH 180369	Luzon/Quirino Prov.	Nagtipunan Munic., Brgy. Matmad, Sitio Mangitagud, Mungiao Mtns	HM370996
<i>Apomys</i>	<i>sierrae</i>	FMNH 180371	Luzon/Quirino Prov.	Nagtipunan Munic., Brgy. Matmad, Sitio Mangitagud, Mungiao Mtns	HM370997
<i>Apomys</i>	<i>sierrae</i>	FMNH 180373	Luzon/Quirino Prov.	Nagtipunan Munic., Brgy. Matmad, Sitio Mangitagud, Mungiao Mtns	HM370998
<i>Apomys</i>	<i>sierrae</i>	FMNH 185806	Luzon/Cagayan Prov.	3.5 km SW Mt. Cetaceo peak	HM370999
<i>Apomys</i>	<i>sierrae</i>	FMNH 185816	Luzon/Cagayan Prov.	2.0 km SW Mt. Cetaceo peak	HM371000
<i>Apomys</i>	<i>sierrae</i>	FMNH 185871	Luzon/Cagayan Prov.	1.5 km SW Mt. Cetaceo peak	HM371001
<i>Apomys</i>	<i>sierrae</i>	FMNH 185906	Luzon/Cagayan Prov.	3.5 km SW Mt. Cetaceo peak	HM371002
<i>Apomys</i>	<i>sierrae</i>	FMNH 185943	Luzon/Cagayan Prov.	2.0 km SW Mt. Cetaceo peak	HM371003
<i>Apomys</i>	<i>sierrae</i>	FMNH 185948	Luzon/Cagayan Prov.	3.5 km SW Mt. Cetaceo peak	HM371004
<i>Apomys</i>	<i>sierrae</i>	FMNH 186728	Luzon/Nueva Vizcaya Prov.	Quezon Munic., 1.3 km NE Mt. Palali	HM371005
<i>Apomys</i>	<i>sierrae</i>	FMNH 186730	Luzon/Nueva Vizcaya Prov.	Quezon Munic., 1.3 km NE Mt. Palali	HM371006
<i>Apomys</i>	<i>sierrae</i>	FMNH 186736	Luzon/Nueva Vizcaya Prov.	Quezon Munic., 1.3 km NE Mt. Palali	HM371007
<i>Apomys</i>	<i>sierrae</i>	FMNH 186739	Luzon/Nueva Vizcaya Prov.	Quezon Munic., 1.3 km NE Mt. Palali	HM371008
<i>Apomys</i>	<i>sierrae</i>	FMNH 186763	Luzon/Nueva Vizcaya Prov.	Quezon Munic., Mt. Palali Peak	HM371009
<i>Apomys</i>	<i>sierrae</i>	FMNH 186765	Luzon/Nueva Vizcaya Prov.	Quezon Munic., Mt. Palali Peak	HM371010
<i>Apomys</i>	<i>sierrae</i>	FMNH 191232	Palau/Cagayan Prov.	Sta. Ana Munic., Brgy. San Vicente, 4.25 km S of Cape Engano Lighthouse	HM371011
<i>Apomys</i>	"sp. A/C"	USNM 458747	Negros/Negros Oriental Prov.	3 km N, 17 km W Dumaguete, Mt. Guinsayawan	AY324486
<i>Apomys</i>	"sp. A/C"	USNM 458751	Negros/Negros Oriental Prov.	3 km N, 17 km W Dumaguete, Mt. Guinsayawan	AY324487
<i>Apomys</i>	"sp. A/C"	FMNH 135715	Sibuyan/Romblon Prov.	Magdiwang, 4.5 km S, 4 km E; NW slope Mt. Guitinguitin	AY324484
<i>Apomys</i>	"sp. A/C"	FMNH 137024	Sibuyan/Romblon Prov.	Magdiwang, 4.5 km S, 4 km E; NW slope Mt. Guitinguitin	AY324485
<i>Apomys</i>	"sp. B"	FMNH 145698	Sibuyan/Romblon Prov.	Magdiwang, 6.75 km S, 4.5 km E; NW slope Mt. Guitinguitin	AY324488
<i>Apomys</i>	"sp. B"	FMNH 145699	Sibuyan/Romblon Prov.	Magdiwang, 4.5 km S, 4 km E; NW slope Mt. Guitinguitin	AY324489
<i>Apomys</i>	"sp. F"	USNM 458762	Leyte/Leyte Prov.	10 km N, 4.5 km E Baybay	AY324474
<i>Apomys</i>	"sp. F"	USNM 459844	Biliran/Leyte Prov.	5 km N, 10 km E Naval	AY324475
<i>Apomys</i>	<i>zambalensis</i>	FMNH 178276	Luzon/Zambales Prov.	Mt. High Peak, Palauig Munic., Brgy. Salasa	HM371012
<i>Apomys</i>	<i>zambalensis</i>	FMNH 178282	Luzon/Zambales Prov.	Mt. High Peak, Palauig Munic., Brgy. Salasa	HM371013
<i>Apomys</i>	<i>zambalensis</i>	FMNH 178288	Luzon/Zambales Prov.	Mt. High Peak, Palauig Munic., Brgy. Salasa	HM371014
<i>Apomys</i>	<i>zambalensis</i>	FMNH 178293	Luzon/Zambales Prov.	Mt. High Peak, Palauig Munic., Brgy. Salasa	HM371015
<i>Apomys</i>	<i>zambalensis</i>	FMNH 178296	Luzon/Zambales Prov.	Mt. High Peak, Palauig Munic., Brgy. Salasa	HM371016

**Appendix I**  
*Continued.*

Genus	Species	Voucher	Island/Province	Locality	GenBank accession
<i>Apomys</i>	<i>zambalensis</i>	FMNH 178297	Luzon/Zambales Prov.	Mt. High Peak, Palauig Munic., Brgy. Salasa	HM371017
<i>Apomys</i>	<i>zambalensis</i>	FMNH 178310	Luzon/Zambales Prov.	Mt. High Peak, Palauig Munic., Brgy. Salasa	HM371018
<i>Apomys</i>	<i>zambalensis</i>	FMNH 178327	Luzon/Zambales Prov.	Mt. High Peak, Palauig Munic., Brgy. Salasa	HM371019
<i>Apomys</i>	<i>zambalensis</i>	FMNH 183348	Luzon/Bataan Prov.	0.7 km N, 0.2 km W Mt. Natib Peak	HM371020
<i>Apomys</i>	<i>zambalensis</i>	FMNH 183393	Luzon/Bataan Prov.	0.7 km N, 0.2 km W Mt. Natib Peak	HM371021
<i>Apomys</i>	<i>zambalensis</i>	FMNH 183395	Luzon/Bataan Prov.	0.7 km N, 0.2 km W Mt. Natib Peak	HM371022
<i>Apomys</i>	<i>zambalensis</i>	FMNH 183405	Luzon/Bataan Prov.	0.3 km N, 0.1 km W Mt. Natib Peak	HM371023
<i>Apomys</i>	<i>zambalensis</i>	FMNH 183407	Luzon/Bataan Prov.	0.3 km N, 0.1 km W Mt. Natib Peak	HM371024
<i>Apomys</i>	<i>zambalensis</i>	FMNH 183414	Luzon/Bataan Prov.	0.1 km N Mt. Natib Peak	HM371025
<i>Apomys</i>	<i>zambalensis</i>	FMNH 183530	Luzon/Zambales Prov.	Palauig Munic.: Brgy. Salasa: Mt. Tapulao	HM371026
<i>Apomys</i>	<i>zambalensis</i>	FMNH 183532	Luzon/Zambales Prov.	Palauig Munic.: Brgy. Salasa: Mt. Tapulao	HM371027
<i>Apomys</i>	<i>zambalensis</i>	FMNH 183535	Luzon/Zambales Prov.	Palauig Munic.: Brgy. Salasa: Mt. Tapulao	HM371028
<i>Apomys</i>	<i>zambalensis</i>	FMNH 183537	Luzon/Zambales Prov.	Palauig Munic.: Brgy. Salasa: Mt. Tapulao	HM371029
<i>Apomys</i>	<i>zambalensis</i>	FMNH 183539	Luzon/Zambales Prov.	Palauig Munic.: Brgy. Salasa: Mt. Tapulao	HM371030
<i>Apomys</i>	<i>zambalensis</i>	FMNH 183604	Luzon/Bataan Prov.	0.7 km N, 0.2 km W Mt. Natib Peak	HM371031
<i>Apomys</i>	<i>zambalensis</i>	FMNH 183610	Luzon/Bataan Prov.	0.7 km N, 0.2 km W Mt. Natib Peak	HM371032
<i>Apomys</i>	<i>zambalensis</i>	FMNH 183617	Luzon/Bataan Prov.	0.3 km N, 0.1 km W Mt. Natib Peak	HM371033
<i>Apomys</i>	<i>zambalensis</i>	FMNH 183618	Luzon/Bataan Prov.	0.3 km N, 0.1 km W Mt. Natib Peak	HM371034